

## SOUND ABSORBING MATERIALS

SOLE DISTRIBUTORS FOR THE U S A AND CANADA  
ELSEVIER BOOK COMPANY, INC, 213, FOURTH AVENUE,  
NEW YORK — FOR THE BRITISH EMPIRE, EXCEPT  
CANADA CLIFTON HUME PRESS LTD, 42, SOUTH  
AUDLEY STREET, LONDON, W 1

# SOUND ABSORBING MATERIALS

by

C. ZWIKKER

PHILIPS ELECTRICAL INDUSTRIES, EINDHOVEN,  
FORMERLY PROFESSOR OF PHYSICS, DELFT TECHNICAL UNIVERSITY

AND

C. W. KOSTEN

LECTURER OF PHYSICS, DELFT TECHNICAL UNIVERSITY  
(NETHERLANDS)

CHBCL333



ELSEVIER PUBLISHING COMPANY, INC.

NEW YORK AMSTERDAM LONDON BRUSSELS

1949

ALL RIGHTS RESERVED NO PART OF THIS BOOK MAY BE  
REPRODUCED IN ANY FORM (INCLUDING PHOTOSTATIC OR  
MICROFILM FORM) WITHOUT WRITTEN PERMISSION FROM  
THE PUBLISHERS.

## PREFACE

The current acoustical literature provides us with numerous data and long tables concerning the sound absorption coefficient of the various materials that are on the market. These data together with the physical features of the material (the thickness of the layer, the porosity, the diameter of the pores, its stiffness) provide the skilled designer of absorbing materials with some idea as to how new materials can adequately be designed. In this book we have tried to give the design a more scientific basis. The principles underlying the wave propagation through media — porous or not — are described. The wave propagation through porous media has been treated at considerable length, being of great importance for the majority of absorbing materials.

Except for the last chapter (VIII) all theoretical considerations and measurements are confined to normal incidence of sound.

With a view to the increasing application of absorbing materials behind perforated panels, due attention is paid to this subject (chapter VII).

The origin of the book has been a request of the editor to the first author for a book on the subject of acoustical materials. The latter wrote the text in the grim war winter of 1944—1945 when all laboratory work was utterly impossible. Due to a serious shortage of printing facilities the actual printing was delayed so much that it was considered necessary to review the text on account of the publications that had become available since the war. At the first author's request the second author accepted the task to do this. It turned out that this meant hardly less than rewriting the whole text. Moreover the chapter on resonators was not included in the original scheme and it due to the initiative of the second author.

As far as we know a book with a similar aim does not exist, which may serve as a justification of adding a new book to the extensive acoustical literature. Furthermore, the existence of the latter may help to meet certain shortcomings in this book, of which the authors are convinced there are. May it, nevertheless, turn out to be valuable for the scientific manufacturer.

August 1949.

C. ZWIKKER

C. W. KOSTEN

# CONTENTS

PREFACE . . . . .	v
I SIMPLE THEORY OF SOUND ABSORPTION BY HOMO- GENEOUS LAYERS . . . . .	1
§ 1 Propagation constant and wave impedance . . .	1
§ 2 Impedance of a layer of finite thickness . . .	2
§ 3 Wave impedance $W_0$ of free air . . . . .	4
§ 4 Geometry in the complex plane . . . . .	6
§ 5 Geometrical representation of $\coth \gamma l$ . . . .	8
§ 6 Geometrical representation of formula (1.12) . .	11
§ 7 Wave impedance of impervious media with in- ternal friction . . . . .	13
§ 8 The general equations governing the wave prop- agation in porous material with rigid frame . .	18
§ 9 The resistance constant $\sigma$ . . . . .	22
II MORE DETAILED THEORETICAL CONSIDERATIONS CON- CERNING VISCOUS AND THERMAL EFFECTS IN POROUS MEDIA . . . . .	25
§ 1 Sound propagation in cylindrical tubes and pores	25
§ 2 The air density in cylinders disregarding thermal effects . . . . .	26
§ 3 The compression modulus of air in cylinders dis- regarding viscous effects . . . . .	29
§ 4 Extension of Kirchhoff's theory of sound propagation in cylindrical tubes and pores . .	34
§ 5 The consequences of Kirchhoff's theory for the wave propagation in porous media . . . .	40
§ 6 Discussion of the theoretical results of Korringa, Kronig, and Smit . . . . .	42
§ 7 Porous materials with high air resistance ( $\mu < 2$ )	44
§ 8 Porous materials with low air resistance ( $\mu > 20$ )	47
§ 9 A method of verification of theoretical results . .	48

III	THEORY OF SOUND ABSORPTION BY HOMOGENEOUS ISOTROPIC AND ELASTIC LAYERS	52
§ 1	Porous materials with elastic frame	52
§ 2	Travelling waves in elastic porous media	55
§ 3	Graphical representation of the roots of the Γ equation	57
§ 4	Simplified theory, $h=1$	64
§ 5	Elastic layer with closed front surface	65
§ 6	Elastic layer with open front surface	72
§ 7	Elastic layer backed otherwise than by a rigid wall	75
IV	EXPERIMENTAL DETERMINATION OF THE ELEMENTARY MATERIAL CONSTANTS OF POROUS ABSORBENTS GOVERNING THE ABSORPTION COEFFICIENT	76
§ 1	Introduction	76
§ 2	The porosity	77
§ 3	The air resistance	79
§ 4	The compression modulus	81
§ 5	Result of measurements of the complex stiffness	82
V	MEASUREMENT OF NORMAL IMPEDANCE AND AB- SORPTION	85
§ 1	Introduction	85
§ 2	Constant length interferometer	86
§ 3	Wente and Bedell's method	89
§ 4	Curve width method	90
§ 5	Reaction-on-source interferometers	91
§ 6	The determination of the absorption coefficient with reaction interferometers Practical aspects	95
§ 7	Geluk's impedance indicator	99
§ 8	Details of Geluk's impedance indicator	101
VI	EXPERIMENTAL RESULTS COMPARISON WITH THEORY	107
§ 1	Introduction	107
§ 2	Experiments on artificial samples	108
§ 3	Impervious materials of high elasticity	111
§ 4	Porous materials with rigid frame	112
§ 5	Porous materials, elastic frame open front surface	114
§ 6	Porous materials elastic frame coated surface	116
§ 7	Porous material backed by a layer of air	119
§ 8	Celotex C—4	124

VII	ABSORPTION BY RESONATORS . . . . .	127
§ 1	Introduction . . . . .	127
§ 2	The single resonator in an infinite wall . . . . .	132
§ 3	The use of single resonators in practice . . . . .	141
§ 4	Perforated panels before a rigid wall . . . . .	143
§ 5	Rules for designing perforated panel absorbers . . . . .	147
§ 6	Rules for designing panel absorbers with slits . . . . .	152
§ 7	Experimental results . . . . .	153
§ 8	Combinations of resonators . . . . .	157
VIII	OBLIQUE AND RANDOM INCIDENCE. PRACTICAL ASPECTS . . . . .	164
§ 1	Introduction . . . . .	164
§ 2	Oblique incidence on locally reacting surfaces . . . . .	167
§ 3	Oblique incidence on a single resonator . . . . .	170
	AUTHOR INDEX . . . . .	172
	SUBJECT INDEX . . . . .	173



## CHAPTER I

### SIMPLE THEORY OF SOUND ABSORPTION BY HOMOGENEOUS LAYERS

#### § 1 PROPAGATION CONSTANT AND WAVE IMPEDANCE

If we consider a plane sound wave travelling in the direction of the positive  $x$ -axis in a homogeneous isotropic medium extending to infinity, the sound pressure depends upon the time  $t$  and on the distance  $x$  as a damped sine:

$$p(x) = A \exp \left\{ j \omega \left( t - \frac{x}{c} \right) - \alpha x \right\} \quad (1.01)$$

in which  $j^2 = -1$ ,  $\omega = 2\pi \cdot \text{frequency}$ ,  $c = \text{velocity of propagation of sound}$ , and  $\exp(\dots)$  is the well-known symbolical notation for  $e^{(\dots)}$ . At the site  $x=0$  we have  $p(0) = A \exp j\omega t$ . Putting  $\omega/c = \beta$  and  $\alpha + j\beta = \gamma$ , we obtain for the damped sine the shorter analytical form

$$p(x) = p(0) \exp(-\gamma x).$$

The constant  $\gamma$ , which, apart from its dependence on  $\omega$ , is determined by the nature of the medium is called the *propagation constant* of this medium; its real part  $\alpha$  is called the *attenuation constant* and its imaginary part  $\beta$  the *phase constant*.

In the same way the velocity of specific volume displacement,  $v$ , can be expressed by a similar formula

$$v(x) = v(0) \exp(-\gamma x),$$

in which the same constant  $\gamma$  enters as in the formula for  $p$ , because in a travelling wave the ratio  $p/v$  must be independent of  $x$ . We shall use the symbol  $v$  for the amount of material volume passing through a unit surface in unit time, or the volume current density. Only in a homogeneous medium (free air, compact solid medium) is  $v$  identical with the material velocity. For example, in a porous medium with rigid solid skeleton, the velocity of

volume displacement  $\iota$  is smaller than the velocity of the vibrating air, the ratio being equal to that of the volume of the accessible holes to the total volume of the medium,  $h$ . The constant  $h$  is called the *porosity* or *cavity factor* and is one of the elementary properties of the material which will play an important rôle in the following pages.

In analogy to electrical practice the quotient

$$z(x) = p(x)/\iota(x) \quad (1.02)$$

is called the specific acoustic impedance at the site  $x$ . For an unlimited medium,  $z$  must be independent of  $x$ . This impedance is a material constant and is called its *wave impedance*, represented by  $W$ . As  $p$  and  $\iota$  are generally not in phase with each other,  $W$  is a complex quantity.

If a periodical pressure  $p(0)$  is applied at the site  $x=0$  of an unlimited medium, the dependence of  $p$  and  $\iota$  upon  $x$  and  $t$  is fully determined by the two quantities  $\gamma$  and  $W$ . Thus  $\gamma$  and  $W$  fully determine the acoustical behaviour of the medium.

## § 2 IMPEDANCE OF A LAYER OF FINITE THICKNESS

We shall next consider a layer of uniform constitution, determined by the properties  $\gamma$  and  $W$ , having a thickness  $l$  ( $x=0$  to  $x=l$ ). Supposing it to be loaded at  $x=l$  by the arbitrary complex impedance  $z_2$ , what is, then, the impedance  $z_1$  at  $x=0$  (Fig. 1)? Part of the sound wave will be reflected at the end  $x=l$ , so that  $p$  is the superposition of an incoming wave and a reflected wave

$$\begin{aligned} p(x) &= p_i \exp \{ \gamma (l-x) \} + p_r \exp \{ -\gamma (l-x) \} \\ \iota(x) &= (p_i/W) \exp \{ \gamma (l-x) \} - (p_r/W) \exp \{ -\gamma (l-x) \}, \end{aligned}$$

in which  $p_i$  and  $p_r$  are obviously the possibly complex pressure of the incoming and the reflected wave at  $x=l$ , just inside the layer.

The pressure adds as a scalar, the velocity as a vector, hence the minus sign in the formula for  $\iota$ . As a boundary condition we have  $p(l)/\iota(l) = z_2$ . With the aid of this it may easily be verified that

$$p_r/p_i = (z_2 - W)/(z_2 + W), \quad (1.03)$$

and introducing this into the preceding equations one finds for the impedance at the site  $x=0$

$$z_1 = W \frac{z_2 \cosh \gamma l + W \sinh \gamma l}{z_2 \sinh \gamma l + W \cosh \gamma l}, \quad (1.04)$$

a formula wellknown from the theory of electric cables and filters.

This formula contains, as a special case, that of the medium extending to infinity. Then  $z_2 = W$  and the formula gives  $z_1 = z_2 = W$ . Another special case is that in which  $z_2 = \infty$ , in which case

$$z_1 = W \coth \gamma l. \quad (1.05)$$

This latter case is of great importance for the investigations, because this is the one which can easily be realized by loading the sheet of absorbent material with a completely hard back wall. Backing absorbent layers with a rigid wall is a normal way of

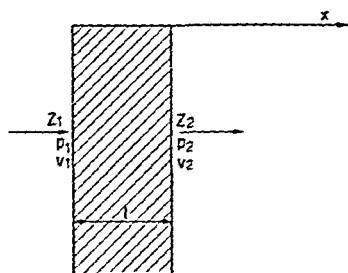


Fig. 1  
Layer backed by an impedance  $z_2$

applying these materials in practice, so that this case is at the same time of great practical importance.

The other limiting case is obtained by putting  $z_2 = 0$ . Then (1.04) yields

$$z_1 = W \tanh \gamma l. \quad (1.06)$$

Because the impedance of a layer of air with a thickness of one quarter of a wave length, backed by a rigid wall, is zero (see (1.05) remembering that  $\gamma = j\omega/c$ , since there is no damping), this case can be realized by placing the absorbent layer at a distance of  $1/4 \lambda$  from the rigid wall.

It is now possible to calculate in principle the acoustic impedance of any combination of sheets of different characters and lengths by the successive application of (1.04) (Fig. 2). One starts

by computing  $z_{n-1}$  from  $z_n$ , then  $z_{n-2}$  from  $z_{n-1}$ , and so on until finally  $z_1$  is found. The calculation is complicated and tiresome and might better be replaced by a geometrical method<sup>1</sup>.

### § 3 WAVE IMPEDANCE $W_0$ OF FREE AIR

The theoretical deduction of the quantities  $W$  and  $\gamma$  for any medium is always accomplished in essentially the same way by starting from the equation of motion for the vibrating medium and from the equation of continuity (conservation of mass). We shall now consider the simplest case, viz., that of free air without taking into account the effects of damping.

The equation of motion is found by applying Newton's

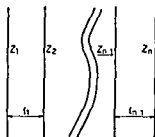


Fig. 2

Successive computation of the impedance of a multilayer system

equation (force = mass  $\times$  acceleration) to a thin layer of air of thickness  $dx$

$$-\frac{\partial p}{\partial x} = \rho_0 \frac{\partial v}{\partial t}, \quad (107)$$

in which  $\rho_0$  = density. The equation of continuity is

$$-\frac{\partial v}{\partial x} = \frac{1}{\rho_0} \frac{\partial p}{\partial t} = \frac{1}{h_0} \frac{\partial p}{\partial t}, \quad (108)$$

in which

$$h_0 = \frac{dp}{d\rho/\rho_0}$$

Eliminating  $v$  by differentiating (107) with respect to  $x$

<sup>1</sup> See e.g. Feldtkeller Vierpoltheorie and Chapter VI § 7 Fig. 6"

and (1.08) with respect to  $t$  and equating the expressions for  $\partial^2 v / \partial x \partial t$  thus obtained, gives a differential equation for  $p$

$$\frac{\partial^2 p}{\partial x^2} = \frac{\rho_0}{K_0} \frac{\partial^2 p}{\partial t^2}. \quad (1.09)$$

Since we expect a solution of the form  $p = A \exp(j\omega t) \exp(-\gamma_0 x)$  we may put:  $-\partial/\partial x = \gamma_0$  and  $\partial/\partial t = j\omega$ , so that (1.09) reduces to

$$\gamma_0^2 = -\frac{\rho_0}{K_0} \omega^2,$$

from which we get

$$\gamma_0 = \pm j\omega \sqrt{\rho_0/K_0}. \quad (1.10)$$

By comparing (1.10) with (1.01) we see that the physical interpretation of the constant  $\sqrt{K_0/\rho_0}$  is the velocity of propagation  $c_0$  of sound waves in free air, the plus (minus) sign for  $\gamma_0$  having to be taken for waves travelling in (opposite to) the direction of the positive  $x$ -axis. Substituting this value of  $-\partial/\partial x$  together with  $j\omega$  for  $\partial/\partial t$  in either equation (1.07) or (1.08) yields for the wave impedance

$$p/v = W_0 = \sqrt{K_0 \rho_0} = \rho_0 c_0. \quad (1.11)$$

From (1.11) we learn that the wave impedance is real. By inserting the known values of  $\rho_0$  and  $c_0$  at room temperature it appears that  $W_0$  has the approximate value of  $420 \text{ kg m}^{-2} \text{ sec}^{-1}$  (42 cgs).

If plane waves from the air impinge upon a wall of specific impedance  $z$ , reflection will take place; the ratio of the pressure of the reflected wave to that of the incoming wave just before the reflecting boundary is given by (1.03), which runs in the present notation

$$r = \frac{p_r}{p_i} = \frac{z - W_0}{z + W_0}. \quad (1.12)$$

We shall call this ratio the complex reflection coefficient. By squaring the absolute value one obtains the reflection coefficient for the energy, which is complementary to the absorption coefficient:

$$a_0 = 1 - \left| \frac{p_r}{p_i} \right|^2 = 1 - \left| \frac{z - W_0}{z + W_0} \right|^2, \quad (1.13)$$

the index zero being added because this coefficient applies only to normal incidence

What is said of free air in this section will be shown to be of quite general validity. The equations of continuity and motion may in many cases be written down in exactly the same form (107 and 108) although the constants  $\rho$  and  $k$  will have a different meaning they will be dependent on several more or less elementary properties of the medium and finally will have to be considered as complex quantities

In order to avoid confusion all symbols relating to free air will when necessary be provided with an index zero as was done in this section  $\rho_0$   $k_0$   $\gamma_0$   $W_0$   $c_0$

A very important way of application of absorbing materials is the direct fixing of a layer of such material to a rigid back wall. In this case the impedance at the front side was shown to be (cf § 2)

$$z = W \coth \gamma l \quad (100)$$

Substituting the general expressions for  $W$  and  $\gamma$  of (110) and (111) yields

$$z = \sqrt{k\rho} \coth j\omega l \sqrt{\rho/k} \quad (114)$$

as a general expression for the impedance of any layer backed by a rigid wall. We have to make an exception for some porous flexible layers. The question of the computation of  $k$  and  $\rho$  will be considered in § 7 to II § 6

#### § 4 GEOMETRY IN THE COMPLEX PLANE

The understanding of such formulae as (100) and (111) may be facilitated by plotting the function  $\coth \gamma l$  and other complex functions  $z$  of  $\omega$  in the complex plane. If we allow  $\omega$  to assume all values from 0 to  $\infty$  the function under consideration follows a certain contour in the complex plane. This curve as a rule appeals more directly to our imagination than does an analytical formula. The point is to separate the real from the imaginary part so that  $z$  takes the form  $z(\omega) = x(\omega) + jy(\omega)$  and to plot  $z$  in the plane with  $x$  and  $y$  (belonging to the same value of the parameter  $\omega$ ) as coordinates

For example the function  $z = 1 - j\omega$  is a straight line startin.,

at the point  $x=1$  of the real axis and going downwards (Fig. 3);  $z = \exp(j\omega) = \cos \omega + j \sin \omega$  is the circle with unit radius.

Multiplying a complex number by  $\exp(j\omega)$  means turning it

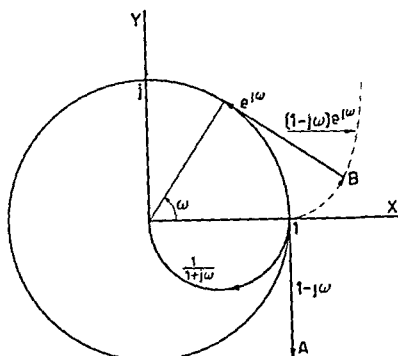


Fig. 3

Complex representation of the circle involute

round the origin through an angle  $\omega$ . So by multiplying the point A (Fig. 3) by  $\exp(j\omega)$  we come to the point B and it is obvious,

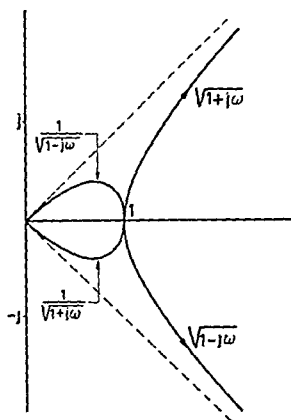


Fig. 4

Complex representation of a hyperbola and a lemniscate

that B lies on the involute of the circle; hence  $z = (1 - j\omega) \exp(j\omega)$  is the circle involute.

The function  $z = \sqrt{1 + j\omega}$  is represented by a rectangular hyperbola (Fig. 4), which may be proved as follows. Put  $z = x +$

$xy = \sqrt{1 + j\omega}$  and square  $x^2 - y^2 + 2jxy = 1 + j\omega$ . Separating the real from the imaginary parts shows us that  $x^2 - y^2 = 1$  and this is the common formula for the rectangular hyperbola. Further  $2xy = \omega$ , now since  $\omega$  is always positive  $x$  and  $y$  have the same sign. The function  $\sqrt{1 + j\omega}$  is represented by the upper branch of the hyperbola, the lower branch being represented by  $\sqrt{1 - j\omega}$ . The generalization  $z = \sqrt{1 \pm jf(\omega)}$ , where  $f(\omega)$  is an arbitrary real function of  $\omega$ , leads to the same hyperbola but the  $\omega$  scale is changed. This remark is one of a general validity, we may always pass on to a new  $\omega$ -scale on the same curve by substituting  $f(\omega)$  for  $\omega$ .

Inverting a complex number  $z = M \exp(j\varphi)$  gives  $\frac{1}{z} = \frac{1}{M} \exp(-j\varphi)$ , so the modulus is inverted, and the sign of the argument is the opposite of the original one. As the lemniscate is the inverse curve of the hyperbola the former is represented by the functions  $(1 \pm j\omega)^{-\frac{1}{2}}$ .

By inverting a straight line, one obtains, as is well known from elementary geometry, a circle. In Fig. 3 the inversion of the half line  $1 + j\omega$  is drawn as a half circle running from the point  $x = 1$  on the real axis towards the origin.

More examples illustrating the simple geometrical representation of functions by contours and vice versa may easily be obtained.

#### § 5 GEOMETRICAL REPRESENTATION OF $\coth \gamma l$

In Fig. 5 the function  $\coth \gamma l$  is plotted with the aid of<sup>1</sup> the formula

$$\coth \gamma l = \coth(\alpha + j\beta)l = \frac{\sinh 2\alpha l - j \sin 2\beta l}{\cosh 2\alpha l - \cos 2\beta l} \quad (1.15)$$

for constant values of  $\alpha$  and  $\beta$ . It looks like a logarithmic spiral. And indeed for large values of the argument,  $\coth \gamma l$  is approximated by a logarithmic spiral. We arrive at this result, because for large values of  $\gamma l$ ,  $\coth \gamma l \sim 1 + 2 \exp(-2\gamma l)$ .

Leaving aside for the moment the shift over the distance 1 in the direction of the real axis, the function

<sup>1</sup> J. Rübner: *Nomograms of Complex Hyperbolic Functions*, p. 25. Copenhagen 1947.



$$2 \exp(-2 \gamma l) = 2 \exp(-2 \alpha l) \cdot \exp(-2 j \beta l)$$

represents a spiral with modulus  $M = 2 \exp(-2 \alpha l)$  and argument  $\varphi = -2 \beta l$ . Hence the relation between  $M$  and  $\varphi$  is

$$M = 2 \exp\left(\frac{\alpha}{\beta} \varphi\right),$$

and this is, for a constant value of  $\alpha/\beta$ , the usual formula for

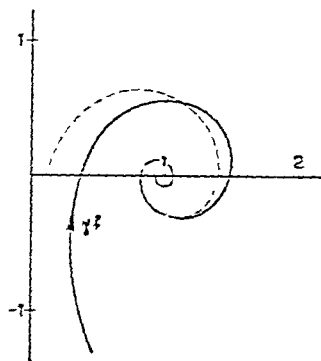


Fig. 5

Complex representation of  $\coth \gamma l$

the logarithmic spiral in polar coordinates. It is indicated by a dashed curve in Fig. 5. In the same way it can be shown that  $\tanh \gamma l$  converges towards the logarithmic spiral  $1 - 2 \exp(-2 \gamma l)$ .

The geometrical interpretation of the constant  $\alpha/\beta$  is this,

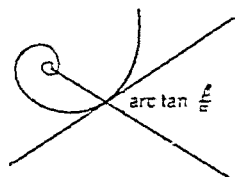


Fig. 6

The slope of  $\coth \gamma l$

that it is the tangent of the "slope" of the spiral, which is constant along the logarithmic spiral (Fig. 6). The greater  $\alpha$ , the greater the slope, and the more rapidly the function converges towards its apex. Figs. 7 and 8 represent two cases with slopes 1 and 0.1 respectively.

For an arbitrary medium  $\alpha$  and  $\beta$  are both functions of  $\omega$  and so is the slope  $\alpha/\beta$ . Taking  $l$  as a constant,  $\gamma l$  varies because of the variations in  $\alpha$  and  $\beta$  with  $\omega$ . In this general case we get a

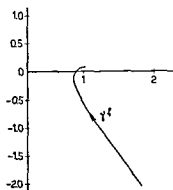


Fig 7

A coth with slope 1  
strong damping

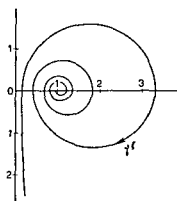


Fig 8

A coth with slope 0.1,  
weak damping

modification of the logarithmic spiral with a slope varying along the curve. In Fig 9 the case  $\alpha/\beta = \text{const}/\omega$  is illustrated, the

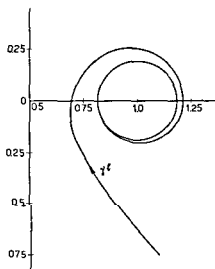


Fig 9

A coth with a slope inversely proportional with frequency

slope approaches the value of zero for large values of  $\omega$  the contour approaches to an asymptotic circle

Multiplication of  $\coth \gamma l$  by a complex number  $W = M \exp j\varphi$  (cf. 1.05) means enlarging the contour by a factor  $M$  and rotating it through an angle  $\varphi$  around the origin, as in the example of the circle involute. Multiplication by a complex number  $W$ , which in itself is a function of  $\omega$ , is accomplished by applying this process for each point of the spiral, taking together corresponding points (for the same value of  $\omega$ ) of the multiplier  $W$  and  $\coth \gamma l$ . If  $W$  does not run fast through the diagram, something resembling a spiral may still be seen; if, on the other hand,  $W$  runs fast, the spiral appearance may be lost, and a kind of damped sine curve with curved axis may result, this curved axis being the contour of  $W$ .

#### § 6 GEOMETRICAL REPRESENTATION OF FORMULA (1.12)

We shall now give a geometrical interpretation of (1.12)

$$r = \frac{z - W_0}{z + W_0}. \quad (1.12)$$

We plot  $z$  in a complex plane and also plot the points  $W_0$  and  $-W_0$  on the real axis.  $z - W_0$  is the vector going from  $W_0$  to  $z$ ;  $z + W_0$  is the vector going from  $-W_0$  to  $z$ , and the complex reflection coefficient is the quotient of these two vectors. Now in general the quotient of two vectors

$$\frac{M_1 \exp(j\varphi_1)}{M_2 \exp(j\varphi_2)} = \frac{M_1}{M_2} \exp\{j(\varphi_1 - \varphi_2)\}$$

is a vector with an absolute value equal to the ratio of the *absolute* values of the two original vectors and an argument equal to the differences of the arguments.

Hence the absolute value of  $p_r/p_i$  is the ratio of the two vectors, shown in Fig. 10, its argument, i. e., the phase angle by which  $p_r$  is ahead of  $p_i$ , is the angle  $\Delta$  in fig. 10<sup>1</sup>.

The absolute value of  $r$  and therefore, the value of the absorption coefficient  $a_0 = 1 - |r|^2$  remains constant along contours for which  $M_1/M_2 = \text{constant}$  and from elementary geometry we know that these contours are circles. For 100 % absorption  $M_1 = 0$ , and the circle reduces to the point  $W_0$  (Fig. 11). On the other hand

<sup>1</sup> In accordance with usage in electrotechnics we denote the real part of  $z$  by  $R$ , its imaginary part by  $X$ ,  $Y$  being reserved for the admittance  $Y = 1/z$ .

we also know from elementary geometry that the locus of point  $z$  with the same value of  $\Delta$  is also a circle, now going through the point  $W_0$  and  $-W_0$  (Fig 11) Moreover the two sets of circles

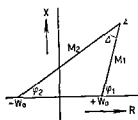


Fig 10

Modulus and argument of the complex reflection coefficient  $r$  (equation 1.12) in the  $z$  plane

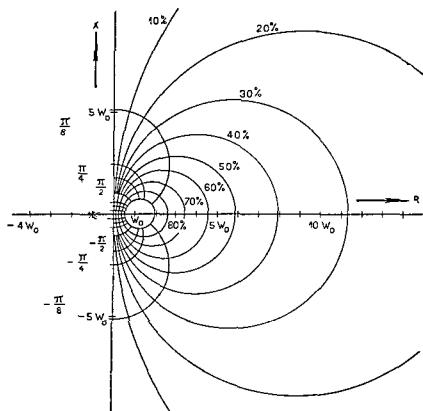


Fig 11

The complex reflection coefficient  $r$  in the impedance plane, phase jump  $\Delta$  and absorption coefficient  $a_0$ , the circle diagram

for constant  $a_0$  and constant  $\Delta$  intersect orthogonally. This may be proved from the general property of transformations in the complex plane which are known to be always conformal, i. e., that angles of intersection are not altered. Now since in the  $r$ -plane the contours of constant  $\Delta$ , which are the radii, intersect orthogonally the contours of constant  $|r|$ , which are circles around the origin, the same must be true for the two sets of contours of  $\Delta$  constant and  $|r|$  constant in the  $z$ -plane which is obtained by the transformation (1.12). The same result may be obtained in a more direct but more tiresome way by calculating the quantities  $\left(\frac{\partial z}{\partial a_0}\right)_\Delta$  and  $\left(\frac{\partial z}{\partial \Delta}\right)_{a_0}$  from (1.12), and observing that they differ only by an imaginary factor, which means that the two directions  $a_0$ -constant and  $\Delta$ -constant intersect orthogonally.

The graphical representation of Fig. 11 is of very great value in two respects. If a theoretical expression for  $z$  as a function of frequency is obtained and the corresponding contour is plotted in Fig. 11. one sees at a glance the dependence of the absorption coefficient  $a_0$  and the phase jump  $\Delta$  upon frequency. Conversely, when, as is the case with most stationary wave methods,  $a_0$  and  $\Delta$  are measured, we have at our disposal a practical means of finding the corresponding value of  $z$  by a graphical method and without any further computation.

#### § 7 WAVE IMPEDANCE OF IMPERVIOUS MEDIA WITH INTERNAL FRICTION

We shall now extend our considerations of § 3 to the case in which internal damping occurs. As soon as this occurs the density variation is no longer in phase with the pressure variation and the quantity  $dp/d\rho$  is no longer a pure real number. Now by its definition the "compression modulus"  $K$  is  $\rho dp/d\rho$  and by  $K_r$  we shall denote its real part. The dynamical value of  $K$  may then be written

$$K = K_r (1 + j \tan \delta). \quad (1.16)$$

in which  $\delta$ , the loss angle, denotes the phase difference between  $p$  and the variation of  $\rho$ . This loss angle is always small and as our own measurements and those of other investigators have

shown, this  $\delta$  is to a reasonable degree independent of  $\omega$ , thus greatly simplifying the problem.  $K_r$ , however, has proved to be dependent on  $\omega$ , at least at very low frequencies.

As before (§ 3) the equation of motion is

$$-\frac{\partial p}{\partial x} = \rho \frac{\partial v}{\partial t} \quad \text{or} \quad \gamma p = j\omega \rho l,$$

restricting ourselves to a single travelling wave in the direction of the positive  $x$  axis. The equation of continuity is

$$-\frac{\partial v}{\partial x} = \frac{1}{K} \frac{\partial p}{\partial t} \quad \text{or} \quad \gamma v = \frac{j\omega}{K} p$$

from which we immediately derive

$$\gamma = j\omega \sqrt{\frac{\rho}{K}} \quad , \quad W = \sqrt{\rho K} \quad (117)$$

As  $\delta$  is small we may put approximately,

$$\sqrt{K} = \sqrt{K_r} \left(1 + j \frac{\delta}{2}\right) \quad , \quad \frac{1}{\sqrt{K}} = \frac{1}{\sqrt{K_r}} \left(1 - j \frac{\delta}{2}\right)$$

in which case

$$\gamma = \alpha + j\beta = \alpha + j \frac{\omega}{c} = j\omega \sqrt{\frac{\rho}{K_r}} \left(1 - j \frac{\delta}{2}\right)$$

which means that the velocity of propagation amounts to

$$c = \sqrt{K_r / \rho},$$

so that

$$\gamma = j \frac{\omega}{c} \left(1 - j \frac{\delta}{2}\right) \quad \text{and} \quad W = \rho c \left(1 + j \frac{\delta}{2}\right) \quad (118)$$

and the impedance of a layer of thickness  $l$  backed by a perfectly hard wall is

$$z = W \coth \gamma l = \rho c \left(1 + j \frac{\delta}{2}\right) \coth \left\{ j \frac{\omega l}{c} \left(1 - j \frac{\delta}{2}\right) \right\} \quad (119)$$

(119) is a special form of the general expression (114)

We see that the acoustical behaviour of impervious materials can be predicted from the values of their stiffness  $K_r$ , their density  $\rho$  and their loss angle  $\delta$ .

As  $\alpha/\beta = \delta/2$  is not dependent on  $\omega$ , the  $\coth$  converges to a logarithmic spiral and as  $\delta$  is small the slope is also small. More

over its apex lies at the point  $\rho c (1 + j\delta/2)$ , that is just a little above the real axis. Comparing this case with that of undamped propagation we see that there are two corrections due to the occurrence of  $\delta$ . The correction of  $W$  is only of slight importance, the correction of  $\gamma$  is more important as it gives rise to the creation of a spiral. The impedance of a layer of finite thickness is, therefore, pretty well illustrated by the curve of Fig. 8 and

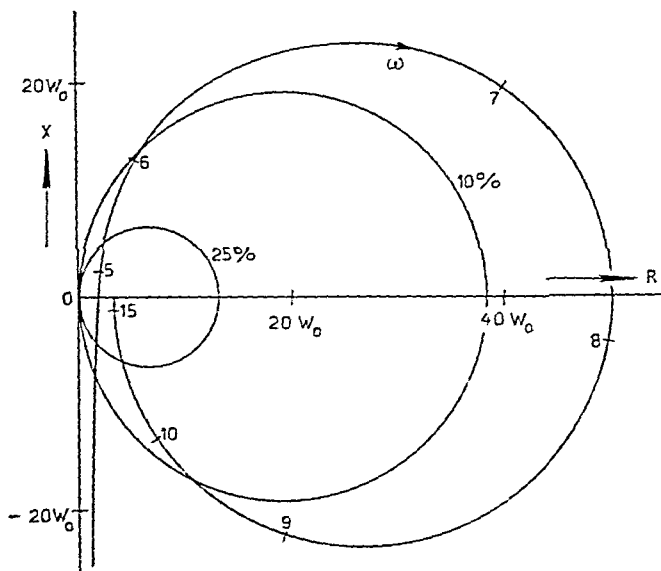


Fig. 12  
Impedance contour of a sample of cellular rubber,  
frequencies added along the contour in 100 Hz<sup>1</sup>

in our subsequent discussion we shall ignore the deviation of  $W$  from the "undamped" value  $\rho c$ .

An example is given in Fig. 12 where the impedance is shown for a sample of cellular rubber with completely closed cellular holes<sup>2</sup>.

<sup>1</sup> In order to avoid misunderstanding we want to make clear that e.g., in the point designated by 7 the frequency is 700 Hz (cycles/sec), but that  $\omega = 2\pi \cdot 700$  radians/sec.

<sup>2</sup> C. W. Kosten and C. Zwicker, *Physica*, 8 (1941) 933.

Without entering into the description of the method of measurement something must be said about how Fig 12 and the following figures of impedance contours have been obtained. Most of the experimental work has been carried out with an older type of interferometer with a rather small accuracy, especially as to the measurement of the phase jump  $\Delta$ . For better understanding the results have been smoothed without changing the character of the contour. The true measuring points may be found in the original publications. The numbers added on the impedance curve are frequencies in 100 Hz.

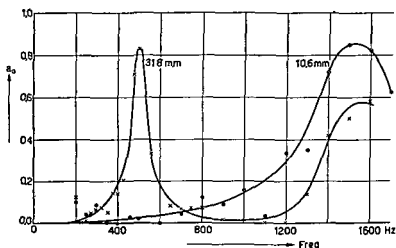


Fig 13

Absorption by cellular rubber strong selective absorption

After each turn of the  $z$  contour it comes into the neighbourhood of the point  $W_0$ , giving rise to a high absorption coefficient over a relatively small range of frequencies, these absorption peaks being separated from each other by large ranges with only poor absorption (Fig 13, true values)

Such resonance peaks occur in the neighbourhood of those frequencies for which  $\coth \gamma l$  is real. From (1.15) we conclude that this is the case when

$$\sin 2\beta l = 0, \quad \text{i.e.} \quad 2\beta l = n\pi$$

(resonance for  $n$  odd, antiresonance for  $n$  even). The resonance frequencies can be computed with the aid of  $\beta = \omega/c$ , giving



$\omega = n\pi c/2l$ . The first resonance ( $n=1$ ) lies at  $\omega = \pi c/2l$ , the second ( $n=3$ ) at  $\omega = 3\pi c/2l$ . Expressed in the wave length  $\lambda = 2\pi c/\omega$ , the resonances are found at:  $\lambda = 4l, 4l/3, 4l/5$ , etc. The distribution of the velocity amplitude is illustrated in Fig. 14 for the three lower resonances. The ratio between the frequencies of the first and the second resonance was well established in our measurements on cellular rubber (Fig. 13, curve for a layer of 31.8 mm thickness).

It should be mentioned here that the constant  $K_r$  cannot be deduced from its static value, the dynamic value being several times greater. If no mechanical measurements are available  $K_r$ ,

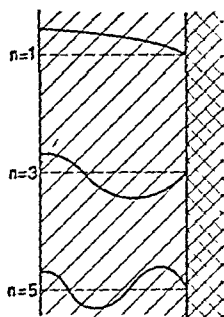


Fig. 14

Velocity amplitude at the first three resonance frequencies

may be computed from the first resonance frequency, which is:

$$\omega = \frac{\pi}{2l} \sqrt{\frac{K_r}{\rho}}.$$

An easy way of determining the loss angle from the acoustical measurements is found by applying (1.15) to the first anti-resonance. Then  $\sin 2\beta l = 0$ ;  $\cos 2\beta l = 1$  and

$$\coth \gamma l = \coth \alpha l \approx 1/\alpha l.$$

Now from (1.18)  $\alpha = \omega\delta/2c$  and in the first anti-resonance

$$l = \pi c/\omega, \text{ hence } \coth \gamma l = 2/\pi\delta.$$

The corresponding impedance is from (1.16)

$$z_{\text{antires.}} = \rho c \, 2/\pi\delta \quad (1.20)$$

and  $\delta$  can now be computed from the measured value of  $z$  in the first anti resonance. The values of  $\delta$  so determined agreed well with those obtained in a purely mechanical way.

We may also deduce a simple formula for  $z$  in the case of resonance. Then  $\sin 2\beta l = 0$ ,  $\cos 2\beta l = -1$ , and from (1.15)

$$\coth \gamma l = \tanh \alpha l \approx \alpha l,$$

and with  $l = \pi c / 2 \omega$ ,  $\alpha = \omega \delta / 2 c$  we obtain

$$z_{\text{res}} = \rho c \tau \delta / 4 \quad (1.21)$$

which formula may also serve for the calculation of  $\delta$ . An accurate value for  $z_{\text{res}}$  may readily be found from (1.13), since  $a_0$  is known with a high precision.

#### § 8 THE GENERAL EQUATIONS GOVERNING THE WAVE PROPAGATION IN POROUS MATERIAL WITH RIGID FRAME

We shall discuss the behaviour of porous materials for the time being with a rigid frame and direct our attention to the motion of the air.

The first difficulty is the definition of the velocity of the air in the material. Whereas in an infinitesimal volume only one pressure  $p$  exists the velocity changes from point to point in the pores owing to their irregularity. Let us define the velocity  $v$  in a certain direction therefore by the volume of air passing through a unit of surface perpendicular to that direction i.e. by the velocity of specific volume displacement. Denoting the porosity (or cavity factor) by  $h$  it will be clear then, that for a given velocity gradient  $\partial v / \partial x$  a  $1/h$  times larger  $\partial p / \partial t$  will be found than in free air. Hence the equation of continuity may be written in close analogy to the preceding cases as

$$-\frac{\partial v}{\partial x} = \frac{h}{\rho_0} \frac{d\rho}{dp} \frac{\partial p}{\partial t}$$

This time the quantity  $\rho_0 dp / d\rho$  need not be real. Leaving viscosity effects aside for the moment there are two limiting cases in which  $\rho$  and  $p$  vibrate in phase with each other. In the first limit the transmission of heat to and from the solid frame is so

rapid that the enclosed air is kept at constant temperature (isothermal case, as was supposed in the old theory of Newton). In air at constant temperature a fixed functional relation between  $p$  and  $\rho$  exists (Boyle's law). In the other limit the transmission of heat is so slow that the air vibrates adiabatically (Laplace's supposition). Then again, a fixed functional relation exists between  $p$  and  $\rho$  (Poisson's law). In both cases  $dp/d\rho$  is real. In general, however, there will be heat exchange with finite speed, so that, during the compression phase, the air is hotter than the solid frame, and during the expansion phase it is colder. Hence for the same value of  $p$  the density is smaller in the compression phase than in the expansion phase (Fig. 15);  $\rho$  and  $p$  are not in

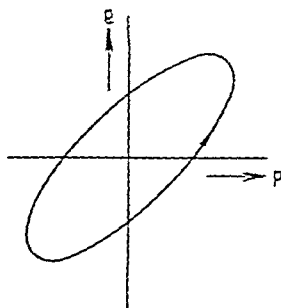


Fig. 15

Losses in the stiffness, hysteresis

phase,  $dp/d\rho$  and also the modulus  $\rho_0 dp/d\rho$  are complex quantities.

It seems unlikely at first sight that viscosity effects might influence the modulus (stiffness) of the air, since the modulus describes the behaviour of air during compression and expansion, which air may be supposed to be motionless as a whole. An important group of absorbent materials is formed by the acoustic porous plasters. Now suppose that part of the holes in the materials can only be entered through one narrow pore. A time lag between  $p$  and the corresponding variation in  $\rho$  will now be found due to the "RC-time" of these side holes, which can only be pumped up with difficulty. Therefore, phase difference between  $p$  and  $\rho$  cannot be put down with certainty either to defective heat exchange or to the latter side holes. Such holes may occur very easily in the interior of the macroscopic globules of which a

plaster consists. Of course this effect will be present to some degree in all practical materials.  $\frac{\rho_0}{h} \frac{dp}{d\rho}$  will be denoted by  $K$ , by which, for a travelling wave, the equation of continuity again attains its universal form

$$\gamma v = \frac{j\omega}{K} p, \text{ in which } K = \frac{\rho_0}{h} \frac{dp}{d\rho} \approx \frac{K_0}{h} \quad (122)$$

The equation of motion for the enclosed air is

$$-\frac{\partial p}{\partial x} = \frac{k}{h} \rho_0 \frac{\partial v}{\partial t} + \sigma v \quad (123)$$

As compared to the case of free air we observe three changes viz the appearance of the *structure constant*  $k$ , the *porosity*  $h$ , and the *resistance constant*  $\sigma$ . The appearance of the latter will be clear from the fact that we have to take account of the viscosity. For the steady flow state the term in  $\partial v / \partial t$  cancels out so that then,  $\sigma$  is defined as the ratio of pressure gradient and velocity of volume displacement.

There are several effects by which the density of the air seems to be enlarged, giving rise to the factor  $k/h > 1$ . This factor has been split up into two parts  $k$  and  $1/h$  the latter describing the rather elementary influence of the porosity, whereas  $k$  comes mainly from two effects, the structural properties of the material playing the most important rôle, this is the reason for calling  $k$  the *structure factor*. Supposing the porosity  $h$  to be decreased without changing the structure, the pressure gradient, needed for the acceleration of the air, should obviously be taken  $1/h$  times greater in order to obtain the same velocity of volume displacement  $v$ .  $k$  contains a factor lying between 1 and  $4/3$ , because, as will be shown in chapter II, owing to the internal friction of the air a term between 0 and  $\rho_0/3$  is apparently added to the density  $\rho_0$ . The influence of the structure may be elucidated by the following examples.

Imagine a structure like that in Fig 16a with pores placed inclined with respect to the macroscopical pressure gradient. Along these pores the pressure gradient is only  $\cos \theta$  times that in pores having the same direction as the macroscopical pressure gradient. The acceleration of the enclosed air has in its turn

a component in the direction of the macroscopical pressure-gradient, which again contains the factor  $\cos \theta$ . For this model, therefore, the structure factor  $k$  contains the factor  $1/\cos^2 \theta$ . Should the orientation of the pores be distributed at random, then the resulting value of this factor amounts to 3.

Again, consider a medium after the model of Fig. 16b, provided with lateral cavities located beside the air current in the main pores. Notwithstanding the application of a pressure-gradient the air in the lateral cavities remains largely at rest, thus acting as if it were heavier than the air in the stream lines and giving rise to a factor  $k$  greater than unity. In other words as far as this effect is concerned: since the pressure-gradient only succeeds in accelerating the air in the main pores, leaving the air in the side holes at rest, the porosity *in the equation of motion* should

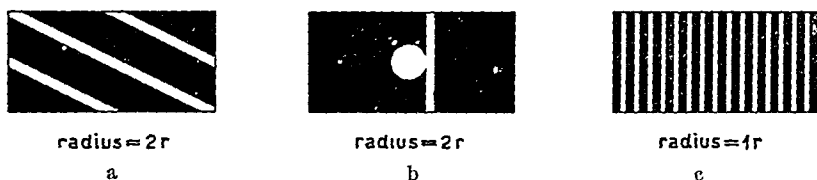


Fig. 16

To the concept of the structure factor. Three models having the same porosity  $h$  and the same resistance  $\sigma$ , but different structure factor  $k$

be taken as the air in the *main pores* per unit of volume, i.e. as  $h/k$ .  $k$ , therefore, is equal to the ratio of the total air contents to that of the main pores and is essentially greater than unity.

Yet another reason for the occurrence of  $k$  is the possible vibration of small parts of the solid skeleton, which also tends to enlarge the apparent inertia of the air. Although it cannot be denied that in principle this effect may occur, there are several reasons for warning the reader against over-estimating of this effect. In most cases (the more rigid absorbent materials) the effect is small indeed and the main contribution to  $k$  is due to the structure (e.g.,  $k = 3$ ). In the case of very flexible materials the motion of the solid material may be considerable; in this case, however, a more adequate mathematical treatment can be given in which the effect of the internal forces between the air and the structure is correctly taken into account (see Chapter III). As we restrict

ourselves in this section to rigid frames this effect may be left out of consideration.

The factor mentioned above between 1 and  $4/3$  is a function of  $\omega$ . Denoting it by  $k_\omega$  we may split up  $k$  into the factors  $k_\omega$  and  $k_s$ , where  $k_s$  now is fully and exclusively determined by the internal structure of the material.

It is hardly possible to calculate  $k$  beforehand from a description of the sample. Nor is it possible to find it experimentally in any other way than by acoustic measurements. This means that we cannot predict the acoustic behaviour of a porous material quantitatively from such simple quantities as its porosity and air resistance. According to experiments the structure factor  $k$  normally lies between 3 and 7, but it may attain any value exceeding 1.

Introducing the complex quantity  $k\rho_0/h + \sigma/j\omega$  as the apparent density,  $\rho$  the equation of motion for a travelling wave is also brought into the universal form

$$\gamma p = j\omega \rho l \quad \text{in which} \quad \rho = k\rho_0/h + \sigma/j\omega \quad (124)$$

and as before we find for  $\gamma$  and  $W$

$$\gamma = j\omega \sqrt{\rho/K} \quad W = \sqrt{K\rho}$$

Putting  $\rho = \frac{k}{h} \rho_0 (1 - j \tan \delta)$  in which

$$\tan \delta_r = \sigma h / \omega k \rho_0 \quad \text{and} \quad K = K_r (1 + j \tan \delta_K),$$

we find for the impedance of a layer of thickness  $l$

$$z = \sqrt{\frac{k}{h} \rho_0 K_r} \sqrt{(1 - j \tan \delta_r) (1 + j \tan \delta_K) \coth \left[ j\omega l \sqrt{\frac{k\rho_0}{hK_r}} \sqrt{\frac{1 - j \tan \delta_r}{1 + j \tan \delta_K}} \right]} \quad (125)$$

## § 9 THE RESISTANCE CONSTANT $\sigma$

According to Poiseuille's law the velocity of volume displacement through a conduit with radius  $r$  in the direction of the positive  $x$  axis for steady flow is

$$v = - \frac{-r^4}{8\eta} \frac{\partial p}{\partial x},$$

in which  $\eta$  denotes the viscosity of air. If there are  $n$  parallel passages distributed over a cross section of unit area the amount is  $n$  times greater, and, as the porosity  $h$  equals  $n\pi r^2$ ,

$$v = -h \frac{r^2}{8\eta} \cdot \frac{\partial p}{\partial x}.$$

In materials with pores inclined to the  $x$ -axis or with pores with side holes (Fig. 16),  $v$  is decreased by the factor  $k$ , so that finally

$$v = -\frac{h}{k} \frac{r^2}{8\eta} \frac{\partial p}{\partial x},$$

from which follows

$$\sigma = \frac{k}{h} \frac{8\eta}{r^2}. \quad (1.26)$$

This is the value of  $\sigma$  for a stationary current with a parabolic distribution of the velocity in the conduits.

The expression (1.26) will also be used for materials not having identical cylindrical pores throughout the material. In such cases  $r$  has to be looked upon as a kind of mean value, defined by (1.26).

In the case of rapid oscillations the character of the current changes. Only the outer layers of air are affected by the rigid walls; the inner parts of the pores, however, are swinging to and fro as a whole, the velocity being only controlled by its mass. In the limiting case of only a thin layer of air along the walls being influenced by friction, Helmholtz' value for  $\sigma$  is to be applied<sup>1</sup>

$$\sigma = \frac{k}{h} \frac{1}{r} \sqrt{2\eta\omega\rho_0}. \quad (1.27)$$

As pointed out by Crandall (l.c.) the thickness of the layer which is hindered in its motion by the walls is of the order  $\sqrt{\eta/\omega\rho_0}$ , and by a thin layer we mean a layer for which this value is small compared with  $r$ . So the conditions depend upon whether the dimensionless quantity  $\mu = \sqrt{\omega\rho_0 r^2/\eta}$  is great or small compared with unity ( $\mu \gg 1$  Helmholtz,  $\mu \ll 1$  Poiseuille).

---

<sup>1</sup> I. B. Crandall, *Theory of vibrating systems and sound*, App. A., London 1927.

$\mu^2$  is comparable with Reynolds' number in hydrodynamics. Both quantities are a measure for the relative importance of inertia forces as compared with viscous forces. Their form is largely analogous ( $Re = \rho v d / \eta$ )

Now, which of the two formulae (126) or (127) will have to be applied in the case of absorbent porous materials? Or will it be necessary to deal with an intermediate case giving rise to more complicated mathematics? The answer to these questions is that all cases may occur on occasion.

The limiting cases will be dealt with in a correct way in II § 4. An approximate (?) expression for  $\sigma$  in the intermediate frequency range will be given in II § 2.

We are fortunate in that the conditions for the two limiting cases, considered here, approximately coincide with those for the two limiting cases of the compression modulus  $K$  mentioned in § 8, and such that Poiseuille's law applies to the nearly isothermal case, while Helmholtz' law holds in the nearly adiabatic case. These coincidences are due to the close connection existing between the viscosity and the thermal conductivity of a gas, which, according to the kinetic theory, are proportional to each other, and, in fact, are both linked up with the mean free path of the molecules. At the same moment, therefore, that the walls cease to influence the motion of the gas current in the middle of the conduit, they cease to exchange heat with it.



## CHAPTER II

### MORE DETAILED THEORETICAL CONSIDERATIONS CONCERNING VISCOUS AND THERMAL EFFECTS IN POROUS MEDIA

#### § 1 SOUND PROPAGATION IN CYLINDRICAL TUBES AND PORES

In §§ 8 and 9 of Chapter I several problems were touched upon that arise when studying the sound propagation through porous rigid media. The behaviour largely depends upon whether low or high frequencies are involved. At extremely low frequencies the air resistance and the compression modulus have their static value, the real density is increased by 33 %; even this increased density is, however, negligible in comparison with the imaginary part of the complex density,  $\sigma/j\omega$ . At extremely high frequencies it is the density which has its normal value; now the air resistance is "abnormal" (Helmholtz' value) and the compression is adiabatic.

We shall now proceed to the case of intermediate frequencies. A correct approach to the solution will be made taking Kirchhoff's theory as a basis (§ 4). We then no longer consider the case of *extremely* low (high) frequencies, but that of simply low (high) frequencies, confining ourselves furthermore to the simple case of the propagation in cylinders. In that case argument and magnitude of the complex quantities  $K$  and  $\rho$ , and therefore of  $W$  and  $\gamma$ , are slightly changed as compared with the corresponding expressions at *extremely* low (high) frequencies, while the mathematics are still relatively simple. In Kirchhoff's theory viscous forces and thermal conductivity are taken into account at the same time. It turns out that the correction factor of  $K$  only contains the thermal effect, that of  $\rho$  only the viscous one. At first sight this is very plausible although we do not see how this can be proved beforehand from the differential equations underlying Kirchhoff's theory. If, however, we assume directly

at the beginning that we may omit the viscous effect when the complex quantity  $K$  is to be calculated and on the other hand the thermal conductivity may be disregarded when calculating  $\rho$ , the derivation of  $K$  and  $\rho$  can be given comparatively simply. Moreover we are then in a position to derive expressions for  $K$  and  $\rho$  for all intermediate frequencies and not only for low and high frequencies, from which of course, corresponding expressions for  $W$  and  $\gamma$  are easily found, also for any frequency.

For convenience of the reader it seems most practical to give the latter derivation first, accepting the necessary assumptions for the time being. The derivation of  $\rho$  (§ 2) is essentially that of Crandall<sup>1</sup>, repeated here for convenience. The derivation of  $K$  will be given taking Kirchhoff's correct theory as a basis (§ 3).

In order to avoid the assumption that  $K$  and  $\rho$  can be computed separately, we shall then give the complete derivation in which viscous and thermal effects are taken into account at the same time (§ 4). We have to confine ourselves then, however, to low and high frequency resp. This derivation is given for completeness but can be omitted by the reader, who is not interested in all details.

## § 2 THE AIR DENSITY IN CYLINDERS DISREGARDING THERMAL EFFECTS

The derivation is analogous to that of Poiseuille's law except for the introduction of an inertia term. The total driving force on an annular ring of volume  $2\pi r dr dx$  is  $-(\partial p / \partial x) dx 2\pi r dr$ . The actual velocity is a function of the radius  $r$ , giving rise to a viscous force on the annular ring

$$\frac{\partial}{\partial r} \left( -2\pi r \eta dx \frac{\partial v}{\partial r} \right) dr$$

Finally an inertia force has to be taken into account

$$j\omega \rho_0 2\pi r dr dx$$

---

<sup>1</sup> I. B. Crandall *Theory of vibrating systems and sound* App. A, London 1927

Equating the driving force to the viscous and inertia forces one obtains

$$-\partial p / \partial x = \left\{ j \omega \rho_0 - \frac{\eta}{r} \frac{\partial}{\partial r} \left( r \frac{\partial}{\partial r} \right) \right\} v.$$

This may be written

$$\frac{1}{\eta} \frac{\partial p}{\partial x} = \left( \frac{\partial^2}{\partial r^2} + \frac{1}{r} \frac{\partial}{\partial r} + k^2 \right) v \quad (k^2 = -j \omega \rho_0 / \eta) \quad (2.01)$$

the solution being

$$v = \frac{1}{\eta k^2} \frac{\partial p}{\partial x} + A J_0(kr) \quad (2.02)$$

in which  $J_0$  is Bessel's function of zero order. At the cylindrical surface ( $r=R$ )  $v$  must vanish, from which  $A$  can be determined. Substituting this value of  $A$  in (2.02) gives

$$v = \frac{-1}{j \omega \rho_0} \frac{\partial p}{\partial x} \left\{ 1 - \frac{J_0(kr)}{J_0(kR)} \right\} \quad (2.03)$$

The mean velocity  $\bar{v}$  over the cross-section is now found by replacing  $J_0(kr)$  by its mean value over the cross-section

$$\overline{J_0(kr)} = \frac{1}{\pi R^2} \int_0^R J_0(kr) 2 \pi r dr.$$

This integral may be evaluated with the aid of the well-known property of Bessel's function<sup>1</sup>

$$\int_0^a x J_0(x) dx = x J_1(x) \Big|_0^a = a J_1(a)$$

in which  $J_1$  stands for Bessel's function of order unity. We obtain

$$\overline{J_0(kr)} = \frac{2}{kR} J_1(kR), \quad (2.04)$$

which substituted in (2.03) yields

<sup>1</sup> E. Jahnke and F. Emde, *Funktionentafeln*, p. 212, Berlin 1933.

$$\bar{v} = -\frac{1}{j\omega\rho_0} \frac{\partial p}{\partial x} \left\{ 1 - \frac{2}{kR} \frac{J_1(kR)}{J_0(kR)} \right\} \quad (2.05)$$

Defining the complex mean density by the equation

$$-\frac{\partial p}{\partial x} = \rho \frac{\partial \bar{v}}{\partial t}$$

we obtain the expression for  $\rho$  by comparison of this equation with (2.05). Replacing  $kR$  by its equivalent  $\mu\sqrt{-j}$ ,  $\rho$  takes the form

$$\rho = \rho_0 \left/ \left\{ 1 - \frac{2}{\mu\sqrt{-j}} \frac{J_1(\mu\sqrt{-j})}{J_0(\mu\sqrt{-j})} \right\} \right. \quad (2.06)$$

Approximations for low (high) frequencies may readily be derived. If  $\mu < 1$  (i.e., at low frequencies or in narrow pores) we may take three terms of the power series for  $J_0$  and  $J_1$ ,

$$J_0(\mu\sqrt{-j}) = 1 + \frac{1}{8}j\mu^2 - \frac{1}{64}\mu^4$$

$$J_1(\mu\sqrt{-j}) = \frac{1}{2}\mu\sqrt{-j} \left( 1 + \frac{1}{8}j\mu^2 - \frac{1}{192}\mu^4 \right)$$

leading to

$$\left. \begin{aligned} \text{or} \quad \rho &= \frac{4}{3}\rho_0 (1 - 6j/\mu^2) \\ \rho &= \frac{4}{3}\rho_0 (1 - 6j\eta/\omega\rho_0 R^2) \\ \text{or} \quad \rho &= \frac{4}{3}\rho_0 + \frac{1}{j\omega} \frac{8\eta}{R^2} \\ \text{or} \quad \rho &= \frac{4}{3}\rho_0 + \frac{1}{j\omega} \sigma_{\text{stat}} \end{aligned} \right\} \begin{array}{l} \mu < 1 \\ \text{low frequencies} \end{array} \quad (2.07)$$

which is in agreement with equation (1.26)

If on the other hand  $\mu > 10$  (i.e. at high frequencies or in wide tubes), we may put  $J_1/J_0$  equal to  $j$  when the imaginary part of  $\sqrt{-j}$  is taken positive, giving

$$\left. \begin{aligned} \text{or} \quad \rho &= \rho_0 (1 - 2\sqrt{-j}/\mu) \\ \rho &= \rho_0 [1 + (1 - j)\sqrt{2\eta/\omega\rho_0 R}] \end{aligned} \right\} \begin{array}{l} \mu > 10 \\ \text{high frequencies} \end{array} \quad (2.08)$$

which is in agreement with equation (1.27)

The contour of  $\rho$  as a function of  $\mu$  is given in Fig. 17a. At low frequencies ( $\mu$  small) the real part is equal to  $4\rho_0/3$  i.e. the

density is increased by 33 % as a consequence of the parabolic velocity distribution over the cross-section. The imaginary part is

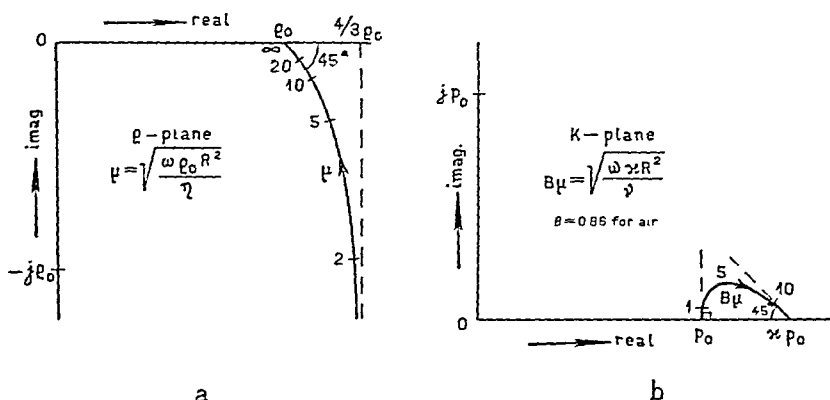


Fig. 17

Density and stiffness of the air in cylinders

equal to the stationary value  $\sigma_{\text{stat.}}/j\omega$ . At high frequencies ( $\mu$  great) the density deviates from the normal density  $\rho_0$  by a *complex* correction with an argument of minus  $45^\circ$  (see (2.08)).

### § 3 THE COMPRESSION MODULUS OF AIR IN CYLINDERS DISREGARDING VISCOUS EFFECTS

If sound waves are travelling in the cylinder under consideration we can distinguish at any point of the tube the sound pressure, the three components of the vector velocity, and the excess temperature. All are functions of the position in the tube and the time. The dependence on time of all quantities will be supposed to be as  $\exp j\omega t$ , so that  $\partial/\partial t$  can be replaced by  $j\omega$ .

The experiment that will virtually be carried out is the periodic compression in the axial direction of a cylindrical volume of air. Compression gives rise to generation of heat which, owing to the thermal conductivity of the air, tends to flow to the cylindrical boundary. Dissipation in the axial direction must of course not be taken into account, since such dissipation is of no importance in travelling waves, and this is the case for which the compression modulus  $K$  is to be computed.

The excess temperature will of course depend upon the radius  $r$  and must be zero at the boundary  $r=R$ . The same will apply to the radial velocity of the air. The variation in density will also depend upon the radius, but will not vanish at the boundary. The pressure will be assumed to be constant in the whole volume under consideration. This is justified by the fact that the radius of the cylinders under consideration is extremely small compared to the wave length.

As to the variation of  $p$  in the axial direction the situation is still simpler.  $\partial p / \partial x$  can be made zero by compressing the layer of air under consideration from either side exactly symmetrically, viz., by equal and opposite displacements of the flat terminal surfaces of the layer. Speaking in terms of waves we can say that a thin layer of air is taken out of a standing wave at the position where  $p$  is a maximum. Then  $\partial p / \partial x$  obviously is zero.

In the next § the correct derivation will be given in close connection with Rayleigh's survey of Kirchhoff's theory<sup>1</sup>, making use of a notation that deviates as little as possible from Rayleigh's. The same notation will be used in this §.

Let

$p, p_0$  = excess and equilibrium pressure resp.,

$\delta\rho, \rho_0$  = excess and equilibrium density resp.,

$\delta T, T_0$  = excess and equilibrium absolute temperature resp.,

$\mathbf{v}$  = particle velocity (vector),

$s$  = condensation =  $\delta\rho / \rho_0$ ,

$\kappa = C_p / C_v$  = ratio of specific heats,

$\theta'$  = a kind of relative excess temperature =  $\delta T / (\kappa - 1) T_0$ ,

$\lambda_h$  = thermal conductivity,

$\nu = \lambda_h / \rho_0 C_p$  = a kind of reduced thermal conductivity

$\Delta$  = Laplacian operator =  $\nabla^2 = \text{div grad} = \partial^2 / \partial x^2 + \text{cyc}$

We then have the following four equations, which can be called the equation of continuity (2.09), the compression equation (2.10), the equation of motion (2.11) and the thermal equation (2.12)

<sup>1</sup> Rayleigh, *Theory of sound* II, 2nd ed., p. 319 a f. Cambridge 1896

$$\operatorname{div} \mathbf{v} = - \partial s / \partial t \quad (2.09)$$

$$p = p_0 \{ s + (\kappa - 1) \theta' \} \quad (2.10)$$

$$- \operatorname{grad} p = \rho_0 \partial \mathbf{v} / \partial t \quad (2.11)$$

$$\partial \theta' / \partial t = \partial s / \partial t + \nu \Delta \theta' \quad (2.12)$$

(2.09) needs no explanation. It is the normal equation of continuity if one bears in mind that  $s = \delta \rho / \rho_0$ . (2.10) is a form of the law of Boyle-Gay-Lussac for small variations in  $p_0$ ,  $\rho_0$  and  $T_0$ . (2.11) again is the normal equation and needs no explanation. Equation (2.12) expresses the fact that the temperature can rise by compression as well as by heat conduction. The compression term again follows from Boyle-Gay-Lussac, since for adiabatic variations

$$T = \rho^{\kappa-1} \text{ . constant}$$

and therefore

$$\delta T / T_0 = (\kappa - 1) \delta \rho / \rho_0 \text{ .}$$

The conduction term is the normal one from the Fourier equation.

Writing  $j\omega$  for  $\partial / \partial t$  and eliminating  $s$  between (2.10) and (2.12) we obtain

$$\left( \Delta - \frac{j\omega\kappa}{\nu} \right) \theta' + \frac{p}{p_0} \frac{j\omega}{\nu} = 0.$$

Since  $p$  is independent of the space coordinates, the solution can be given at once

$$\theta' = \frac{1}{\kappa} \frac{p}{p_0} + A J_0 r \left( \sqrt{-\frac{j\omega\kappa}{\nu}} \right),$$

the second term being the solution of the reduced equation, the first a particular solution of the whole equation.

$A$  is found from the boundary condition  $\theta' = 0$  for  $r = R$ , giving

$$\theta' = \frac{1}{\kappa} \frac{p}{p_0} \left[ 1 - \frac{J_0(r \sqrt{-j\omega\kappa/\nu})}{J_0(R \sqrt{-j\omega\kappa/\nu})} \right].$$

Substitution of this expression for  $\theta'$  in (2.10) gives

$$s = \frac{p}{\kappa p_0} \left[ 1 + (\kappa - 1) \frac{J_0(r \sqrt{-j\omega\kappa/\nu})}{J_0(R \sqrt{-j\omega\kappa/\nu})} \right]$$

The normal definition of the compression modulus  $K$  is

$$K = \rho \frac{dp}{ds} = \frac{p}{s}$$

The ratio  $p/s$  is, however, a function of  $r$ . We, therefore, are in need of a definition of the mean value of  $K$  over the cross-section.

Denoting again mean values over the cross-section by a bar, the required mean value of  $K$  must be computed according to the definition

$$\bar{p} = K \bar{s},$$

for, then, the equation of continuity is again brought into its usual form (108), since

$$-\frac{\partial \bar{s}}{\partial t} = \frac{\partial \bar{u}_x}{\partial x}$$

Now  $p$  is constant, so we only have to compute  $s$ . Averaging means averaging of the Bessel function in  $r$ . This is accomplished as in § 2 equation (204) by increasing the order of the Bessel function by 1, dividing it by half the argument and finally replacing  $r$  by  $R$ .

If we furthermore replace  $R \sqrt{-j\omega\kappa/\nu}$  by its equivalent  $B_\mu \sqrt{-j}$  in which  $B_\mu = \sqrt{\eta\kappa/\rho_0\nu} = 0.86$  for air, we obtain

$$K = \kappa p_0 / \left[ 1 + \frac{2}{B_\mu \sqrt{-j}} (\kappa - 1) \frac{J_1(B_\mu \sqrt{-j})}{J_0(B_\mu \sqrt{-j})} \right] \quad (213)$$

Comparison with the expression for  $\rho$  of § 2 (206) reveals several analogous features. Most important is that the arguments of the Bessel functions are almost identical, since  $B \approx 1$ . This means that the significance of the expressions "low", "high" and "intermediate frequency" is the same for the density  $\rho$  and the compression modulus  $K$ .

Approximations for low (high) frequencies for  $K$  are easily derived from (213). At low frequencies the argument of the Bessel functions is small, we then have



$$\frac{2}{B_\mu \sqrt{-j}} \frac{J_1(B_\mu \sqrt{-j})}{J_0(B_\mu \sqrt{-j})} = 1 + \frac{1}{8} (B_\mu \sqrt{-j})^2,$$

and

$$K = p_0 \left[ 1 + \frac{1}{8} j \frac{\kappa - 1}{\kappa} (B_\mu)^2 \right] \quad (\mu < 1) \quad (2.14)$$

The modulus of  $K$  therefore does not change to the degree of approximation involved (see Fig. 17b).

At high frequencies the argument of the Bessel functions is large, giving

$$\frac{2}{B_\mu \sqrt{-j}} \frac{J_1(B_\mu \sqrt{-j})}{J_0(B_\mu \sqrt{-j})} = \frac{2}{B_\mu \sqrt{-j}} j,$$

if  $\sqrt{-j}$  is assumed to have a positive imaginary part, and

$$K = \kappa p_0 [1 + 2 \sqrt{-j} (\kappa - 1) / B_\mu]. \quad (\mu > 10) \quad (2.15)$$

Therefore, both argument and modulus of  $K$  now change,  $K$  attaining the limiting adiabatic value  $\kappa p_0$  in a direction that is inclined  $45^\circ$  to the real axis (see Fig. 17b).

Comparing the results of  $\rho$  and  $K$  there turn out to exist very simple relations between the loss angles (the arguments) of both quantities, viz., (for air)

$$\begin{aligned} \tan \delta_\rho \cdot \tan \delta_K &= 0.16 & \text{for } \mu < 1 \\ \tan \delta_K &= 0.46 \tan \delta_\rho & \text{for } \mu > 10. \end{aligned}$$

Without giving the derivation we shall write down the expression for  $K$  arrived at if  $p$  is not assumed to be independent of  $r$ , but still independent of  $x$ . The latter assumption is irrelevant, since  $K$  will be equal whether the volume under consideration is part of a travelling or of a standing wave, therefore, whether  $\partial p / \partial x = 0$  or  $\neq 0$ .

$$K = p_0 \times$$

$$1 + (\kappa - 1) \frac{\frac{2}{R \sqrt{-\lambda_1}} \frac{J_1(R \sqrt{-\lambda_1})}{J_0(R \sqrt{-\lambda_1})} - \frac{2}{R \sqrt{-\lambda_2}} \frac{J_1(R \sqrt{-\lambda_2})}{J_0(R \sqrt{-\lambda_2})}}{\left(1 - \frac{\nu \lambda_1}{j \omega}\right) \frac{2}{R \sqrt{-\lambda_1}} \frac{J_1(R \sqrt{-\lambda_1})}{J_0(R \sqrt{-\lambda_1})} - \left(1 - \frac{\nu \lambda_2}{j \omega}\right) \frac{2}{R \sqrt{-\lambda_2}} \frac{J_1(R \sqrt{-\lambda_2})}{J_0(R \sqrt{-\lambda_2})}}$$

in which  $\lambda_1$  and  $\lambda_2$  are roots of a quadratic equation from Kirchhoff's theory<sup>1</sup> and  $K$  is defined as  $\bar{p}/s$

#### § 4 EXTENSION OF KIRCHHOFF'S THEORY OF SOUND PROPAGATION IN CYLINDRICAL TUBES AND PORES

Taking into account at the same time viscosity and heat conduction, Kirchhoff developed his brilliant theory describing the sound propagation, among other things, in tubes and pores of cylindrical shape

The way in which we shall tackle the problem is that expressions are derived for  $W$  and  $\gamma$  at low (high) frequencies, from which  $K$  and  $\rho$  then can be computed. An expression for  $\gamma$  at high frequencies is already given by Kirchhoff. Also an expression for  $\gamma$  at *extremely* low frequencies is available. The corresponding expression for  $\gamma$  for *simply low* frequencies will be derived in this § by giving the derivation to a higher approximation.

Expressions for  $W$  will be derived from the definition  $W = \bar{p}/\bar{u}$ , in which  $\bar{p}$  and  $\bar{u}$  mean the average pressure and axial velocity over the cross section. Properly speaking  $\bar{p}$  ought to be the mean force per unit surface, which is not exactly equal to the mean hydrostatic pressure. The difference is the  $xx$  term of the friction tensor (see Rayleigh<sup>2</sup>) which can be shown, however, to be negligible as compared with the hydrostatic pressure.

In order to avoid a repetition of Kirchhoff's theory we shall take Rayleigh's version of it as our starting point. References to Rayleigh are given with §, page and equation from the second edition (Cambridge 1896). Rayleigh's notation will be slightly changed.

The four fundamental differential equations of the previous section remain valid except for the equation of motion (2.11) in which frictional terms enter. The new equations of motion are Rayleigh's § 348 p. 319 (2)

$$\frac{\partial u}{\partial t} + \frac{1}{\rho_0} \frac{\partial p}{\partial x} = \frac{\eta}{\rho_0} \Delta u - \frac{1}{3} \frac{\eta}{\rho_0} \frac{\partial^2 s}{\partial x \partial t}$$

<sup>1</sup> Rayleigh *Theory of sound* II, 2nd ed., p. 321, equation 19, Cambridge 1896

<sup>2</sup> Rayleigh, *Theory of sound* II, 2nd ed., § 345, Cambridge 1896

and cyclic equations for  $v, w, y, z$ , when  $u, v, w$  denote the three components of the vector velocity.

Elimination of all other variables than  $\theta'$  gives an equation in  $\theta'$ , from which

$$\theta' = A_1 Q_1 + A_2 Q_2 \quad (2.16)$$

is a solution, if

$$\Delta Q_1 = \lambda_1 Q_1, \Delta Q_2 = \lambda_2 Q_2,$$

where  $\lambda_1$  and  $\lambda_2$  are the roots of a quadratic equation, viz. Rayleigh's § 348, p. 320 (16). Good approximations are  $\lambda_1 = (j\omega/c_0)^2$ ,  $\lambda_2 = j\omega\kappa/\nu$ . The viscosity turns out to be of much less importance for  $\lambda_1$  and  $\lambda_2$  than the heat conductivity.

Now our object is supposed to be cylindrical in shape, furthermore all quantities are supposed to vary as  $\exp(-\gamma x)$ , i.e., a travelling wave is supposed to exist. Finally a rotationally symmetrical solution is the only one that interests us, therefore the velocity at any point is given by the axial component  $u$  and the radial component  $q$ .

$A, A_1, A_2$  being constants to be determined next, correct expressions for  $u, q$  and  $\theta'$  as functions of  $r$  are given (§ 350, p. 324, (8) (9) (10)), running in our notation:

$$u = A Q + A_1 \gamma (j\omega/\lambda_1 - \nu) Q_1 + A_2 \gamma (j\omega/\lambda_2 - \nu) Q_2 \quad (2.17)$$

$$q = A \frac{\gamma}{j\omega/\eta' - \gamma^2} \frac{dQ}{dr} - A_1 \left( \frac{j\omega}{\lambda_1} - \nu \right) \frac{dQ_1}{dr} - A_2 \left( \frac{j\omega}{\lambda_2} - \nu \right) \frac{dQ_2}{dr} \quad (2.18)$$

$$\theta' = A_1 Q_1 + A_2 Q_2 \quad (2.19)$$

in which

$$\eta' = \eta/\rho_0,$$

$$Q = J_0(r \sqrt{\gamma^2 - j\omega/\eta'})$$

$$Q_1 = J_0(r \sqrt{\gamma^2 - \lambda_1}),$$

$$Q_2 = J_0(r \sqrt{\gamma^2 - \lambda_2}).$$

These exact solutions have to fulfil the boundary conditions at the cylindrical surface  $r=R$ :

$$\left. \begin{array}{l} u=0 \\ q=0 \\ \theta'=0 \end{array} \right\} \text{ for } r=R. \quad (2.20)$$

In these equations  $A$ ,  $A_1$  and  $A_2$  are unknown quantities still to be determined. To permit a solution the determinant of the coefficients should be zero, whence at  $r=R$

$$\frac{\gamma^2 j\omega}{j\omega/\eta' - \gamma^2} \left( \frac{1}{\lambda_1} - \frac{1}{\lambda_2} \right) \frac{d \ln Q}{dr} + \left( \frac{j\omega}{\lambda_1} - \nu \right) \frac{d \ln Q_1}{dr} - \left( \frac{j\omega}{\lambda_2} - \nu \right) \frac{d \ln Q_2}{dr} = 0 \quad (2.21)$$

This equation is Rayleigh's § 350 p 324 (11)

To a *third* approximation we may write for small values of the argument of the Bessel functions (which applies to  $Q$ ,  $Q_1$  and  $Q_2$  at low frequencies (§ 350, p 326))

$$d \ln J_0(z)/dz = -\frac{1}{2}z(1 + \frac{1}{8}z^2 + \frac{1}{48}z^4) \quad (2.22)$$

Introducing this into (2.21) taking for  $Q$ ,  $Q_1$  and  $Q_2$  the expressions given above, an equation in  $\gamma^0$ ,  $\gamma^2$  and  $\gamma^4$  is obtained from which  $\gamma^2$  must be calculated. In doing this only the leading terms should be retained. This means that  $j\omega\nu/c^2$ ,  $R/\text{wave length}$  and  $j\omega R^2/\eta'$  are considered as negligibly small quantities in comparison with unity. All terms in  $\gamma^4$  cancel out among other terms and one finally retains

$$\gamma^2 = \frac{8 j\omega \eta' \kappa}{c^2 R^2} \left[ 1 + \frac{1}{6} \frac{j\omega R^2}{\eta'} - \frac{1}{8} (\kappa - 1) \frac{j\omega R^2}{\nu} \right] \quad (2.23)$$

(for low frequencies)

This equation is in complete agreement with the equations for  $\rho$  (2.07) and  $K$  (2.14) calculated separately. The relation should be  $\gamma^2 = (j\omega)^2 \rho/K$  and turns out to be complied with.

For high frequencies we may at once borrow a suitable expression from Rayleigh § 350, p 325 (15)

$$\gamma^2 = \left( \frac{j\omega}{c} \right)^2 \left[ 1 + \frac{2 \sqrt{\eta'}}{R \sqrt{j\omega}} + 2 \left( \sqrt{\kappa} - \frac{1}{\sqrt{\kappa}} \right) \frac{\sqrt{\nu}}{R \sqrt{j\omega}} \right] \quad (2.24)$$

which again complies with  $\rho$  and  $K$ , calculated separately and given by (2.08) and (2.15) respectively.

Once  $\gamma$  has been taken as to fulfil the condition (2.21) the ratios  $A/A_1$  and  $A/A_2$  can be derived from equations (2.17) (2.18) and (2.19). Giving a suitable value to  $A$  one finds

$$\left. \begin{aligned} A &= j\omega \left( \frac{1}{\lambda_1} - \frac{1}{\lambda_2} \right) / Q(\alpha R), \\ A_1 &= -1/\gamma Q_1(\alpha_1 R), \\ A_2 &= 1/\gamma Q_2(\alpha_2 R). \end{aligned} \right\} \quad (2.25)$$

$\alpha_1 R$  stands for the complex argument of the quantities  $Q$ , at  $r = R$ . The argument of  $Q$  at a variable point  $r$ , is, therefore,  $\alpha_1 r$ .

Introducing (2.25) in (2.17) gives

$$u = j\omega \left( \frac{1}{\lambda_1} - \frac{1}{\lambda_2} \right) \frac{Q(\alpha r)}{Q(\alpha R)} - \left( \frac{j\omega}{\lambda_1} - \nu \right) \frac{Q_1(\alpha_1 r)}{Q_1(\alpha_1 R)} + \left( \frac{j\omega}{\lambda_2} - \nu \right) \frac{Q_2(\alpha_2 r)}{Q_2(\alpha_2 R)}.$$

The average value  $\bar{u}$  is obtained by averaging  $Q$ , over the cross-section, which may be performed as in § 2, see (2.04). The integrated Bessel function of order zero leads to a Bessel function of order unity.

A corresponding equation for  $p$  is obtained by successively introducing (2.25) in (2.19), calculating the condensation  $s$  from

$$s = \theta' - (\nu/j\omega) \Delta \theta', \quad (2.12)$$

where  $\Delta$  is put equal to  $\lambda_1$  and  $\lambda_2$  respectively, substituting  $s$  and  $\theta'$  in the expression for  $p$  (2.10)

$$p = p_0 [s + (\kappa - 1) \theta'],$$

and averaging over the cross-section with the aid of (2.04).

Now this value of  $p$  is not exactly equal to the mean force per unit surface, since it is only the hydrostatic part of it. Properly speaking a frictional term corresponding to § 345, p. 313 (5) should be added. It can be shown, however, that this additional term can be neglected for the approximation required. We then obtain

$$\begin{aligned} & p_0(\kappa - \nu\lambda_1/j\omega) \bar{Q}_1/Q_1(\alpha_1 R) - p_0(\kappa - \nu\lambda_2/j\omega) \bar{Q}_2/Q_2(\alpha_2 R) \\ & - j\omega\gamma(1/\lambda_1 - 1/\lambda_2) \bar{Q}/Q(\alpha R) + \gamma(j\omega/\lambda_1 - \nu) \bar{Q}_1/Q_1(\alpha_1 R) - \gamma(j\omega/\lambda_2 - \nu) \bar{Q}_2/Q_2(\alpha_2 R) \end{aligned} \quad (2.26)$$

In order to derive approximate expressions for low and high frequencies suitable expressions for  $\bar{Q}_i/Q_i(\alpha_i R)$ ,  $\lambda_1$ ,  $\lambda_2$  and  $\gamma$  are introduced. Retaining the leading terms, we obtain

$$W = \rho_0 c_0 \left[ 1 + \sqrt{\frac{\eta}{j\omega\rho_0 R^2}} - \left( \sqrt{\kappa} - \frac{1}{\sqrt{\kappa}} \right) \sqrt{\frac{\nu}{j\omega R^2}} \right]$$

for high frequencies (2 27)

$$W = j\omega \left[ \frac{1}{3} \rho_0 + \frac{1}{j\omega} \frac{8\eta}{R^2} \right] / \gamma \quad \text{for low frequencies (2 28)}$$

From these equations and the corresponding equations for  $\gamma$  (2 24) and (2 23)  $h$  and  $\rho$  are easily obtained with the aid of the well known equations (1 17) The result is given in Table 1

TABLE 1

$\gamma$   $W$   $h$  AND  $\rho$  IN CYLINDERS DERIVED FROM  
KIRCHHOFF'S THEORY

low frequencies $\mu = \sqrt{\omega\rho_0 R^2/\eta} < 1$	high frequencies $\mu = \sqrt{\omega\rho_0 R^2/\eta} > 10$
$\gamma = \frac{8j\omega\eta}{\rho_0 R^2} \left[ 1 + \frac{j\omega\rho_0 R^2}{6\eta} - \frac{1}{3}(\kappa - 1) \frac{j\omega R^2}{\nu} \right]$	$\gamma = \left( \frac{j\omega}{c_0} \right) \left[ 1 + \sqrt{\frac{\eta}{j\omega\rho_0 R^2}} + \left( \sqrt{\kappa} - \frac{1}{\sqrt{\kappa}} \right) \sqrt{\frac{\nu}{j\omega R^2}} \right]$
$W = j\omega \left[ \frac{1}{3} \rho_0 + \frac{1}{j\omega} \frac{8\eta}{R^2} \right] / \gamma$	$W = \rho_0 c_0 \left[ 1 + \sqrt{\frac{\eta}{j\omega\rho_0 R^2}} - \left( \sqrt{\kappa} - \frac{1}{\sqrt{\kappa}} \right) \sqrt{\frac{\nu}{j\omega R^2}} \right]$
$h = \rho_0 \left[ 1 + \frac{1}{3}(\kappa - 1) \frac{j\omega R^2}{\nu} \right]$	$h = \kappa \rho_0 \left[ 1 - 2 \left( \sqrt{\kappa} - \frac{1}{\sqrt{\kappa}} \right) \sqrt{\frac{\nu}{j\omega R^2}} \right]$
$\rho = \frac{1}{3} \rho_0 + \frac{1}{j\omega} \frac{8\eta}{R^2}$	$\rho = \rho_0 \left[ 1 + 2 \sqrt{\frac{\eta}{j\omega\rho_0 R^2}} \right]$

Substituting  $\omega \rho_0 R^2 / \eta = \mu^2$  and some numerical constants for air, these formulae may be put into the simplified form of Table 2.

TABLE 2  
SIMPLIFIED EXPRESSIONS FOR  $\gamma$ ,  $W$ ,  $K$  AND  $\rho$   
FOR CYLINDERS AND AIR

low frequencies $\mu = \sqrt{\omega \rho_0 R^2 / \eta} < 1$	high frequencies $\mu = \sqrt{\omega \rho_0 R^2 / \eta} > 10$
$\gamma = \sqrt{8 j \omega \eta / \rho_0 R^2} (1 + 0.07 j \mu^2)$	$\gamma = (j \omega / c_0) (1 + 1.46 / \mu \sqrt{j})$
$\gamma W = \frac{4}{3} j \omega \rho_0 (1 + 6 / j \mu^2)$	$W = \rho_0 c_0 (1 + 0.54 / \mu \sqrt{j})$
$K = \rho_0 (1 + 0.028 j \mu^2)$	$K = \kappa \rho_0 (1 - 0.92 / \mu \sqrt{j})$
$\rho = \frac{4}{3} \rho_0 (1 + 6 / j \mu^2)$	$\rho = \rho_0 (1 + 2 / \mu \sqrt{j})$
$\tan \delta_\rho \cdot \tan \delta_K = 0.16$	$\tan \delta_K = 0.46 \tan \delta_\rho$

Summarizing the theoretical results for  $\rho$ ,  $K$ ,  $W$  and  $\gamma$ , we may state that independent computation of  $\rho$  and  $K$  gives expressions which have turned out correct at low and high frequencies. There seems to be no argument against assuming the validity of the formulae in the intermediate frequency range. In principle we can check the validity in the intermediate frequency range, for we can compute  $\gamma = j \omega \sqrt{\rho / K}$  from the expressions for  $\rho$  and  $K$ .

$$\gamma^2 = \left( \frac{j \omega}{c_0} \right)^2 \frac{1 + \frac{2}{B \mu \sqrt{-j}} (\kappa - 1) \frac{J_1(B \mu \sqrt{-j})}{J_0(B \mu \sqrt{-j})}}{1 - \frac{2}{\mu \sqrt{-j}} \frac{J_1(\mu \sqrt{-j})}{J_0(\mu \sqrt{-j})}}.$$

Now this expression for  $\gamma$  should be in agreement with Rayleigh's § 350, p. 324 (11), the verification of which seems to be a cumbersome task.

Numerous attempts have been made by different investigators to verify the theoretical result in the Helmholtz-Kirchhoff region; a survey is to be found in Wood<sup>1</sup>, showing that theory

<sup>1</sup> A. Wood, *Acoustics*, p. 252, London 1947.

and experiment are in good agreement. Experiments by the authors and Mr Van den Eyk<sup>1</sup>, although less accurate than those of Kaye and Sherratt<sup>2</sup> gave the same result.

#### § 5 THE CONSEQUENCES OF KIRCHHOFF'S THEORY FOR THE WAVE PROPAGATION IN POROUS MEDIA

We may raise the question, whether the results of Table 1 can be applied directly or after small alteration to porous media. We shall see that this is only the case for media with pores of cylindrical shape of the same diameter throughout the whole material, a rather hypothetical case. Ordinary materials, especially those containing pores varying greatly in cross-section along their length, give rise to great difficulties. For materials which only contain pores of one diameter, the equations of Table 1 are valid, provided  $K$  is divided by  $h$ , and  $\rho$  is multiplied by  $h/h$ . The loss angles  $\delta_\rho$  and  $\delta_K$  will obviously remain unchanged, because in every pore the propagation is exactly as given in Table 1. Therefore the ratio of resistance forces to inertia or stiffness forces, i.e.,  $\tan \delta_\rho$  and  $\tan \delta_K$  respectively, will be unchanged for the whole as well.

Whether the propagation mechanism is of the Poiseuille Kirchhoff type or of the Helmholtz Kirchhoff type, may readily be found by calculating  $\mu$  from

$$\mu = \sqrt{\omega \rho_0 R^2 / \eta} = \sqrt{8 \omega h \rho_0 / h \sigma_{\text{stat}}},$$

see (1.26). The quantities  $l$ ,  $h$  and  $\sigma_{\text{stat}}$  have to be inserted,  $h$  and  $\sigma_{\text{stat}}$  are taken from measurements, whereas  $l$  is found from the resonance frequency of an absorbing layer or put equal to 3 as a rough estimate. If  $\mu < 1$ , Poiseuille Kirchhoff holds, whereas  $\mu > 10$  certainly indicates that the Helmholtz Kirchhoff mechanism is valid.

The theory fails in the case of media containing pores the cross sections of which vary greatly along their length. In order to make this clear, consider the extreme case of a material in

<sup>1</sup> C. Zwicker, J. Van den Eyk, and C. W. Kosten *Physica* 10 (1943) 239.

<sup>2</sup> Kaye and Sherratt, *Proc Roy Soc A*, 141 (1933) 123.



which the air content is present in rather large holes, mutually connected by very narrow pores. The air resistance is mainly due to these latter pores and, owing to their small cross-section, may essentially be of the Poiseuille character. The behaviour of the compression modulus is governed by the velocity of heat exchange of the air, and, because the greater part of the total air content is found in the rather large holes, this heat exchange may occur so slowly that Helmholtz—Kirchhoff applies. Therefore, it may happen that  $1 < \mu < 10$ , and that nevertheless  $\rho$  complies with the first column of Table 1, whereas  $K$  is found from the second column of Table 1; in other words: the motion might take place almost isothermally, the compression almost adiabatically. The viscosity losses are governed by the conditions in the narrowest parts of the pores, the heat losses by those in the widest parts.

The following general trend, therefore, may be expected:

a. If  $\mu = 1$ , as calculated from  $\sigma_{\text{stat.}}$ , Poiseuille's law for  $\tan \delta_\rho$  will hold good, but  $\tan \delta_K$  may be considerably greater than  $0.028 \mu^2$ . This will be shown to be of the utmost importance for the absorption at low frequencies.

b. If  $\mu = 2$ , which may be about the limit for the applicability of Poiseuille's law,  $\tan \delta_K$  may already have reached values in the neighbourhood of its maximum (0.1—0.2).

c. If  $\mu > 20$ , Helmholtz—Kirchhoff's theory might be applicable both as to  $\tan \delta_K$  and  $\tan \delta_\rho$ , i.e., column 2 of Table 1 might hold good (after the changes  $K \rightarrow hK$  and  $\rho \rightarrow h\rho/k$ ).

A rough estimate of  $\mu$  at 500 Hz for different materials is

acoustic plasters :	$\sigma = 5 \cdot 10^3 - 10^5$	$k/h = 4$	$\mu = 4.5 - 1$
hair felt :	$\sigma = 5 \cdot 10^4 - 10^6$	$k/h = 3$	$\mu = 1 - 0.3$
wood fibre plates:	$\sigma = 5 \cdot 10^5 - 10^7$	$k/h = 3$	$\mu = 0.3 - 0.1$

This means that cases a and b will indeed occur, that is that the motion will frequently be isothermal, while  $\tan \delta_K$  will be greater than according to the first column of Table 1.

As we shall see, the complex quantities  $\rho$  and  $K$ , and therefore, also their loss angles, may be calculated from impedance measurements, so a check of our theoretical considerations is possible. A question of more or less academic importance may be answered

too in the mean time. In the equation of motion the structure factor  $k$  was necessarily introduced, it seemed impossible, however, to check whether  $k$  originated in oblique pores or in side holes. Now an idea about the relative importance of both effects may be expected to be gained from measurements of  $K$ . If oblique pores are preponderant, Table 1 should apply, if side holes are more important, the required  $\mu$  value for  $K$  will be greater than for  $\rho$ .

The same results as described in this section would have been found if the heat conductivity  $\lambda_h$  were supposed to be several times smaller than the actual one. This causes a shift of  $K$  along its complex contour (Fig. 17b) in the direction of the adiabatical value, giving rise to greater  $\delta_K$  values at low frequencies, smaller at high frequencies. The ratio of the apparent heat conductivity  $\lambda_{app}$  and the normal value  $\lambda_h$  must be looked upon as a new material "constant". It will depend upon the frequency and the structure and must be obtained from experiment.

#### § 6 DISCUSSION OF THE THEORETICAL RESULTS OF KORRINGA, KRONIG, AND SMIT

The behaviour of porous materials was described in the beginning by the material constants  $h$ ,  $k$  and  $\sigma$ . For materials with ideally cylindrical pores these constants seemed to be sufficient. Considering practical materials, however, a further "constant" had to be introduced, the ratio  $\lambda_{app}/\lambda_h$  ( $< 1$ ). Although the need for the introduction of the latter constant is obvious and the constant has a physical meaning which is easily grasped, it is clear that this way of attack ceases to be elegant, the more so since it is rather difficult to give an even rough estimate of the ratio  $\lambda_{app}/\lambda_h$ . A mathematically more sound way of attack was proposed by Korrington, Kronig, and Smit<sup>1</sup>, although this method has the disadvantage of only being applicable in geometrically well defined and simple cases, even then being quite laborious. They considered the propagation of sound waves in a medium consisting of spheres, situated on a cubic lattice, taking into account viscosity and heat effects, thus applying Kirchhoff's method

---

<sup>1</sup> J. Korrington, R. Kronig, and A. Smit, *Physica*, 11 (1945) 209

(who considered viscosity and heat effects in tubes) to a problem treated by Rayleigh, viz., the propagation in a medium of spheres, neglecting damping effects<sup>1</sup>.

Their results are given in a few simple graphs, giving  $\gamma$  (disregarding a factor  $j\omega/c_0$ ) and  $W/\rho_0 c_0$  as a function of frequency for different radii of the spheres and porosities. Their results essentially corroborate our views and give us an idea of the magnitude of the ratio  $\lambda_{app.}/\lambda_h$  for the media under consideration.

TABLE 3

$k$  AND  $\lambda_{app.}/\lambda_h$  FROM KORRINGA, KRONIG, AND SMIT'S  
THEORY FOR PACKED SPHERES

$h$	$\frac{\text{diam.}}{\text{dist.}}$	$k$	$\lambda_{app.}/\lambda_h$
0.85	0.66	1.1	0.45
0.75	0.78	1.1	0.45
0.65	0.87	1.2	0.45
0.55	0.95	1.2	0.45
0.48	1.00	1.3	0.45

Table 3 gives a survey of our interpretation of their results. The arguments of  $\rho$  and  $K$ , in the frequency range for which Korringa et al. gave numerical results, are rather small indicating that we are working in the Helmholtz' region. According to our scheme the wave impedance at high frequencies should be  $\sqrt{k}/h$  times  $\rho_0 c_0$ , and, since  $h$  is known,  $k$  may be computed. One really finds figures greater than unity of the expected magnitude. From  $\gamma$  and  $W$  the complex  $K$  and  $\rho$  can be computed and, of course, the ratio  $\tan \delta_K / \tan \delta_\rho$  interests us greatly; Kirchhoff predicts in the case of tubes 0.46 for this ratio, which according to our conception should be  $0.46 \sqrt{\lambda_{app.}/\lambda_h}$ .

The results, obtained in the paper under discussion lead to

<sup>1</sup> Rayleigh, *Phil. Mag.*, 34 (1892) 481; *Scientific papers*, Vol. 4 (1903) p. 19.

ratio's  $\lambda_{app}/\lambda_h$  of about 0.4 to 0.5, very acceptable values for this case. Because we are, now, in the Helmholtz' region, this means that Kirchhoff's correction is two times smaller than in tubes. On the other hand it completely corroborates our views and justifies the suggestion that the contribution of heat exchange losses in the more important case of Poiseuille flow is increased by the irregularity in cross-section of the pores.

### § 7. POROUS MATERIALS WITH HIGH AIR RESISTANCE ( $\mu < 2$ )

We shall now proceed with the consideration of the absorption characteristics of media in the extreme cases of small and large  $\mu$ , and, in order to give some idea of the influence of the above mentioned ratio of conductivities, this ratio will be inserted into the equations. We must bear in mind, then, that the quantity  $v$  is proportional to the thermal conductivity.

The general expression (1.14) for the impedance of a layer of thickness  $l$

$$z = \sqrt{K\rho} \coth j\omega l \sqrt{\rho/K}$$

may be written for small values of the argument of the  $\coth$  (i.e., far below resonance) as

$$z = K/j\omega l + j\omega l\rho/3 \quad (2.29)$$

For, if  $x \ll 1$ ,

$$\coth x = \frac{1}{x} + \frac{x}{3} \quad (2.30)$$

(2.29) is the impedance of a mass  $l\rho/3$  mounted on a stiffness  $K/l$ . The effective mass of the layer per unit surface, therefore, turns out to be  $1/3$  of the total mass/m<sup>2</sup>.

If  $\mu < 1$ , the values of the first column of table 1 for  $K$  and  $\rho$  may be inserted (with  $h$  and  $h'$ ), which yields in the case of air

$$\begin{aligned} \frac{z}{\rho_0 c_0} = \frac{\sigma l}{3 \rho_0 c_0} \left\{ 1 + \left( \frac{3 \rho_0 c_0}{\sigma l} \right)^2 \frac{\lambda_h}{\lambda_{app}} \frac{h}{20 h^2} \right\} + \frac{p_0}{j\omega l \rho_0 c_0 h} + \\ + \frac{j\omega l \frac{4}{3} \rho_0}{3 \rho_0 c_0} = \frac{R - jX}{\rho_0 c_0} \end{aligned} \quad (2.31)$$

in which  $\sigma$  denotes the steady flow air resistance. It should be borne in mind that  $c_0$  stands for the sound velocity in free air,

$c_0 = \sqrt{\kappa p_0 / \rho_1}$ . Far below resonance the mass reactance term in  $X$  may be dropped. The layer behaves like a spring with losses. We then have

$$X = p_0 / \omega l h \quad (2.32)$$

$X$  is neither dependent on  $k$ , nor on  $\sigma$ , and indeed all experimental contours of  $z$  show the same trend at low frequencies (Fig. 18).

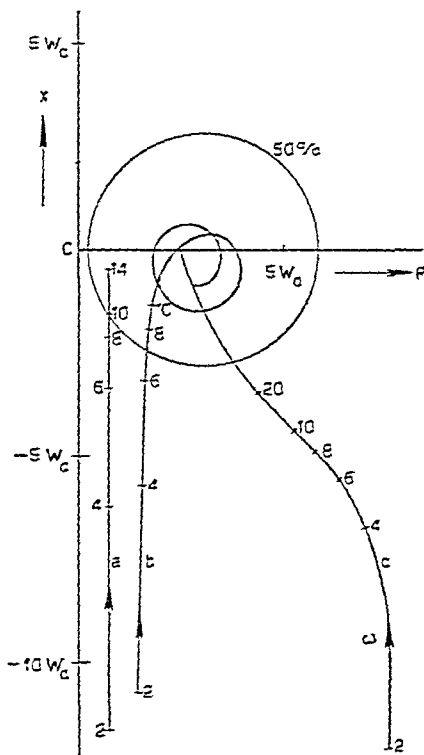


Fig. 18

Smoothed curves of measured contours, frequencies added in 100 Hz

The absorption coefficient in this region is approximately proportional to  $R$ .

$$\alpha_1 = \frac{1}{2} \rho_1 c_0 R / X^2. \quad (2.33)$$

Therefore,  $R$  is of great importance for the absorption coefficient.  $R$  passes through a minimum if  $\sigma$  varies. As a rule (since  $\lambda_1 k / \lambda_{app} \approx 1$ )  $R_{min.} = 2 \rho_1 c_0$ , corresponding with a

vertical line for  $z$  at a distance  $2\rho_0 c_0$  from the imaginary axis  
 Under extreme conditions ( $\lambda_{app} \approx \lambda_h$ ,  $h=1$ ,  $h=1$ )  $R_{min} \approx 1/2 \rho_0 c_0$

Inserting  $\lambda$  from (2.32) and taking  $R_{min} = \rho_0 c_0$  equation (2.33) gives

$$\alpha_{min} = (2 \kappa \omega l h / c_0)^2$$

We should like to emphasize that (2.29) and (2.31) only hold

- 1) if Poiseuille's law holds (i.e., about  $\omega < h\sigma/2 \lambda \rho_0$ ), and
- 2) if the expansion of  $\coth$  into two terms is allowed (i.e., about  $\omega < p_0 / \sigma h l^2$ )

The lowest of these limiting frequencies forms, of course, the limit of applicability of the equation. For materials with low  $\sigma$  (plasters) the first condition is the more severe and traces a limit at 50–1000 Hz. On the other hand, for materials with high  $\sigma$ , the first condition is satisfied at all audiofrequencies but the second is passed already at rather low frequencies (10 Hz for very high air resistance). An easy control is obtained in the complex plane. According to the second condition, all impedances to which equation (2.29) applies should have an imaginary part about 1.5 times greater than the real one, i.e., the argument should be between  $-55^\circ$  and  $-90^\circ$ .

The correction in  $R$  between the brackets of (2.31) due to Kirchhoff's effect in  $K$ , is only of importance if  $\sigma l < 5 \rho_0 c_0$ . To give some idea of the magnitude of this factor in practice, it is given in Table 4 for a few materials. It is of great importance when the air resistance is low.<sup>1</sup>

TABLE 4  
 ROUGH ESTIMATE OF KIRCHHOFF'S CORRECTION  
 IN THE POISEUILLE RANGE ( $i=0.02$ )

material	corr factor
plasters	25–100
felt	1–2
wood fibre	1

<sup>1</sup> C. W. Kosten *Appl sci Research*, B1 (1949) 241

For large values of  $\omega$  we know that  $\coth$  converges towards 1, and,  $\rho$  being almost purely imaginary, a frequency contour for  $\coth$  as in Fig. 7 is to be expected. Putting  $\coth \gamma l = 1$ ,  $z$  equals the wave impedance, approximately

$$z = \sqrt{K_r \rho_r} \sqrt{1 - j \tan \delta_r}.$$

Now  $\sqrt{1 - j f(\omega)}$  is a rectangular hyperbola (Fig. 4 lower branch), which explains the form of the upper part of the contour shown in Fig. 18 curve c. This is the case with materials with extremely high  $\sigma$ . At low frequencies their absorption is relatively high, but they do not reach really high values of  $a_0$ , even at high frequencies, because their wave impedance remains appreciable. Materials with smaller  $\sigma$  behave like Fig. 18 curve a and b. At high frequencies Poiseuille no longer holds,  $\coth$  shows maxima and minima (Figs. 5, 8, 9), giving rise to a spiral-like impedance contour and an absorption characteristic with pronounced maxima and minima. Fig. 18 curve a holds approximately for 20 mm hair felt, c for wood fibre plates.

#### § 8 POROUS MATERIALS WITH LOW AIR RESISTANCE ( $\mu > 20$ )

As in § 7 equation (1.14) holds for the impedance of a layer  $l$  on rigid background, and, again (2.29) is its approximation for low frequencies. Furthermore, because the modulus of  $\rho$  is much smaller than in the case of  $\mu < 2$ , the approximation is valid up to higher frequencies this time. A further approximation is allowed, since both  $K$  and  $\rho$  have arguments,  $\delta_K$  and  $\delta_\rho$ , of the same order, whereas the modulus of the mass reactance at low frequencies is negligible as compared with that of  $K$ . Dropping, therefore, the term in  $\rho$  gives for low frequencies

$$z = \frac{K}{j\omega l} = \frac{\kappa p_0}{\omega l h} \left[ 0.23 \sqrt{\frac{h \sigma_{\text{stat.}}}{\omega h \rho_0}} - j \right]$$

leading to an absorption coefficient proportional to  $\sqrt{\omega}$ . Of course this dependence cannot remain valid for extremely low frequency, since Helmholtz's value must then be replaced by Poiseuille's. This time the real part of  $z$  varies as  $\omega^{-3/2}$ , giving rise to the curved impedance contour often found for materials with very low resistance at low frequencies.

For the higher frequencies we obtain, when only the leading terms are retained, and, moreover the irrelevant small loss angle in the wave impedance is dropped

$$z = \sqrt{K_r \rho_r} \coth \{ j \omega l \sqrt{\rho_r / K_r} \{ 1 - j (1 + 0.46 \sqrt{\lambda_{app} / \lambda_h}) \delta_r / 2 \} \},$$

which is represented in the complex plane by a spiral with a small slope of less than  $0.73 \delta_r$ . Now since  $\delta_r$  in this case is proportional to  $\omega^{-1/2}$  the slope steadily decreases, although there is no asymptotic circle as in fig. 9

For very high  $\omega$   $z$  approaches

$$z = \sqrt{K_r \rho_r} = \frac{1}{h} \sqrt{k} \rho_0 c_0 \approx (2 \text{ to } 3) \rho_0 c_0,$$

therefore, the absorption characteristic will have very pronounced maxima and minima "around" a mean value, which amounts to about 80% almost independently of the material under consideration

$h$  can be determined from resonance frequencies, for which

$$\omega_{\text{res}} l \sqrt{\rho_r / K_r} = \omega_{\text{res}} l \sqrt{k} / c_0 = \pi/4, 3\pi/4, \text{ etc}$$

or from anti resonance frequencies, for which

$$\omega_{\text{antires}} l \sqrt{k} / c_0 = \pi/2, \pi, \text{ etc}$$

## § 9 A METHOD OF VERIFICATION OF THEORETICAL RESULTS

The correctness of theoretical results can be verified by experimentally measuring the impedance of a layer of thickness  $l$ . If the wave impedance and propagation exponent, used for the theoretical expression of  $z$ , were correct, good agreement with experiment should be found. Discrepancies will generally be found, it, then, turns out to be rather difficult to find the reason for these discrepancies. The best way of getting a good insight into the material and its behaviour is, however, to compute the complex quantities  $K$  and  $\rho$  from the experiments. The reason for discrepancies between the actually found  $K$  and  $\rho$  on the one hand and any couple of theoretical expressions for  $K$  and  $\rho$  on the other, can be found much more easily than when comparing experimental and theoretical results of the impedance  $z$  of a layer of thickness  $l$ ,



because the mathematical distance between the fundamental assumptions and  $K$  and  $\rho$  is much shorter than that between these assumptions and  $z$ .

This way of attack, which is common practice in the electrical field, was perhaps first applied to the propagation of sound waves in absorbing media by Wüst<sup>1</sup>. A possible scheme for the computation of  $K$  and  $\rho$  from adequate measurements is the following

$$\begin{aligned} z_1 = W \coth \gamma l & \quad W = \sqrt{z_1 z_2} & \quad K = j\omega W / \gamma \\ \rightarrow & & \rightarrow \\ z_2 = W \tanh \gamma l & \quad \coth \gamma l = \sqrt{z_1 / z_2} & \quad \rho = W \gamma / j\omega \end{aligned}$$

$z_1$  and  $z_2$  are the measured impedances for the layer backed by a rigid wall and a column of air of one quarter of a wave length

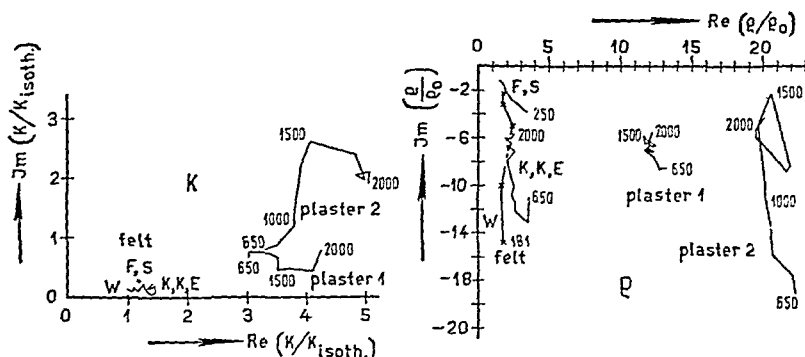


Fig. 19

Measurements of the complex stiffness and density

respectively (see equations (1.05) and (1.06)).  $W$  is now calculated from the product  $z_1 z_2$ ,  $\gamma$  from the ratio  $z_1 / z_2$ . The next step is the computation of  $K$  and  $\rho$  from the well-known relations between  $W$ ,  $\gamma$  and  $K$ ,  $\rho$  (1.17).

Although this way of attack is doubtless the most promising one, only a few measurements of this kind have been carried out.

In Fig. 19 a general survey of results is given comprising those of Wüst ( $W$ ), Ferrero and Sacerdote<sup>2</sup> ( $F$ ,  $S$ )

<sup>1</sup> H. Wüst, *Hochfrequenztechn. u. Elektroakustik*, 44 (1934) 73.

<sup>2</sup> M. Ferrero and G. Sacerdote, *Nuovo Cimento*, 4 (1947) 3.

and of C W Kosten, M L Kasteleyn, and J Van den Eyk<sup>1</sup> (K, K, E) Wust, Ferrero, and Sacerdote described results for felt only, whereas the results of the last group of investigators (Kosten et al) also include measurements made on acoustic plasters. These latter results especially lack accuracy probably due to the fact that the samples of plaster were insufficiently homogeneous.

All  $\rho$  curves show the upward trend with frequency which was to be expected (see Fig 17a). Except for the measurements of Ferrero and Sacerdote, the real parts of  $\rho$  are nearly constant indicating that the structure factor is constant. With the results of Ferrero and Sacerdote, the structure factor obviously decreases with increasing frequency. The structure factor is of the order 2 for all felt samples.

The compression modulus  $K$  of felt lies somewhere in between the isothermal and the adiabatic value. In the results of Wust an unmistakable progression towards the adiabatic value is to be noticed. The loss angle  $\delta_K$  of Ferrero and Sacerdote has about the maximum value in agreement with their  $\delta_\rho$ .

The general tendency of Wust's results is the same as that of the results of Kosten et al for felt. His resistance seems to be a little smaller giving rise to the theoretically expected frequency dependence of  $K$ . The results of Ferrero and Sacerdote, although extremely accurate deviate much more in general trend. Moreover it seems rather difficult to give a theoretical explanation of them. Since  $\tan \delta_\rho$  is of the order unity  $K$  might be expected to be rather strongly dependent on the frequency which is not the case.

The behaviour of the plasters 1 and 2 is much more complicated. The real part of  $\rho$  is  $h\rho_0/h$ , yielding  $h/h$  values of 12.5 and 21 resp. The real part of  $K$  is proportional to  $1/h$ . Assuming the variation to take place about midway isothermal to adiabatic this yields  $h$  values of 0.34 and 0.3 resp. The structure factor therefore, is found to be approximately 4.2 and 6.3 resp., which are reasonable values. The low  $h$ -values are not in agreement with the statically measured ones, which are about 0.7. This will be due

---

<sup>1</sup> C W Kosten, M. L. Kasteleyn and J Van den Eyk, unpublished.

to the fact that in the statical measurements all cavities are taken into account, also those, which, in the dynamical situation, do not take any part in the mechanism. This fact also explains other features of the curves. In the case of plaster 2  $\delta_K$  is much greater than its theoretical maximum. Moreover the variation of the real part of  $K$  is greater than could be explained from the mere transition from  $K_{\text{isoth.}}$  to  $K_{\text{adlab.}}$  (1:1.4). The effective porosity obviously decreases more or less with frequency, which decrease is accompanied by extra losses in  $K$ .

The question arises whether the measured loss angles are in agreement with those calculated from measurements on the steady flow resistance  $\sigma_{\text{stat.}}$ . This turns out to be the case for  $\delta_p$ ; the calculated values for  $\delta_K$  are, however, smaller than the measured ones. Since  $\delta_p$  for the plasters is rather small, the relations between  $\delta_p$  and  $\sigma_{\text{stat.}}$  for the Helmholtz-Kirchhoff case will approximately apply

$$\tan \delta_p = \sqrt{\sigma_{\text{stat.}}/4 \omega \rho_r}$$

(see (1.26) and (2.08), bearing in mind that  $\rho_r = k\rho_0/h$ )

and furthermore  $\delta_K$  can be calculated from

$$\tan \delta_K = 0.46 \tan \delta_p.$$

The results are given in Table 5, showing good agreement for  $\delta_p$ .

TABLE 5  
CALCULATED AND MEASURED LOSS ANGLES AT 1500 Hz  
FOR PLASTERS

plaster no.	$\sigma_{\text{stat.}}$	$\rho_r$	$\tan \delta_p$		$\tan \delta_K$	
			calc.	meas.	calc.	meas.
1	5500	12	0.11	0.1	0.05	0.15
2	34000	24	0.19	0.15	0.1	0.5

## CHAPTER III

### THEORY OF SOUND ABSORPTION BY HOMOGENEOUS POROUS AND ELASTIC LAYERS

#### § 1 POROUS MATERIALS WITH ELASTIC FRAME<sup>1</sup>

If the possibility of vibration of the solid material, due to its finite stiffness, is taken into account, the mathematical problem of the coupled vibrations of frame and air arises

This problem will be dealt with in this and the following sections. In order to distinguish clearly between the quantities of frame and air respectively all quantities relating to the *frame* are written with an index 1, those relating to the *air* with the index 2. Let

$p_1$  = force acting on the frame per unit area of cross-section of the sample,

$v_1$  = mean velocity of the solid material at  $x$ ,

$\rho_1$  = density of the solid material as given by the mass of solid material per unit volume of porous material,

$K_1$  = specific stiffness of the frame to be taken complex if necessary,

$p_2$  = excess force acting on the air per unit area of cross-section of the sample, the equilibrium force has been subtracted therefore it is called the *excess* force,  $p_2$  is closely related to the mean sound pressure at  $x$ , which is  $1/h$  times greater, if  $h$  denotes the porosity,

$v_2$  = mean velocity of the air at  $x$ , this quantity is  $1/h$  times greater than the velocity of volume displacement, used up to now,

$\rho_2$  = density of the air as given by the mass of the air content per unit volume of porous material, it is  $h$  times the density of free air,

---

<sup>1</sup> C. W. Kosten and C. Zwicker, *Physica*, 8 (1941) 963, C. W. Kosten, Thesis Delft 1942

$K_2$  = normal modulus of air, if necessary to be taken complex in the case of losses being present (thermal or viscous),  
 $P_0$  = total equilibrium pressure of the air,  
 $P$  = total pressure of the air during the vibration,  
 $s$  = coupling coefficient, to be defined next.

The equations of motion are

$$-\frac{\partial p_1}{\partial x} = \rho_1 \frac{\partial v_1}{\partial t} + s(v_1 - v_2) \quad (3.01)$$

$$-\frac{\partial p_2}{\partial x} = \rho_2 \frac{\partial v_2}{\partial t} + s(v_2 - v_1). \quad (3.02)$$

The first term of the right hand side of the first equation is the ordinary mass reaction force; the second term stands for the force per unit volume of porous material exerted by the air on the frame if  $v_1 \neq v_2$ . The definition of  $s$  is obviously the force per unit volume per unit difference between the velocities of frame and air. Owing to the law of action and reaction the same term also occurs in the equation of motion of the air, however, of course, with the opposite sign.

The coupling coefficient  $s$  can easily be connected with well-known quantities. Supposing  $v_1$  to become zero without changing the structure, (3.02) must assume the usual form (1.23) from which follows

$$s = j\omega\rho_2(k-1) + h^2\sigma \quad (\rho_2 = h\rho_0) \quad (3.03)$$

This means that coupling even occurs in the case where  $\sigma = 0$ .

The equations of continuity will be shown to be

$$-\frac{\partial p_1}{\partial t} = K_1 \frac{\partial v_1}{\partial x} - \frac{1-h}{h} \frac{\partial p_2}{\partial t} \quad (3.04)$$

$$-\frac{\partial p_2}{\partial t} = hK_2 \frac{\partial v_2}{\partial x} + (1-h)(K_2 - P_0) \frac{\partial v_1}{\partial x}. \quad (3.05)$$

The first equation expresses the fact that the force in the frame will increase by a concentration of solid matter as well as of air. The term containing  $K_1$  is the normal contribution which would be present in vacuum, arising from the stiffness of the frame. The necessity of the second term can easily be demonstrated as follows.

Suppose  $\partial v_1 / \partial x$  to be zero in a special point of the material.

If, furthermore, it is supposed that the frame does not deform if submitted to a hydrostatic pressure (e g, porous sample in vacuo as compared to porous sample in free air), then it is clear that  $p_1$  must increase together with  $p_2$ , if the frame does not deform ( $\partial v_1/\partial x = 0$ ). Indeed  $p_1/(1-h)$  and  $p_2/h$  are the pressures in solid material and air resp, which should vary by equal amounts if  $\partial v_1/\partial x$  be zero

Equation (3 05) states that the air pressure will increase by a concentration of air as well as of solid matter, the first term of the right hand side relating to the influence of air concentration, the second to that of solid material (3 05) may be derived as follows

$$p_2 = hP - h_0P_0 = \text{actual force} - \text{equilibrium force}, \quad (3\ 06)$$

$$p_2 = h\rho, \quad (3\ 07)$$

if  $\rho$  denotes the variable density of air

$P$  and  $\rho$  are connected through the compression modulus of air (complex if necessary)

$$\frac{dP}{K_2} = \frac{d\rho}{\rho_0},$$

which equation, with the aid of (3 06) and (3 07) yields

$$\frac{1}{h} \frac{\partial p_2}{\partial t} - \frac{P_0}{h} \frac{\partial h}{\partial t} = \frac{K_2}{\rho_2} \left( \frac{\partial \rho_2}{\partial t} - \frac{\rho_2}{h} \frac{\partial h}{\partial t} \right)$$

Now  $\partial h/\partial t$  can be replaced by  $(1-h) \partial v_1/\partial x$  and  $\partial \rho_2/\partial t$  by  $-\rho_2 \partial v_2/\partial x$ , which after substitution yields the equation of continuity of the air (3 05)

The physical meaning of (3 05) can be elucidated by the following qualitative consideration. If in an infinitesimal volume solid material is introduced owing to  $\partial v_1/\partial x$  not being zero, the air pressure will increase. The air force  $p_2$  will not be increased if the compression takes place isothermally, for, then, the pressure increases in the same ratio as the porosity decreases. Indeed the second term of the right hand side of (3 05) cancels out in this case, owing to  $K_2 = P_0$  if the compression is isothermal. This will apply at low frequencies, thus materially simplifying the considerations. As we do not confine ourselves to this case the complete expression will be used.

## § 2 TRAVELLING WAVES IN ELASTIC POROUS MEDIA

In order to find expressions for a travelling sine-shaped wave we substitute  $-\gamma$  for  $\partial/\partial x$  and  $j\omega$  for  $\partial/\partial t$  in equations (3.01), (3.02), (3.04) and (3.05).  $j\omega$  is a given number,  $\gamma$  has to be solved, giving us damping and velocity of propagation of the supposed wave.

Indeed the quoted equations of motion and continuity now form a set of four homogeneous linear equations in  $p_1$ ,  $p_2$ ,  $v_1$ , and  $v_2$ , which only permits a solution, if the determinant of the coefficients is zero, thus giving an equation for determining  $\gamma$ . If furthermore we write

$$\begin{aligned}\Gamma &= \gamma/j\omega \quad (=1/\text{complex sound velocity}), \\ S &= s/j\omega \quad (= \text{generalized air density}).\end{aligned}\quad (3.08)$$

this determinant is

$$D = \begin{vmatrix} p_1 & p_2 & v_1 & v_2 \\ \Gamma & 0 & -(\rho_1 + S) & S \\ 0 & \Gamma & S & -(\rho_2 + S) \\ -1 & \frac{1-h}{h} & K_1\Gamma & 0 \\ 0 & -1 & (1-h)(K_2 - P_0)\Gamma & hK_2\Gamma \end{vmatrix} \quad (3.09)$$

The equation  $D=0$  is

$$\begin{aligned}\Gamma^4 - \Gamma^2 \left[ \frac{h\rho_1 + S}{hK_1} + \frac{\rho_2 + S}{hK_2} + \frac{\rho_2(1-h) + S}{hK_1K_2} \frac{(1-h)(K_2 - P_0)}{h} \right] + \\ + \frac{\rho_1\rho_2 + (\rho_1 + \rho_2)S}{hK_1K_2} = 0\end{aligned}\quad (3.10)$$

Since only even powers of  $\Gamma$  enter into (3.10), the four roots of the equation may be written  $\pm \Gamma'$  and  $\pm \Gamma''$ . For the moment the negative roots may be omitted as they are related to waves in the negative  $x$ -direction which do not interest us for the general considerations.

We see that at a given frequency two waves are possible in the positive  $x$ -direction. The amplitude of each wave will be dependent on the boundary conditions. We should like to

emphasize that these two waves may not be considered as the wave in air and that in the frame resp. The wave type relating to  $\Gamma'$  takes place both in the air and in the frame, and so does that of  $\Gamma''$ .

A fairly good analogy is to be found in optics, where double refracting media exist. One single wave impinging on such a medium gives two refracted waves. In the acoustical case it seems however rather inadequate to distinguish between an ordinary and an extraordinary beam.

In special cases  $\Gamma'$  or  $\Gamma''$  may assume a numerical value which reminds one strongly of the propagation constant of a wave in the air or frame separately. This will be the case if the coupling is weak. However such a wave in air or frame is always accompanied by a wave in frame or air of the same  $\Gamma$ .

For  $\Gamma$  equal to either  $\Gamma'$  or  $\Gamma''$  the equations in  $p_1$ ,  $p_2$ ,  $v_1$  and  $v_2$ , of which the coefficients may be taken from (3.09), may be used for computing all ratio's between  $p_1$ ,  $p_2$ ,  $v_1$  and  $v_2$ , e.g.,  $p_1/v_1$  and  $p_2/v_2$ , which have the character of partial wave impedances. Since  $\Gamma$  may take one of the two values  $\Gamma'$  and  $\Gamma''$ , all ratio's have also two values. We can distinguish, therefore, four wave impedances

$$\left. \begin{aligned} W'_1 &= (p_1/v_1)' & W''_1 &= (p_1/v_1)'' \\ W'_2 &= (p_2/v_2)' & W''_2 &= (p_2/v_2)'' \end{aligned} \right\} \quad (3.11)$$

The ratio's  $(v_2/v_1)'$  and  $(v_2/v_1)''$  decide whether the rôle of the air or the frame is preponderant in the wave type under consideration. The wave to which the smaller ratio belongs, may be called the disturbed frame wave, the other the disturbed air wave, since  $v_2$  is the velocity of the air.

The ratio of any two quantities may be derived from the four fundamental equations. The following general expressions for  $W_1$ ,  $W_2$  and  $v_2/v_1$  may easily be derived

$$\left. \begin{aligned} W_1 &= \frac{p_1}{v_1} = \frac{\rho_1 \rho_2 + (\rho_1 + \rho_2) S + SK_1 \Gamma^2 h / (1-h)}{\{ \rho_2 + S / (1-h) \} \Gamma} = \\ &= \Gamma \frac{-(1-h)SK_2 + hK_1 K_2 \Gamma^2 - \rho_2 K_1 - SK_1 - (1-h)^2 (\rho_2 + S) (h_2 - P_0) / h}{h h_2 \Gamma^2 - \rho_2 - S} \end{aligned} \right\} \quad (3.12)$$



$$W_2 = \frac{p_2}{v_2} = \frac{\rho_1 \rho_2 + (\rho_1 + \rho_2) S - \rho_2 K_1 \Gamma^2 - S K_1 \Gamma^2}{(-K_1 \Gamma^2 + S/h + \rho_1) \Gamma} = \left\{ \begin{aligned} &= \frac{(\rho_2 + S)(1-h)(K_2 - P_0) \Gamma + h K_2 S \Gamma}{(1-h)(K_2 - P_0) \Gamma^2 + S}, \end{aligned} \right. \quad (3.13)$$

$$\frac{v_2}{v_1} = \frac{-h K_1 \Gamma^2 + h \rho_1 + S}{(1-h) \rho_2 + S} = \frac{(1-h)(K_2 - P_0) \Gamma^2 + S}{-h K_2 \Gamma^2 + \rho_2 + S}. \quad (3.14)$$

All special cases are comprised in the general one. E. g., putting  $K_1 = \infty$  will yield the case of acoustic plasters,  $S = \infty$  applies to materials with extremely high air resistance or to normal materials at extremely low frequencies (see equations (3.03) and (3.08)). At low frequencies  $K_2$  will assume its isothermal value  $P_0$ . At high frequencies  $S$  is equal to  $(k-1)\rho_2$  and a reasonable assumption for  $K_2$  is  $1.4 P_0$  (adiabatic value).

A few results for special cases may be taken from Table 6.

Two interesting cases deserve special attention. If  $\omega = 0$  one of the wave types is completely coupled,  $(v_2/v_1)' = 1$ .  $\Gamma'$  and  $(W_1' + W_2')$  have the values which are to be expected. The second wave type is infinitely slow ( $\Gamma'' = \infty$ ); the corresponding wave impedances are infinite, so that this wave type seems to be of little importance. It is, however, the only possible type in rigid materials like acoustic plasters. This case is especially worth while studying for more or less flexible wood fibre materials. These are generally treated as rigid ones ( $\Gamma''$ ), whereas it is very likely that the other wave type ( $\Gamma'$ ) is often of much more importance.

The other extreme case is that of complete decoupling, which turns out to occur only if at the same time  $\omega = \infty$  (or  $\sigma = 0$ ),  $h = 1$  and  $k = 1$ . That decoupling does indeed take place is clear from the values of  $v_2/v_1$  (0 and  $\infty$ ). Moreover  $\Gamma$  and  $W$  have the normal values.

If  $k \neq 1$  (last column but one of Table 6) frame and air remain coupled systems, even at high frequencies, where the air friction is of no importance.

### § 3 GRAPHICAL REPRESENTATION OF THE ROOTS OF THE $\Gamma$ -EQUATION

The roots of the  $\Gamma$ -equation (3.10) can be computed without difficulty. Their dependence on the frequency and the material

VALUES OF  $\Gamma'$ ,  $\Gamma''$ ,  $W'$ ,  $W''$ ,  $W'_1$ ,  $W''_1$ ,  $W'_2$ ,  $W''_2$ ,  $(v_2/v_1)'$  AND  $(v_2/v_1)''$  IN SPECIAL CASES (SEE ALSO TABLE 7)  
 ABBREVIATIONS, USED IN THIS TABLE ONLY, ARE INDICATED UNDER THE COLUMNS

	$\omega = 0$ , isothermal	$\omega = \infty$ , $\rho_2 \ll \rho_1$	$\omega = \infty$ , $\rho_2 \ll \rho_1$ , $h = 1$	$\omega = \infty$ , $h = k = 1$
$\Gamma'^2$	$\Sigma\rho/\Sigma K$	$\rho_1/K_1$	$\rho_1/K_1$	$\rho_1/K_1$
$\Gamma''^2$	$\infty$	$k\rho_2/hK_2$	$h\rho_2/K_2$	$\rho_2/K_2$
$W'_1$	$\sqrt{\Sigma K} \sqrt{\Sigma\rho(1-h+hK_1/\Sigma K)}$	$\sqrt{K_1\rho_1}$	$\sqrt{K_1\rho_1}$	$\sqrt{K_1\rho_1}$
$W''_1$	$\infty$	$\sqrt{K_2 h \rho_2 h (A\rho_1/\rho_2 + BK_1/K_2)}$	$(k-1)\sqrt{K_2 k \rho_2} K_1/K_2$	indefinite
$W'_2$	$\sqrt{\Sigma K} \sqrt{\Sigma\rho(h-hK_1/\Sigma K)}$	$\sqrt{K_1\rho_1} \frac{k\rho_2 K_2' + h\rho_2' K_2}{\rho_1 K_2' + \rho_2' K_1}$	$\frac{K_2}{K_1} \sqrt{K_1\rho_1}$	indefinite
$W''_2$	$\infty$	$\sqrt{K_2 k \rho_2 h}$	$\sqrt{K_2 k \rho_2}$	$\sqrt{K_2 \rho_2}$
$W'_1 + W'_2$	$\sqrt{\Sigma K} \sqrt{\Sigma\rho}$	—	—	—
$W''_1 + W''_2$	$\infty$	—	—	—
$(v_2/v_1)'$	1	$\frac{\rho_1 K_2' + \rho_2' K_1}{-h\rho_1 K_2 + k\rho_2 K_1}$	$\frac{(k-1)\rho_2 K_1}{k\rho_2 K_1 - \rho_1 K_2}$	0
$(v_2/v_1)''$	$\sim K_1/K_2$	$\frac{h\rho_1 K_2 - k\rho_2 K_1}{h(k-h)\rho_2 K_2}$	$\frac{\rho_1 K_2 - k\rho_2 K_1}{(k-1)\rho_2 K_2}$	$\infty$
Abbrev	$\Sigma\rho = \rho_1 + \rho_2$ $\Sigma K = K_1 + K_2$	$A = (1-h)/(k-h)$ $B = k-1$ $K_2' = (1-h)(K_2 - P_0)$ $\rho_2' = (k-1)\rho_2$		

constants is very complex and hardly surveyable. The following graphical representation of the dependence on frequency under various circumstances may be of great help.

Writing

$$u = \Gamma^2$$

$$E = \frac{h\rho_1 + S}{hK_1} + \frac{\rho_2 + S}{hK_2} + \frac{\rho_2(1-h) + S}{hK_1K_2} \cdot \frac{(1-h)(K_2 - P_0)}{h}$$

$$F = \frac{\rho_1\rho_2 + (\rho_1 + \rho_2)S}{hK_1K_2}$$

the  $\Gamma$ -equation takes the form

$$u^2 - Eu + F = 0.$$

Its solutions are  $u'$  and  $u''$

$$2u' = E + \sqrt{D},$$

$$2u'' = E - \sqrt{D},$$

if  $D$  denotes the discriminant of the  $\Gamma$ -equation

$$D = E^2 - 4F.$$

In order to allow for a graphical interpretation something must be assumed about  $K_1$  and  $K_2$ , and to simplify things we shall suppose both  $K_1$  and  $K_2$  to be real constants, i.e. it is assumed that internal friction in the frame is of negligible importance and that the Kirchhoff effect (II § 3) and other effects, which might cause  $K_2$  to be complex, are absent. As we saw before, the loss angle for  $K$  is often small indeed and the contribution to sound absorption is for far the greater part due to viscosity.  $\rho_1$  and  $\rho_2$  are constants by definition,  $K_1$  and  $K_2$  are assumed to be constants, so the frequency now only enters implicitly through  $S$ , since

$$S = (k - 1)\rho_2 + h^2\sigma/j\omega.$$

Assuming  $K_1$  and  $K_2$  to be real and constant means, of course, a restriction to the general theory.

One sees at a glance that  $E$  is of the general form  $a + b/j\omega$ ; furthermore it is easily verified that  $D$  can be written

$$D = A - B/\omega^2 + C/j\omega \quad (3.15)$$

in which  $A$  and  $B$  are essentially positive constants,  $C$  can be negative or positive

$$A \approx \left( \frac{\rho_1}{K_1} - \frac{k\rho_2}{hK_2} \right)^2 \quad (\text{if } \rho_2 \ll \rho_1)$$

$$B = \frac{h^2 \sigma^2}{K_1^2 K_2^2} (K_1 + K_2)^2$$

$$C \approx \frac{2h\sigma\rho_1}{K_2^2} \left\{ \left( \frac{K_2}{K_1} \right)^2 - \frac{K_2}{K_1} + \frac{k\rho_2}{h\rho_1} \right\} \quad (\text{if } \rho_2 \ll \rho_1) \quad (3.16)$$

The character of the frequency dependence of  $D$ , and therefore of  $u'$  and  $u''$ , changes discontinuously if  $C$  changes its sign. From (3.16) one easily deduces that this takes place when approximately

$$\frac{K_2}{K_1} = \frac{k\rho_2}{h\rho_1} \quad \text{and } 1 \text{ resp} \quad (\text{if } \rho_2 \ll \rho_1)$$

If the ratio  $K_2/K_1$  has a value in between these limits  $C$  is negative, in the other cases it is positive.

Fig. 20 shows the way in which  $\Gamma'$  ( $=\gamma'/j\omega$ ) and  $\Gamma''$  ( $=\gamma''/j\omega$ )

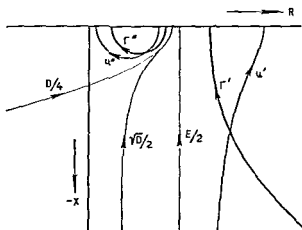


Fig. 20  
The construction of  $\Gamma'$  and  $\Gamma''$

may be constructed.  $E/2$  is represented by an upward straight line parallel to the imaginary axis.  $D$  is obviously a parabola (see (3.15)),  $D/4$  has been drawn in Fig. 20 for a positive value of  $C$ . For negative values of  $C$  the other half of the parabola (above the real axis) would have been found.

The square root of  $D/4$  yields  $\sqrt{D}/2$ , which added to or sub-

tracted from  $E/2$  yields  $u'$  or  $u''$  resp..  $\Gamma'$  and  $\Gamma''$  are finally found by taking the square root of  $u'$  and  $u''$ . The unit of the scales of Fig. 20 can be chosen arbitrarily. For simplicity we took  $A$  as unit.

The contour of  $\Gamma'$  is mainly hyperbolic, that of  $\Gamma''$  very much resembles a semi-circle.

Fig. 20 has been drawn with the assumption  $K_2/K_1 < k\rho_2/h\rho_1$  (rather stiff frame).

This comes down to saying  $C = \text{positive}$ ,  $\sqrt{A} = \rho_1/K_1 - k\rho_2/hK_2$ .

Three essentially different types of figures like Fig. 20 can occur, according to the value of the ratio  $K_2/K_1$ .

TABLE 7

FREQUENCY DEPENDENCE OF  $\Gamma'$  AND  $\Gamma''$  IN THE THREE MAIN CASES

$K_2/K_1 < k\rho_2/h\rho_1$	$k\rho_2/h\rho_1 < K_2/K_1 < 1$	$1 < K_2/K_1$
$\sqrt{A} = k\rho_2/hK_2 - \rho_1/K_1$ $C = \text{positive}$	$\sqrt{A} = \rho_1/K_1 - k\rho_2/hK_2$ $C = \text{negative}$	$\sqrt{A} = \rho_1/K_1 - k\rho_2/hK_2$ $C = \text{positive}$

On the one hand the value of  $K_2/K_1$  determines the sign of  $C$ ; if  $C$  is positive the "hyperbola" remains to the right of the "semi-circle" and conversely. The condition  $K_2/K_1 = k\rho_2/h\rho_1$  at the same time gives a critical value of  $K_2/K_1$  as to the expression for  $\sqrt{A}$ , viz.

$$\sqrt{A} = \pm (\rho_1/K_1 - k\rho_2/hK_2) \text{ for } K_2/K_1 \gtrless k\rho_2/h\rho_1.$$

The consequence of this is to be seen in the values near the end points of the  $\Gamma$ -curves (the interchanging of  $\sqrt{\rho_1/K_1}$  and  $\sqrt{k\rho_2/hK_2}$  in passing from the first to the second case)

If  $K_2/K_1$  is varied continuously the  $\Gamma$  graph also varies continuously from the first to the third graph of Table 7. The 'hyperbola' and 'semi circle' approach each other, at a certain value of  $K_2/K_1$  the curves come into contact. This requires  $D=0$ , i.e.  $C=0$  and  $A-B/\omega^2=0$  from which we see that  $\Gamma'$  may coincide with  $\Gamma''$  if  $K_2/K_1$  has a definite value and the frequency is chosen adequately. The same coincidence again occurs if  $D$  becomes zero for the second time.

A high value of  $\sigma$  (or low frequency) means that the roots are situated at the extreme beginning of the respective curves. One of the roots is then equal to  $\sqrt{(\rho_1 + \rho_2)/(K_1 + K_2)}$ . A low value of  $\sigma$  (or high frequency) means the opposite, i.e., roots at the extreme end points.

Which of the two curves of the graph is called the  $\Gamma'$ -curve or the  $\Gamma''$ -curve respectively is arbitrary. It seems a good system to denote all curves ending in  $\sqrt{\rho_1/K_1}$  by  $\Gamma'$  and to call the corresponding wave the disturbed frame wave. The curves ending in  $\sqrt{k\rho_2/hK_2}$  may then be labeled with  $\Gamma''$  and considered to belong to the disturbed air wave. This nomenclature can be justified by considering numerical values of the ratio  $v_2/v_1$ . It might be expected that the ratio  $v_2/v_1$  for the disturbed air wave has a greater value than unity or at least greater than that for the disturbed frame wave. This indeed turns out to be true. This may be verified with the aid of the expressions for  $v_2/v_1$  at  $\omega=0$  and  $\omega=\infty$  in Table 6, if  $K_2/K_1$  is supposed to be very small and very large respectively.

From a practical point of view it is important to know whether frame and air are to be considered as closely coupled or not. This can be estimated as follows. For the frame-wave  $v_1 > v_2$ . The transition between coupled and rather decoupled vibrations of this wave type may be assumed to take place where the inertia term  $j\omega\rho_1 v_1$  equals the friction term  $h^2\sigma v_1$  in magnitude (see equations (3.01) and (3.03) for  $v_1 \gg v_2$ ), from which the decoupling frequency is found

$$\omega' = h^2\sigma/\rho_1$$

Partial decoupling of the air-wave may be expected for similar reasons at the higher frequency

$$\omega'' = h^2 \sigma / k \rho_2.$$

The practical importance of partial decoupling may be seen from the following reasoning. At low frequencies (complete coupling) one wave type is undamped ( $\Gamma = \text{real}$ ), the other is indeed strongly damped but absent owing to the high wave impedance. As soon as the frame-wave becomes free it will begin to contribute to the absorption. The air-wave will start its contribution to the absorption at a higher frequency. It should be borne in mind that  $K_1$  and  $K_2$  have been assumed to be real; as this is not strictly true, damping takes place owing to the loss angles in  $K_1$  and  $K_2$ , even at very low frequencies.

To give some idea of the decoupling frequencies in ordinary materials a rough estimate is given in Table 8; the steady flow value of  $\sigma$  is taken for simplicity. From Table 8 it is clear that the study of coupled vibrations is of the utmost importance for many usual materials.

TABLE 8  
DECOUPLING FREQUENCIES FOR PRACTICAL MATERIALS

material	$\sigma$	$\nu' = \omega'/2\pi$	$\nu'' = \omega''/2\pi$
ac. plasters	$5 \cdot 10^3 - 10^5$	1 — 20 Hz	100 — 2000 Hz
felt	$5 \cdot 10^4 - 10^6$	100 — 3000	1000 — 20000
wood-fibre	$5 \cdot 10^5 - 10^7$	500 — 15000	$10^4 - 2 \cdot 10^5$

Figs. 21 and 22 give two numerical examples for sponge rubber layers. They may be deemed to be rather flexible. Other materials like soft wood-fibre plates, rockwool, etc., may have, however, a compliance of the same order.

Expressions for the decoupling frequencies have been derived from the equations of motion. We should bear in mind, however, that also the equations of continuity are coupled and even remain so at high frequencies. What  $\omega'$  and  $\omega''$  really mean can perhaps best be elucidated with the aid of Fig. 21 and 22, where  $\nu'$  and

$\nu''$  are indicated on the corresponding curves. One sees that they are easy means for giving a rough idea of the frequency scale that belongs to each curve. The transition points on the  $\Gamma''$ -curves, i.e., on the curves corresponding to the air wave, may be thought to be too much in the neighbourhood of the region of free vibrations to be considered as belonging to the decoupling frequency range. It can be shown that at frequencies which are about three times smaller than the indicated frequencies  $\nu''$  the argument of  $\Gamma''$ , i.e., the damping of the air wave, is about maximum, whereas the maximum of the imaginary part of  $\Gamma''$  is already reached

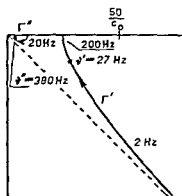


Fig 21

Theoretical curves for  $h=1$ ,  $l=7$ ,  
 $K_1=0.24 \cdot 10^9 \text{ N/m}^2$ ,  $K_2=1.4 \cdot 10^9$ ,  
 $\rho_1=120 \text{ kg/m}^3$ ,  $\rho_2=1.2$ ,  $\sigma=2 \cdot 10^4$   
 mks-units

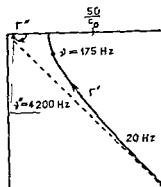


Fig 22

Theoretical curves for  $h=1$ ,  $l=7$ ,  
 $K_1=0.46 \cdot 10^9$ ,  $K_2=1.4 \cdot 10^9$ ,  $\rho_1=200$ ,  
 $\rho_2=1.2$ ,  $\sigma=2.2 \cdot 10^4$  mks-units

at frequencies which are again three times smaller. Although we did not check this in other cases we might perhaps conclude that the decoupling frequency range is 0.1 to 1 times the decoupling frequencies given above.

#### § 4 SIMPLIFIED THEORY, $h=1$

If the porosity is put equal to unity, as was done in the authors' original publication, the mathematical treatment can be given in a much more symmetrical, and therefore, elegant way. This is due to the coupling between the equations of continuity canceling out.



The most important results of the general theory will be summarized for this case.

$$\Gamma^4 - \Gamma^2 \left[ \frac{\rho_1 + S}{K_1} + \frac{\rho_2 + S}{K_2} \right] + \frac{\rho_1 \rho_2 + (\rho_1 + \rho_2) S}{K_1 K_2} = 0$$

$$W_1 = K_1 \Gamma$$

$$W_2 = K_2 \Gamma$$

$$\frac{v_2}{v_1} = \frac{-K_1 \Gamma^2 + \rho_1 + S}{S} = \frac{S}{-K_2 \Gamma^2 + \rho_2 + S} = -\frac{K_1 \Gamma^2 - \rho_1}{K_2 \Gamma^2 - \rho_2}.$$

The latter expression for  $v_2/v_1$  makes it easy to verify that

$$(v_2/v_1)' (v_2/v_1)'' = -K_1/K_2.$$

It should be emphasized that this simple relation exists independently of the frequency. For the derivation one needs  $\Gamma'^2 \cdot \Gamma''^2$ , and  $\Gamma'^2 + \Gamma''^2$ , which quantities are taken from the  $\Gamma$ -equation.

If a function  $\chi$  be defined according to

$$v_2/v_1 = \chi \sqrt{K_1/K_2} \quad (3.17)$$

one obtains

$$\chi' \chi'' = -1, \quad (3.18)$$

furthermore from the equations of continuity

$$\frac{p_2}{p_1} = \frac{K_2}{K_1} \frac{v_2}{v_1} = \chi \sqrt{\frac{K_2}{K_1}}, \quad (3.19)$$

which simple relation holds for both wave types (insert  $\chi'$  or  $\chi''$  resp.).

Finally one easily verifies with the aid of (3.17), (3.18) and (3.19) the reciprocity relations

$$\frac{p_2''}{v_1'} = -\frac{p_1''}{v_2'} \quad ; \quad \frac{p_2'}{v_1''} = -\frac{p_1'}{v_2''}.$$

From (3.18) it follows that one of the  $\chi$ 's is, in absolute value, smaller than unity and the other greater, the former belonging to the frame-wave, the latter to the air-wave.

## § 5 ELASTIC LAYER WITH CLOSED FRONT SURFACE

We now consider the particular case of an elastic layer to which the general theory applies, backed by a rigid wall and

at the front surface closed by a thin non porous covering layer of negligible mass (e g, a thin layer of paint)

The way in which this problem, that of the next section and other problems concerning elastic layers may be dealt with is in all cases essentially the same Four waves are supposed to be present in the layer, viz, an incident and reflected  $\gamma'$  wave, and similar waves of the  $\gamma''$ -type The amplitude of the first wave — the incident  $\gamma'$  wave — is completely fixed if the velocity of the frame at  $x=0$  is given Let us denote this quantity by  $v'_{1i}$  Once  $v'_{1i}$  is given all other quantities  $v'_{2i}$ ,  $p'_{1i}$ , and  $p'_{2i}$  at  $x=0$  can be computed since all ratio's  $(v_{2i}/v_{1i})'$ , etc, are fixed for the wave under consideration The dependence on  $x$  is also known through  $\gamma'$  The same reasoning applies to the other three wave types so that the wave pattern is completely determined if the four velocities at  $x=0$ ,  $v'_{1i}$ ,  $v'_{1r}$ ,  $v''_{1i}$ , and  $v''_{1r}$  are given Finally the problem is to compute the ratio's between these four amplitudes from the boundary conditions and from these ratio's again the impedance at the front surface

We shall demonstrate this procedure for the case of a layer with closed surface, this being perhaps the easiest case

For brevity we shall introduce single letters for ratio's of pressures and velocities, viz

$$p_2/p_1 = \pi \quad (\text{not to be confused with the number } 3.14),$$

$$v_2/v_1 = \varphi \quad (\text{thus distinguishing clearly from } \chi, \text{ which was used in the case } h=1),$$

$$p_2/v_2 = W_2,$$

$$p_1/v_1 = W_1$$

These four ratio's occur of course with a single or a double dash according to the wave type involved

The boundary conditions are (see Fig 23)

$$\Sigma v_1 = 0 \quad \text{for } x=l$$

$$\Sigma v_2 = 0 \quad \text{for } x=l$$

$$\Sigma v_1 = \Sigma v_2 \quad \text{for } x=0$$

These conditions give three equations in the four amplitudes from which their mutual ratio's can be computed Written in full we obtain

$$\begin{aligned}
v'_{1i} \exp(-\gamma' l) + v'_{1r} \exp \gamma' l + v''_{1i} \exp(-\gamma'' l) + v''_{1r} \exp \gamma'' l &= 0 \\
v'_{2i} \exp(-\gamma' l) + v'_{2r} \exp \gamma' l + v''_{2i} \exp(-\gamma'' l) + v''_{2r} \exp \gamma'' l &= 0 \\
v'_{1i} + v'_{1r} + v''_{1i} + v''_{1r} &= v'_{2i} + v'_{2r} + v''_{2i} + v''_{2r}.
\end{aligned}$$

Expressing all velocities in the four frame velocities at  $x=0$  yields for the matrix of coefficients

$$\begin{vmatrix}
v'_{1i} & v'_{1r} & v''_{1i} & v''_{1r} \\
\exp(-\gamma' l) & \exp \gamma' l & \exp(-\gamma'' l) & \exp \gamma'' l \\
\varphi' \exp(-\gamma' l) & \varphi' \exp \gamma' l & \varphi'' \exp(-\gamma'' l) & \varphi'' \exp \gamma'' l \\
1 - \varphi' & 1 - \varphi' & 1 - \varphi'' & 1 - \varphi''
\end{vmatrix}$$

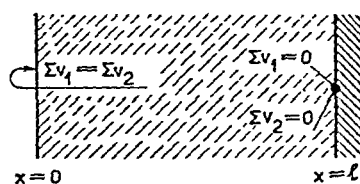


Fig. 23

Boundary conditions for a layer with closed front surface

with the aid of which one easily verifies that

$$\begin{aligned}
v'_{1r}/v'_{1i} &= -\exp(-2\gamma' l); \quad v''_{1r}/v''_{1i} = -\exp(-2\gamma'' l); \\
\frac{v''_{1i}}{v'_{1i}} &= -\frac{1 - \varphi'}{1 - \varphi''} \cdot \frac{\cosh \gamma' l}{\cosh \gamma'' l} \cdot \frac{\exp \gamma'' l}{\exp \gamma' l}. \quad (3.20)
\end{aligned}$$

The impedance at the front surface is

$$\begin{aligned}
z &= \left( \frac{\Sigma p_1 + \Sigma p_2}{\Sigma v_1} \right)_{x=0} = \\
&= \frac{p'_{1i} + p'_{2i} + p'_{1r} + p'_{2r} + p''_{1i} + p''_{2i} + p''_{1r} + p''_{2r}}{v'_{1i} + v'_{1r} + v''_{1i} + v''_{1r}}.
\end{aligned}$$

The double dash velocities of the denominator can be eliminated with the aid of the third boundary condition (see the last line of the matrix of coefficients); the numerator can be written in  $v'_{1i}$ ,  $v'_{1r}$ ,  $v''_{1i}$ ,  $v''_{1r}$  by first writing  $p_2$  as  $\pi p_1$  and then changing all pressures into velocities with the aid of  $p = \pm Wv$ .

After introduction of (3.20) one finally obtains

$$\begin{aligned}
z = & W'_1 (1 + \pi') \frac{1 - \varphi'}{\varphi' - \varphi''} \coth \gamma' l + \\
& + W''_1 (1 + \pi'') \frac{1 - \varphi''}{\varphi'' - \varphi'} \coth \gamma'' l
\end{aligned} \quad (3.21)$$

The impedance may be considered as a series connection of two impedances. We are not allowed to interpret this result thus that the impedance is composed of that of the frame and that of the air. In the extreme case of very loose coupling ( $\omega = \infty$ ,  $h = 1$ ) and  $h = 1$  (3.21) may be greatly simplified owing to (see Table 6)

$$\begin{aligned}
W'_1 &= \sqrt{K_1 \rho_1} & \varphi'' &= \infty, \\
\pi &= \frac{K_2}{K_1} \varphi \quad \left( \begin{array}{l} \text{from (3.04) and} \\ \text{(3.05) for } h = 1 \end{array} \right), & W''_1 &= W''_2 \varphi'' / \pi'', \\
\varphi' &= 0 & W''_2 &= \sqrt{K_2 \rho_2}
\end{aligned}$$

We then get

$$z = \sqrt{K_1 \rho_1} \coth j\omega l \sqrt{\rho_1 / K_1} + \sqrt{K_2 \rho_2} \coth j\omega l \sqrt{\rho_2 / K_2} \quad (3.22)$$

Now there is no objection against speaking of the frame impedance and the air impedance separately.

In the other extreme case of tight coupling the second coth in (3.21) cancels out leaving

$$z = \sqrt{(K_1 + K_2) (\rho_1 + \rho_2)} \coth j\omega l \sqrt{(\rho_1 + \rho_2) / (K_1 + K_2)} \quad (3.23)$$

as was to be expected.

Let us now discuss the results with a view to the absorption coefficient of the layer. To begin with we shall consider in more detail the case of slight coupling in which the two terms of the impedance may be looked upon more or less as giving the impedance of frame and air separately. Both terms are of spiral form in the complex plane the spiral of the second term (air) being essentially the same as discussed in Chapters I and II showing resonances and antiresonances in the audio frequency range the lowest resonance frequency will occur somewhere between 800—2000 Hz.

The first spiral (frame impedance) must be superposed upon the air spiral. The general appearance of the resulting impedance

contour is materially influenced by the ratio of the lowest resonance frequencies of frame and air. If the frame resonance frequencies are much lower than the corresponding resonance frequencies of the air ( $\rho_1 \gg \rho_2$ ;  $K_1 \approx K_2$ ; soft materials like sponge rubber, rockwool, loose wood-fibre plates of low air resistance) the character is as shown in Fig. 24.

The general upward trend of the air contour is retained. The frame resonances cause fluctuations thereon. The most important

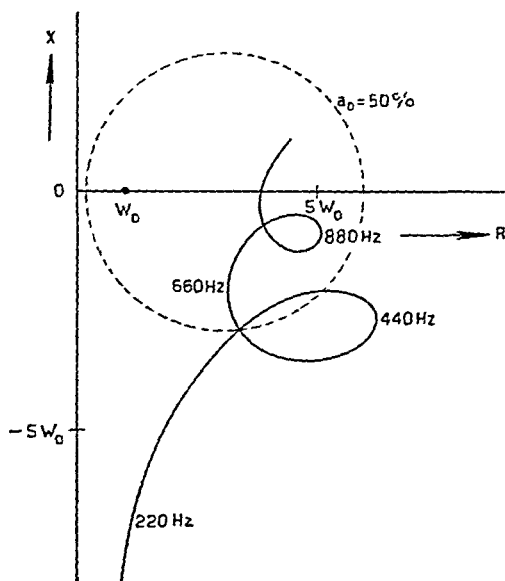


Fig. 24

Theoretical impedance contour for a layer with closed front surface

consequence, however, is the shifting of the air contour to the right along the distance of the order of the wave impedance of the frame ( $\sqrt{K_1 \rho_1}$ ). The air impedance for materials of low air resistance at low and moderate frequencies normally has a real part of the order  $W_0$ . Especially at low frequencies an increase of this real part materially increases the absorption, which may be deemed a great advantage.

In the reverse case of comparatively stiff frame ( $\rho_1 \gg \rho_2$ ;  $K_1 \gg K_2$  so that  $K_1/\rho_1 \gg K_2/\rho_2$ ; acoustic plasters, stiff wood-

fibre plates) the character of Fig 24 changes in so far that now the general upward trend is due to the frame spiral, while the fluctuations are to be imputed to the air, these fluctuations now occur at much higher frequencies (e g, 2500 and 5000 Hz instead of 440 and 880 Hz) while the shifting to the right ( $\sqrt{h_1 \rho_1}$ ) is so great that the contour comes in the low absorption part of the complex plane

The latter case is generally known, plasters and stiff wood fibre plates no longer absorb when superficially closed. The

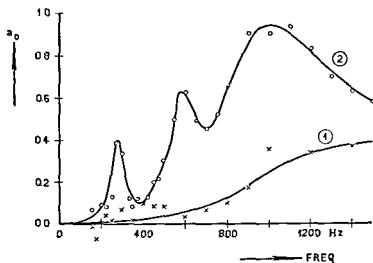


Fig 23  
Improvement of the absorption by closing the surface  
of a very elastic layer 1 open 2 closed

former case (superficially closed rather compliant materials) is the most interesting one. Much better results than with the same layers in non closed condition may be obtained especially in the important low frequency range. In Fig 25 an example of measurements is given for a sponge rubber layer of very low air resistance. The impedance curves (Fig 26, smoothed) indeed show the expected form.

The intermediate case, where the resonance frequencies of frame and air occur in the same frequency range gives rise to very complex results.

More results and detailed discussions of the agreement between

experiment and theory may be found in the original publication<sup>1</sup>.

If a material has a small coupling between frame and air we are in a position to increase the thickness of the layer of air without changing the thickness of the frame by placing the layer at a certain distance before a rigid wall.

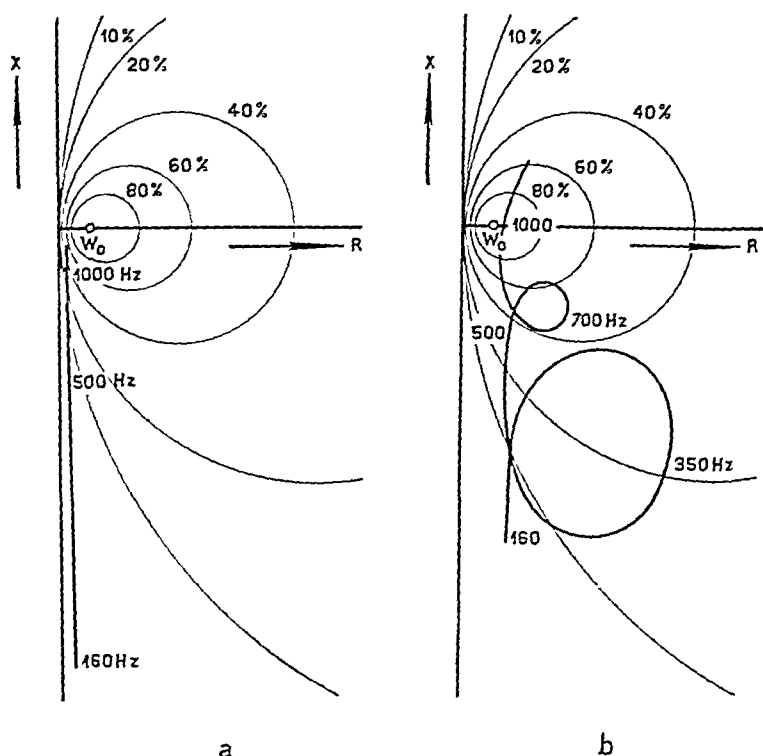


Fig. 26

Impedance contours to fig. 25

Fig. 27 shows results of such measurements, carried out on the same layer to which Fig. 25 applies. Indeed we succeeded in lowering the resonance frequencies of the air, thus obtaining a compact impedance curve in the high absorption part of the complex plane.

<sup>1</sup> C. W. Kosten and C. Zwicker, *Physica*, 8 (1941) 933.

Up to now the coating layer was assumed to be massless, a hypothetical case as a matter of fact. This mass may very easily be taken into account, if, namely, the mass per unit surface be denoted by  $m$  we only have to add  $j\omega m$  to the impedance. This means an increase of the upward trend of the impedance curve. At high frequencies  $j\omega m$  may be appreciable. The coating layer thus gives rise to a rather vague cut off frequency. For the low frequency absorption  $j\omega m$  is advantageous. Another rather important advantage of resilient, superficially closed, layers is doubtless that they can be washed and painted.

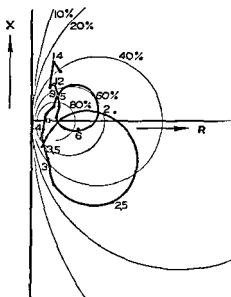


Fig 27

Impedance contour of a superficially closed layer backed with a layer of air of 78 mm frequencies indicated in 100 Hz

#### § 6 ELASTIC LAYER WITH OPEN FRONT SURFACE

This case is perhaps of more importance in practice. The mathematics are a little more complicated.

As boundary conditions, we now have

$$\Sigma v_1 = 0 \quad \text{for } x = l$$

$$\Sigma v_2 = 0 \quad \text{for } x = l$$

$$\frac{\Sigma p_1}{1-h} = \frac{\Sigma p_2}{h} \quad \text{for } x = 0$$



The latter condition is obvious since both frame and air at  $x=0$  are acted upon by the outer air pressure, the surfaces per unit surface of porous material being  $1-h$  and  $h$  respectively, the forces  $p_1$  and  $p_2$  by definition.

If again four waves are supposed to be present, given by  $v'_{1i}, v'_{1r}, v''_{1i}, v''_{1r}$  (velocities at  $x=0$ , i.e., at the front surface), the third boundary condition may be expressed in these variables as was done in the preceding § 5.

All pressures  $p_2$  are expressed in  $p_1$  by  $p_2 = \pi p_1$ ; then all remaining pressures  $p_1$  are changed into the corresponding velocities with the aid of  $p = \pm Wv$ . We obtain

$$W'_1 \{ h - (1-h) \pi' \} (v'_{1i} - v'_{1r}) + \\ + W''_1 \{ h - (1-h) \pi'' \} (v''_{1i} - v''_{1r}) = 0.$$

From this equation and the first two boundary conditions, which are equal to those of the preceding section, all ratio's between  $v'_{1i}, v'_{1r}, v''_{1i}$ , and  $v''_{1r}$  can be computed.

After insertion in the expression for the impedance

$$z = \left( \frac{\Sigma p_1 + \Sigma p_2}{\Sigma (1-h) v_1 + \Sigma h v_2} \right)_{x=0}$$

we finally find after tiresome but elementary calculations

$$\frac{1}{z} = \frac{(1-h+h\varphi') \{ h-(1-h)\pi'' \}}{W'_1(\pi' - \pi'')} \tanh \gamma' l + \\ + \frac{(1-h+h\varphi'') \{ h-(1-h)\pi' \}}{W''_1(\pi'' - \pi')} \tanh \gamma'' l. \quad (3.24)$$

For materials for which  $h=1$  holds to a good approximation equation (3.24) simply runs

$$\frac{1}{z} = \frac{\varphi'}{W'_1(\pi' - \pi'')} \tanh \gamma' l + \frac{\varphi''}{W''_1(\pi'' - \pi')} \tanh \gamma'' l. \quad (3.25)$$

The impedance turns out to be the result of a shunt-connection of two impedances. In the case of slight coupling the impedance may be considered to be the air-impedance, more or less short-circuited by the frame-impedance. This short-circuiting is most effective for small frame-impedances, i.e., when the frame is in the neighbourhood of resonance.

Theoretical results of shunt-connections like (3.24) may best

be represented in an acoustical admittance diagram. From the general equation, giving the absorption coefficient as a function of the impedance (equation (112)) one sees at once that the absorption coefficient does not change, when instead of the impedance the admittance is inserted, provided impedances are measured in  $W_0$  as unit. This means that the lines of constant absorption in the complex admittance plane are the same circles as used up to now in the impedance plane.

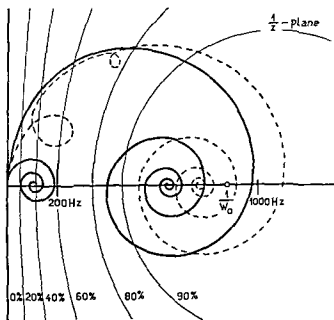


Fig 28

Admittance contour of a layer with open front surface

In Fig 28 an example is given. The assumptions underlying this figure are slight coupling,  $\rho_1 \gg \rho_2$ ,  $K_1 \approx K_2$ . The second term (air admittance) is a normal spiral with its first resonance at about 1000 Hz. A complex  $\tanh$  is represented by a spiral like a coth, only it begins in the origin instead of at infinity. It should be noticed that the apex of the spiral shifts towards the origin if the wave-impedance increases. In our case, therefore the frame spiral is small and turns rapidly owing to the low resonance frequencies. The superposition of the two spirals gives a more or less modified air spiral (dotted in Fig 28). The in

fluence may be of some importance in the low frequency range.

If the coupling is not small the terms air-spiral and frame-spiral gradually loose their significance. In the limit of very tight coupling one of the spirals cancels out, the remaining being related to the normal coupled wave (see equation (3.23)).

# § 7 ELASTIC LAYER BACKED OTHERWISE THAN BY A RIGID WALL

If an elastic layer is backed by a membrane of impedance  $z_b$ , the boundary conditions ( $\Sigma v_1 = 0$  and  $\Sigma v_2 = 0$  for a rigid wall) should be replaced by

$$\left( \frac{\Sigma p_1 + \Sigma p_2}{\Sigma(1-h)v_1 + \Sigma hv_2} \right)_{x=l} = z_b; \quad v_1 = v_2 \text{ at } x=l.$$

The condition  $v_1 = v_2$  expresses the fact that the receiving material of impedance  $z_b$  is essentially not double-refracting. If this material is a rigid porous one, we have to substitute the boundary conditions by

$$v_1 = 0 \text{ at } x=l, \quad \frac{p_2/h}{hv_2} = z_b \text{ at } x=l,$$

if now  $z_b$  is the impedance of the receiving material as for instance measured in an interferometer.

## CHAPTER IV

### EXPERIMENTAL DETERMINATION OF THE ELEMENTARY MATERIAL CONSTANTS OF POROUS ABSORBENTS GOVERNING THE ABSORPTION COEFFICIENT

#### § 1 INTRODUCTION

A few elementary material constants entered into the theoretical considerations of Chapters I to III, viz., the porosity  $h$ , the structure factor  $k$ , the air resistance  $\sigma$  and, for elastic layers, the "compression modulus" of the frame  $K_1$ . As we saw (I § 8) the structure factor can hardly be expected to follow from any statical or steady flow measurement. It is very compheately linked up with the structure of the material. The porosity can easily be determined from steady-state or low frequency measurements, although there is some evidence (see II § 9) that the value thus found is too great to meet the acoustical situation. Anyhow, the measurement of the steady state or low frequency value will give us a rough estimate of the true value. The measuring method for determining this value is given in IV § 2.

The dynamical value of the air resistance can be computed from the steady state value, provided we know whether Poiseuille's law or Helmholtz's theory applies. Therefore the steady state value is no doubt of importance (see IV § 3).

The measurement of  $K_1$  seems easy, but really it is not. What we really want is a knowledge of the complex quantity  $K_1$ , which can only be obtained dynamically. It seems plausible that a statical measurement of the stiffness of a sample should give us the modulus of  $K_1$ . However it is a rather well known fact that the dynamical modulus may be several times the statical one. At low frequencies (say 5—50 Hz)  $K_1$  normally varies so little with the frequency that an extrapolation to acoustical frequencies seems allowed. One disagreeable restriction should however be made. We ought to measure the frame stiffness freed from any air stiffness. So if  $\sigma$

is high (tight coupling) the measurement should be carried out in vacuo; if  $\sigma$  is low it may be sufficient to provide for ample passage to the surrounding air. This difficulty may be avoided by computing  $K_1$  from the measurement of the rigidity modulus  $G$  (against shearing). Properly speaking this only holds good for isotropic materials, but also for non-isotropic materials (e.g., wood-fibre plates) this procedure will probably provide us with a reasonable accurate value of the complex quantity  $K_1$  (see IV § 4). An idea of the degree of inhomogeneity might moreover be obtained by taking samples of different orientation.

## § 2 THE POROSITY

Making use of Boyle's law  $pV = \text{constant}$ , the porosity can be determined with the aid of the apparatus shown in Fig. 29<sup>1</sup>. The specimen of known external volume is placed in the vessel of volume  $V_0$  this being filled up, when necessary, with glass plates to reduce the dead volume. Increase of volume is effected by opening the tap F, and by adding the volume of one or more of the spheres  $V'$ ,  $V''$ , etc., to  $V_0$  by lowering the vessel B. The change of pressure is measured with the manometer E. Meanwhile the level at C is kept at the same height with the aid of the taps at the top of tube D.

The following details are worth mentioning. Both the set of bulbs  $V'$ ,  $V''$ , etc., and the manometer part E—D have to be placed in a water thermostat. As manometer fluid, o-di-iso-amyl-phthalate was chosen, because of its combination of low density, low volatility and low viscosity. Some results may be mentioned here.

Porous plasters have porosities ( $h$ ) between the values 0.50 and 0.75.

For wood-fibre plates, values were found in the neighbourhood of  $h = 0.80$ .

Felt, sponge rubber, and cork samples all have high porosities, varying between 0.85 and 0.95.

Recently an attractive device was described by Leonard<sup>2</sup>

<sup>1</sup> J. Van den Eijk and C. Zwikker, *Physica*, 8 (1941) 149.

<sup>2</sup> R. W. Leonard, *J. Acoust. Soc. Am.*, 20 (1949) 39.

which permits the measurement of the porosity under low frequency conditions. At extremely low frequencies the wave character of the sound inside the absorbing material may be left

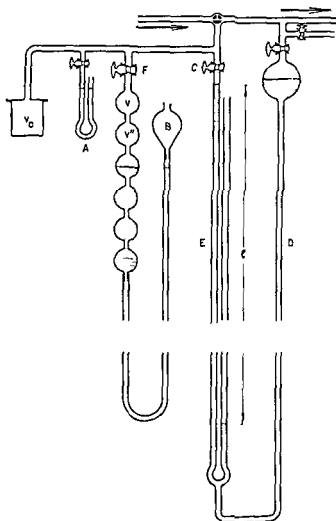


Fig. 20  
Porosity meter

out of consideration. The air content mainly behaves as a spring the compliance per  $m^2$  of which is proportional to the total amount of air per  $m^2$  included in the material, i.e., proportional to the thickness and the porosity. The main features of *Leonard's*

apparatus may be seen from the schematical figure 30. A resonant system is built up of which the stiffness is for the greater part due to the air content. Therefore the porosity can be computed from the resonance frequency. Leonard claims as advantages

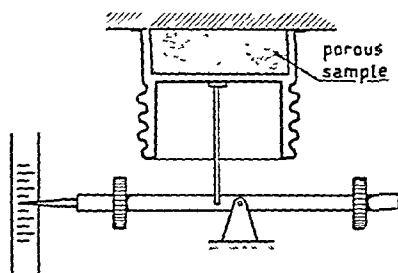


Fig. 30  
Leonard's porosity meter

that his method is not sensitive to changes of temperature, a great advantage as a matter of fact; moreover the volume of difficultly accessible pores and holes does not contribute to the porosity found. Indeed (see Chapter II § 9) the effective porosity will decrease with increasing frequency.

### § 3 THE AIR RESISTANCE

An apparatus for the determination of the stationary air-resistance  $\sigma$  is given in outline in Fig. 31. On the specimen A

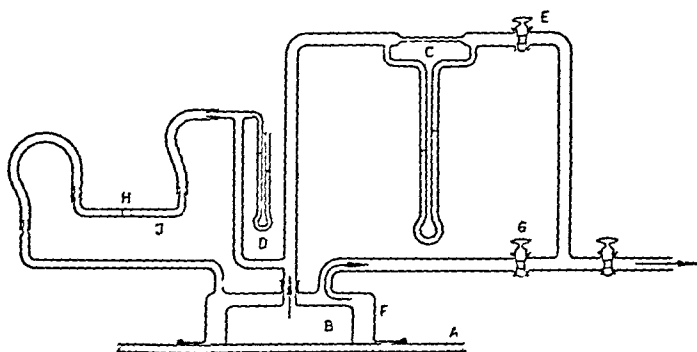


Fig. 31  
Air resistance meter

a box B is placed in which a small subatmospheric pressure is maintained with the aid of an air pump. This pressure is measured with a F u e s s micromanometer D. The velocity of the air current is measured by a capillary flowmeter C. In order to prevent any radial currents in the specimen, box B is enclosed in a wider box F in which the pressure is kept at exactly the same values as in B (principle of the guard ring). This equality is checked by means of a drop of o-di-iso amyl-phthalate H, which is to remain at rest inside the capillary J. Box F is fastened along the edge on the specimen A by means of plaster of Paris.

Practical values of the air resistance vary between  $10^4$  and  $10^7$  mks units. In order to meet this wide range different capillary tubes have to be used, or what comes to the same thing but is much easier the air resistance of the capillary tube may be changed by inserting one or more chromel wires of different diameter in the tube.

An apparatus was constructed along these lines in the laboratory of the authors. The calibration characteristics of the flowmeter were not straight lines, neither when the volume velocity was plotted against the pressure difference, nor when it was plotted against the difference between the squares of the pressure. Pressure differences of the order of 0.02 to 2 mm water height (i.e., 0.2 to 20 N/m<sup>2</sup>) were used, yielding air-currents of about 3 to 180 cm<sup>3</sup>/sec. The inner surface of the samples was always 400 cm<sup>2</sup>. Specific air resistance between  $10^3$  and  $3 \cdot 10^7$ , therefore, could be measured. The relative error amounted to about 15 % (see for practical values of  $\sigma$  II § 5).

Measurements without a guard ring are also common practice. The cylindrical samples, needed for the measurements in the acoustic interferometer, are then used. For the air resistance measurement the side surfaces of the sample have to be closed with solid paraffin in order to procure a parallel flow of air through the sample.

Leonard<sup>1</sup> developed an apparatus for measuring the air resistance in which an analytical balance is used at the same time as air pump, pressure meter and velocity meter (see Fig 32),

---

<sup>1</sup> R. W. Leonard, *J. Acoust. Soc. Am.*, 17 (1946) 240



which can be used for values of air-resistance as low as 1000 mks, using air-pressure differences as low as  $1 \text{ N/m}^2$ . The accuracy is about 2 %.

The uniformity of a material may be checked by taking samples of different thickness of one and the same material. As a rule the surface of every layer is less impervious than the interior part.

For high absorption  $\sigma l/3$  should be of the order of  $\rho_0 c_0$  (420 mks) (see II § 7). This demands specific air-resistances of the order of  $5 \cdot 10^4$  mks; these are found in high-resistance plasters and low resistance felts.

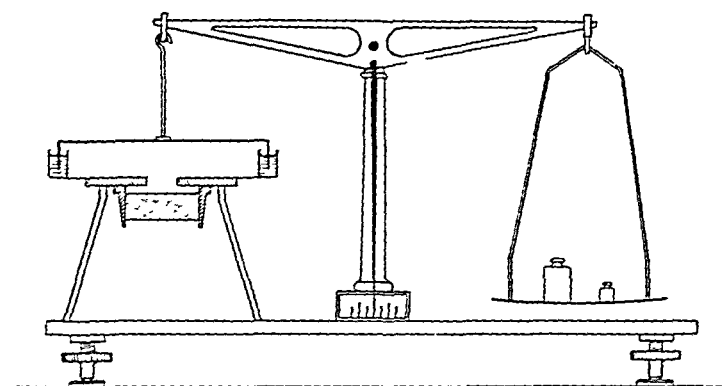


Fig. 32  
Leonard's air resistance meter

#### § 4 THE COMPRESSION MODULUS

As pointed out in IV § 1  $K_1$  cannot be measured statically. If measured at low frequencies, the results have to be extrapolated to audiodrequencies; moreover due account should be taken of the influence of the enclosed air. The air may virtually increase both the stiffness and the losses.

In order to avoid measurements in vacuo we can have recourse to shearing measurements. Since shearing of a material does not give rise to a change of volume the stiffness of a sample against shearing is independent of the air-content, and since displacements of air in the interior might be assumed to be absent or small, the air will not materially increase the losses. So the rigidity

modulus  $G$  will practically coincide with the value in vacuo

$K_1$  is, according to its definition, the stiffness of unit volume of porous material if sideways extensions or contractions are prohibited. Now this is neither the definition of the compression modulus  $K$  nor that of the modulus of elasticity (Young's modulus)  $E$ . If the material under consideration is isotropic, one can easily derive

$$2 G (m - 1) = K_1 (m - 2),$$

where  $m$  is Poisson's ratio ( $m > 2$ )

Now for all practical porous materials  $m$  will be rather high (say 10 or more) so that we may approximately put  $m$  equal to infinity, yielding

$$K_1 \approx 2 G$$

The measurements can be accomplished with any one of the apparatus for measuring mechanical impedances. Suitable apparatus have been described by Meyer and Keidel<sup>1</sup>, Costadoni<sup>2</sup>, Böhme<sup>3</sup> and the authors<sup>4</sup>. In principle the normal acoustic interferometer may be used for this purpose too, though special precautions have to be taken.

If the measurements are carried out at audiofrequencies with samples, the resonance frequencies of which be in the frequency range used, the impedance will be spiral like as in Chapter I. Marvellous results of this type have been obtained by Böhme<sup>3</sup> with solid materials (e.g., rubber). The authors measured at low frequencies so that inertia effects are of no importance. Then, of course, the results must be extrapolated very far.

#### § 5 RESULTS OF MEASUREMENTS OF THE COMPLEX STIFFNESS

Experimental data on the specific stiffness  $K_1$  and the loss angle  $\delta$  of porous materials from measurements in vacuo or derived from shearing experiments are not available.

The static value of  $K_1$  is readily measured. Its magnitude may

<sup>1</sup> E. Meyer and L. Keidel, *Z. tech. Phys.*, 18 (1937) 209.

<sup>2</sup> B. C. Costadoni, *Z. tech. Phys.*, 17 (1936) 100.

<sup>3</sup> H. Böhme, *Akust. Z.*, 2 (1937) 303.

<sup>4</sup> C. W. Kosten and C. Zwicker, *Physica*, 4 (1937) 221.

be as low as  $1/_{100}$  of that of air for soft fibrous materials,  $1/_{10}$  for soft sponge rubber and up to practically infinite values for plasters.

The best estimate of the dynamic complex value of  $K_1$  is perhaps obtained by multiplying the static value by the ratio  $K_{1 \text{ dyn.}}/K_{1 \text{ stat.}}$  obtained for non-porous materials of the same kind and assigning a loss angle to the value thus obtained at least equal to that of the solid material. It is therefore worth while to summarize briefly a few results of the ratio  $K_{1 \text{ dyn.}}/K_{1 \text{ stat.}}$  and of the loss angle  $\delta$  for solid materials.

An instructive example of a soft non-porous material for which data are available<sup>1</sup> is rubber. If properly vulcanized and relatively "pure", i.e., without unnecessary filling materials, dynamic and static stiffness are practically equal, the loss angle is only of the order of  $1^\circ$ . If the material is more or less under-vulcanized the dynamic stiffness exceeds the static one by a factor of 2 or even more. At the same time the loss angle increases to values of  $5^\circ$ — $10^\circ$ . Moreover the material is also less ideally elastic under static load; after removing the static load the initial height turns out to be less (permanent set, flow). The same effects as caused by under-vulcanization are found by using filling materials like barium sulphate, carbon black, etc. Synthetic rubbers generally show the same behaviour as under-vulcanized natural rubber, i.e., greater dynamic than static stiffness, loss angles between  $5^\circ$  and  $10^\circ$ , although it greatly depends, of course, on the kind and manufacture. The behaviour of this class of rubber and rubber-like materials is governed, therefore, to a great extent by elastic after-effect during the deformation.

It is not within the scope of this book to enter into the theoretical aspects of the dynamic behaviour and the internal friction in metals, wood, etc. Since the characteristic frequencies of bodies of such solid materials, as computed from the static elastic constants agree with those actually found, it may be inferred that static and dynamic stiffness for these materials are practically equal. The loss angle is mostly small, say  $0^\circ$ — $1^\circ$ .

It is very doubtful whether porous structures of similar

---

<sup>1</sup> C. W. Kosten, *Proc. Rubb. Techn. Conf.*, p. 987, London 1938.

materials as wood fibre plates hair felt glass silk etc have the same behaviour Measurements carried out in air<sup>1</sup> yield dynamic stiffness values up to 10 times the static one and in extreme cases even higher Friction between the fibres may increase the losses the loss angle  $\delta$  varies between  $2^\circ$  and  $20^\circ$  Values of  $\delta$  greater than  $10^\circ$  are almost undoubtedly due to the streaming of the air in and out of the sample In the case that the flow of air contributes much to the losses both  $K_1$  and  $\delta$  are strongly dependent on frequency<sup>2</sup> The low frequency values of  $K_1$  and  $\delta$  approximate to the values in vacuo It should be emphasized that whereas for normal incidence of sound on an infinite layer of absorbing material the coupling is highest at the lower frequencies the reverse is true in measuring the compression of small samples where the air may escape sideways The sample behaves as an air-container with leakage requiring a minimum time to assume the atmospheric pressure inside after having been pumped up by compression

---

C Van Gijn and C Zwicker *Ingenieur* (Dutch) 56 (1941) O 11  
 E Meyer and L Keidel *Z tech Phys* 18 (1937) 299 E Meyer  
*Z Ver deut Ing* 78 (1934) 1907

<sup>2</sup> C W Kosten and C Zwicker *Physica* 4 (1937) 843

## CHAPTER V

### MEASUREMENT OF NORMAL IMPEDANCE AND ABSORPTION

#### § 1 INTRODUCTION

Practically all devices for measuring the impedance of materials (from which the absorption coefficient may be derived with the aid of Fig. 11) make use of a measuring tube in order to create plane travelling waves. At the one end the sound source is placed, whereas the tube is terminated at the other end by the sample under test. The number of methods for measuring the impedance is practically unlimited. The sound pressure is measured as a function of the distance from the sample, of the frequency or of the length of the tube. Three adequate quantities are necessary in general (e.g., two pressures and one distance), provided damping of the travelling waves in the tube owing to the Helmholtz—Kirchhoff effect is neglected. A rather complete survey of the various possibilities has been given by Beranek<sup>1</sup>. It is impossible and unnecessary to mention all methods here. We shall confine ourselves to the description of a few of them, viz.

a. constant length method, measuring maximum and minimum pressure in the tube (see § 2).

b. variable length method, measuring maximum and minimum pressure at the sound source (see § 3).

c. variable length method, measuring curve width of pressure at the source (see § 4).

d. variable length method, measuring the electrical impedance of the sound source (see §§ 5 and 6),

e. short length tube, measurement of pressure and velocity (see § 7).

---

<sup>1</sup> L. L. Beranek, *J. Acoust. Soc. Am.*, 12 (1940) 3, table I, p. 4.

## § 2 CONSTANT LENGTH INTERFEROMETER

If the sound source operates at such a low frequency that the wave length is greater than 1707 times the diameter  $D$  of the tube, only plane waves can travel in the tube<sup>1</sup> In the neighbourhood of the source these plane waves are disturbed if the sound source generates non plane waves The same holds for the neighbourhood of the sample A non homogeneous sample may reflect the incoming plane wave as a distorted reflected one At some distance from the sample the reflected wave will be plane again if the wave length is long enough Therefore all interferometers can only be used up to frequencies less than  $c_0/17D$  This restriction can not be neglected if the source provides us with ideally plane waves since all samples are more or less inhomogeneous and will reflect travelling non plane waves if the frequency is chosen too high Assuming that this restriction is fulfilled and denoting the impedance of the sample by  $z$  we may describe the sound field in the tube as the superposition of two plane waves an incoming and a reflected one Owing to absorption the reflected one will be of smaller intensity than the incoming one We may borrow from equation (112) the relation between the reflection coefficient  $r = p_r/p_i$  directly before the sample and the impedance  $z$

$$r = \frac{z - W_0}{z + W_0} \quad \text{or} \quad \frac{z}{W_0} = \frac{1 + r}{1 - r} \quad (5.01)$$

Remembering that the propagation constant  $\gamma$  of air is  $j\omega/c_0$  we can write down the pressure at a distance  $x$  in front of the sample

$$p(x) = p_i \exp(-j\omega x/c_0) + r p_i \exp(+j\omega x/c_0) \quad (5.02)$$

The exponentials have modulus unity and only change the phase of the travelling waves (damping is neglected!)

Writing as previously

$$r = |r| \exp j\Delta,$$

(5.02) takes the form

$$p(x) = p_i \exp(-j\omega x/c_0) + |r| p_i \exp j(\omega x/c_0 + \Delta) \quad (5.03)$$

---

<sup>1</sup> Rayleigh, *Theory of Sound* II, 2nd ed, p 161, Cambridge 1896

The pressure  $p(x)$  will be a minimum for those values  $x_n$  of  $x$  for which both terms are in opposite phase, i. e., for

$$(\omega x_n/c_0 + \Delta) - (-\omega x_n/c_0) = -(2n+1)\pi,$$

where  $n$  is an integer. The latter equation yields

$$\Delta = -(2n+1)\pi - 4\pi n/\lambda. \quad (5.04)$$

This equation offers us a means of measuring  $\Delta$ .  $\Delta$  may be computed from the position of the places of minimum sound pressure in the tube. It turns out to be too inaccurate to compute  $\lambda$  from frequency and sound velocity. More reliable values of  $\Delta$  are obtained by measuring the positions of two minima (e. g.,  $x_0$  and  $x_1$ ) and eliminating  $\lambda$ . One sees at a glance from (5.03) that the ratio of maximum and minimum pressure is

$$\frac{p_{\max.}}{p_{\min.}} = \frac{1 + |r|}{1 - |r|} \quad (5.05)$$

This ratio can easily be measured, from which  $|r|$  is found. So (5.04) and (5.05) are a basis for measuring modulus and argument of  $r$ .

Numerous instruments have been designed along these lines, mutually differing only in the way the pressure is measured. Tuma<sup>1</sup> used the ear, and attained only inaccurate results. Taylor<sup>2</sup> used the Rayleigh disc, placed in a side tube. Paris<sup>3</sup> made use of anemometer wires. So did Goldbaum and Waetzmann<sup>4</sup>. Eckhardt and Chrisler<sup>5</sup> used an exploring tube, a tube of very small diameter in comparison with that of the interferometer, forming an acoustical connection between the microphone outside the interferometer and the measuring point inside. This technique was, then, adopted by numerous other investigators. Although the use of an exploring tube is convenient and rather reliable it cannot be denied that it is a source of error. Its impedance is not infinitely high, so

<sup>1</sup> J. Tuma, *Sitzber. Kaiserl. Akad. Wiss.*, 3 (1902) 402.

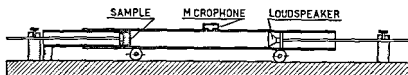
<sup>2</sup> H. O. Taylor, *Phys. Rev.*, 2 (1913) 270.

<sup>3</sup> E. T. Paris, *Proc. Phys. Soc.*, 39 (1927) 269.

<sup>4</sup> G. Goldbaum and E. Waetzmann, *Z. Physik*, 54 (1929) 179.

<sup>5</sup> E. A. Eckhardt and V. L. Chrisler, *Bur. Standards Sci. Paper No. 526* (1926).

it disturbs the sound field. Moreover even if its impedance were infinite it would disturb the field by its geometrical shape. Rough calculations show that errors of the order of the ratio of the cross sections of the exploring tube and the interferometer tube in the impedance are to be expected. A method that has the great advantage of not disturbing the sound field is shown in Figs 33 and 34. The microphone is built into the tube wall



F g 33

Constant length interferometer without exploring tube

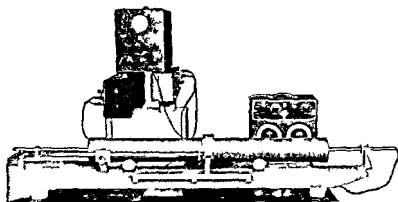


Fig 34

Fotography to F g 33

(see also Fig 35) behind a stiff membrane and can be moved together with the whole tube in which loudspeaker and sample holder fit in an airtight way like pistons. This method seems to have been developed independently by various investigators. It might seem a source of error to use a membrane of  $1 \text{ cm}^2$

<sup>1</sup> W. V. Hall, *J. Acoust. Soc. Am.* 11 (1939) 140. J. Harman, *Acust. Z.* 5 (1940) 215. J. v. d. Engk, C. W. Kosten and W. Kok, *Appl. Sci. Research B* 1 (1947) 50.



or more, since it will be impossible to measure in that way the sound pressure at a "single" point. This objection, however, is not correct. If, for example,  $r=1$   $p_{\min.}$  is zero; the pressure of the standing wave varies as  $\sin \omega x/c_0$  with the place in the tube, if  $x$  is the distance from the point under consideration to the place of minimum pressure, so the pressure is not zero in the vicinity of this point, but is in opposite phase at either side; no force is therefore exerted on a membrane, placed symmetrically with respect to the measuring point. In a similar way it can be shown that also in the general case  $|r| < 1$  no error is made in measuring the ratio  $p_{\max}/p_{\min.}$  (see Van den Eijk, Kosten, and Kok page 88<sup>1</sup>).

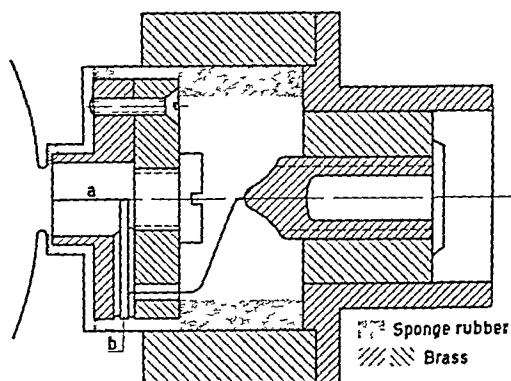


Fig. 35

Details of the microphone of the interferometer of Fig. 33

### § 3 WENTE AND BEDELL'S METHOD<sup>1</sup>

If the length of the tube is changed by moving the sample in the tube and provision is made to keep the strength (velocity) of the source constant, the sound pressure at the source will be proportional to the impedance of the tube at the source, looking into the tube terminated by the sample. The ratio of  $p_{\max.}$  to  $p_{\min.}$  is, therefore, equal to the ratio of  $z_{\max}$  and  $z_{\min.}$ . If the impedance  $z$  of the sample is known, we might compute this ratio with the aid of equation (1.04), a tiresome way, as a matter of fact. With-

<sup>1</sup> E. C. Wente and E. H. Bedell, *Bell Syst. Tech. J.*, 7 (1928) 1.

out any calculations the result may be read from the circle diagram, Fig 11. If the length of the tube varies, the impedance at the source must run through a circle of constant absorption in Fig 11, for the absorption of the sample alone is equal to that of the sample with a layer of air in front of it. The extreme values of the impedance obviously are the points of intersection of the impedance circle with the real axis, for which one easily finds from (5.01)

$$z_{\max}^{\min} = W_0 \frac{1 \pm |r|}{1 \mp |r|}.$$

Therefore, the ratio of  $p_{\max}$  and  $p_{\min}$  is

$$\frac{p_{\max}}{p_{\min}} = \left( \frac{1 + |r|}{1 - |r|} \right)^2, \quad (5.06)$$

the same expression as (5.05) except for the second power. (5.06) is the basis for measuring  $|r|$ . The argument  $\Delta$  is readily obtained from the tube lengths at which extreme values of  $z$  are found, again with the aid of Fig 11. With increasing length of the tube the impedance runs through the absorption circle in a clockwise sense, covering  $2\pi$  in  $\Delta$  for every half wave length. So the first maximum will be found for

$$l/\frac{1}{2}\lambda = \Delta/2\pi,$$

the first minimum for

$$l/\frac{1}{2}\lambda = (\Delta + \pi)/2\pi, \text{ etc}$$

In order to provide a sound source with constant strength Wente and Bedell used a telephone acting upon a heavy piston, the sound pressure at the source was measured with an exploring tube

#### § 4. CURVE WIDTH METHOD

This method resembles Wente and Bedell's method in so far that it is also a variable length method with a source of constant strength, what is measured is also the pressure at the source end of the tube. There are, however, essential differences

---

<sup>1</sup> L. L. Beranek *J. Acoust. Soc. Am.*, 12 (1940) 3

To begin with, Beranek uses a "point" source at the centre of the source end by supplying the sound energy through a high impedance *thin* tube. The sound source, therefore, has a high internal impedance and gives a velocity independent of the load. The pressure at the source end is a function of the radius, since the waves are not plane in the vicinity of the source. Beranek derives this function and shows that the most adequate place for measuring the pressure is at the source side quite near to the wall of the interferometer tube. Furthermore he does not measure maximum and minimum pressure, but derives the damping of the standing longitudinal wave from the curve width near maximum pressure if the tube length varies. This has the great advantage that no measurements are necessary at low pressure level. Damping, caused by energy losses at the interferometer wall itself is taken into account by determining the damping with a perfectly reflecting wall instead of the sample. From these two values of the damping and the two corresponding resonant lengths the impedance can be computed. Various provisions have been made for improving the accuracy, e.g., a precision screw for accurate measurement of the displacement of the sample.

Beranek's method is original and in many respects admirable. His proof of orthogonality of the eigenfunctions seems to be incorrect (*loc. cit.*, p. 7), since the ratio of the normal component of the particle velocity to the pressure should be independent of the eigenvalues at the tube wall, which certainly is not the case. Moreover it seems questionable whether all refinements of his apparatus are necessary in view of other sources of error, e.g., mounting conditions of the sample, differences between various samples of the same material, the uncertainty of the definition of what is called the surface of the sample.

## § 5 REACTION-ON-SOURCE INTERFEROMETERS

The electrical impedance of all electrical sources of sound depends more or less upon the acoustical load. If the source is prevented from vibrating by fixing the cone, the membrane or the emitting surface in general, the electrical impedance, as measured in the normal way at the input terminals of the source,

will be called the *blocked* impedance  $Z_b$ . If the emitting surface can vibrate, a different impedance  $Z$  is found. The difference  $Z - Z_b$  is generally called the motional impedance, it will be labeled  $Z_{\text{mot}}$ . Now  $Z_{\text{mot}}$  depends upon the acoustical impedance at the vibrating surface. It is, therefore, plausible that the latter can be calculated from the measured value  $Z_{\text{mot}}$ . The method is extremely attractive in that the whole measuring equipment is an audiofrequency generator and an electrical impedance bridge. Attenuators, amplifiers, microphones, etc., are no longer necessary. The method has the disadvantage that it has not yet been worked out in all details. The results, obtained up to now, justify the opinion, however, that it can turn out to be of great value.

It can be shown that for all normal sources the following general equation holds

$$Z = L + \frac{M}{N + z}, \quad (5.07)$$

in which  $L$ ,  $M$  and  $N$  are in general complex constants which should be measured as a function of frequency and  $z$  is the acoustical impedance at the source. We shall derive this equation for the electrodynamic loudspeaker and the telephone.

*a Reaction on an electrodynamic loudspeaker* Let

$u$  = voltage on the coil,

$i$  = current through the coil,

$B$  = the constant magnetic induction in the slit

$l$  = the total length of the winding,

$v$  = velocity of the coil,

then

$$u = Z_b i + Blv, \quad (5.08)$$

in which  $Blv$  is the e.m.f. of induction due to the motion. The equation of motion, in the case that the only external force acting on the system is the reaction force of the acoustical load, may be written

$$0 = -Bl i + Z_{\text{mech}} v, \quad (5.09)$$

where  $Bl i$  stands for the Lorentz force on the winding.  $Z_{\text{mech}}$

is built up of two parts, the internal mechanical impedance of the cone (mass, stiffness, and resistance) and the mechanical impedance at the site of the coil due to the acoustical load.

Elimination of  $v$  from (5.08) and (5.09) and putting  $Z$  for  $u/i$  gives

$$Z = Z_b + (Bl)^2/Z_{\text{mech}}. \quad (5.10)$$

If the cone were replaced by a piston and if this piston were acoustically loaded with a specific acoustic impedance  $z$ , constant over the entire surface  $S$  of the piston, e. g., by placing the source in a suitable interferometer tube, we should have

$$Z_{\text{mech.}} = Z_{\text{piston}} + zS,$$

which brings (5.10) into the general form (5.07). A normal loud-speaker does not in the least comply with this idealized situation. It was shown, however, by one of the authors<sup>1</sup> that (5.10) may be transformed into (5.07) in the general case that the velocity of the vibrating surface varies over the surface and the loud-speaker does not fit into the tube without leakage. Now  $M$  and  $N$  of (5.07) become complex functions of frequency which have to be determined, moreover  $L$  is not the blocked impedance, but the impedance that is found when the acoustical load is infinite. Owing to flexibility of the cone and air leakage around the speaker the coil is not completely blocked if  $z = \infty$ .

*b. Reaction on a telephone.* Kennely and Pierce<sup>2</sup> were probably the first to measure the mechanical load of a telephone by its influence on the electrical impedance. Fay and Hall<sup>3</sup> applied this method to a tube of variable length, closed by a sample. The validity of (5.07) in this case is simply proved by Fay and Hall from energy considerations. We shall follow their derivation, which they also applied to the preceding case. We must, however, define very precisely the quantities used. If

<sup>1</sup> C. W. Kosten, *Appl. sci. Res. B*, 1 (1947) 35.

<sup>2</sup> A. E. Kennely and G. W. Pierce, *J. Franklin Inst.*, 200 (1912) 467.

<sup>3</sup> R. D. Fay and W. M. Hall, *J. Acoust. Soc. Am.*, 5 (1933) 46.

no current is supplied to the telephone the permanent magnet supplies the equilibrium flux that exerts an attractive force on the iron membrane. If we give a small displacement to the membrane the flux, and thereby the force, will increase. This force has nothing to do with any electrical input. It is considered as an internal force of the magneto-mechanical system. The magnetic set up, therefore, behaves and is treated as a system with a *negative* stiffness. If at the same time a current is supplied, an *other* contribution to the flux is made, increasing the force on the membrane. This force, which originates in the current will be called the force on the mechanical system, and is labeled  $F$ . A similar distinction must be made in the e.m.f. of induction due to variations in flux. If the membrane is blocked and a current is supplied there is an e.m.f. of self induction. If at the same time the membrane is given a velocity there occurs an extra e.m.f. of induction caused by the velocity. This e.m.f. will be called the back e.m.f. and be labeled  $e$ .

If furthermore  $i$  be the current and  $v$  the velocity of the point to which  $F$  is applied the extra power supplied at any instant to maintain the motion  $ei$ , will be equal to the product  $Fv$ , i.e., to the power transmitted at that moment by the system. therefore

$$ei = Fv$$

Now if

$$e = Lv$$

we have

$$i = F/L,$$

and therefore

$$e/i = L^2 v/F$$

or

$$Z_{mot} = L^2/Z_{mech} \quad (5.11)$$

From this derivation it is clear that  $Z_{mech}$  is the sum of the internal mechanical impedance of the system negative magnetic spring included and the mechanical impedance of the external acoustical load, as felt at the driving point of  $F$ . We have now arrived at an equation corresponding to (5.10) of the electro-dynamical loudspeaker and follow the same method to transform the result into the general equation (5.07) in order to allow for non plane motion of the membrane and air leakage in the interferometer (see Kosten, page 93<sup>1</sup>)

## § 6 THE DETERMINATION OF THE ABSORPTION COEFFICIENT WITH REACTION INTERFEROMETERS. PRACTICAL ASPECTS

Equation (5.07) is the general basis for measuring impedances. The constants  $L$ ,  $M$  and  $N$ , however, have to be determined by calibration. This can be done by measuring the electrical impedances  $Z_1$ ,  $Z_2$  and  $Z_3$  if the source is loaded by three known acoustical impedances  $z_1$ ,  $z_2$  and  $z_3$ .

We can then express  $L$ ,  $M$  and  $N$  in  $Z_1$ ,  $Z_2$  and  $Z_3$ , by which (5.07) can be shown to assume the form

$$\frac{z}{\rho_0 c_0} = j \frac{Z_1 - Z_3}{Z_1 - Z_2} \cdot \frac{Z - Z_2}{Z - Z_3}.$$

The quotient  $(Z_1 - Z_3)/(Z_1 - Z_2)$  has to be looked upon as a new constant of the apparatus, being a function of the frequency only.

If we choose for  $z_1$ ,  $z_2$  and  $z_3$  arbitrarily the impedance of a column of air of  $3/8$ ,  $1/4$  and  $1/2$  wave length respectively, we have

$$z_1 = j\rho_0 c_0, \quad z_2 = 0 \quad \text{and} \quad z_3 = \infty.$$

Since only *differences* of impedances enter in this equation, which are, as a rule, one order smaller than the impedances themselves, some simple sort of compensation bridge is recommended by which the major part of the impedance can be compensated.

Although this procedure seems to be correct, it cannot compete with the methods described in the foregoing sections as to accuracy and ease of handling. If a telephone is used, the impedance differences are only of reasonable magnitude when the telephone is tuned rather sharply to resonance. It, then, is, however, very sensitive to changes of frequency, either of the audiofrequency generator or of the resonance frequency itself, and therefore, to temperature. Using a loudspeaker, temperature sensitivity seems to be of much less importance, but now the atmospheric conditions influence the behaviour of the paper cone. This means, that  $Z_1$ ,  $Z_2$  and  $Z_3$  cannot be measured once for all as a function of frequency, but must be measured for each  $Z$ -measurement.

If we content ourselves, however, with the mere measurement of the absorption coefficient, rapid and accurate measurements

are possible from which the result can be obtained from two graphs without any calculation. For full details the reader is referred to the original publications<sup>1,2</sup>. The outlines are the following:

According to (5.07) every point in the complex  $z$  plane corresponds to a point in the complex plane of the quantity  $M/(N+z)$ , so every contour in the  $z$  plane corresponds to a contour in the other plane. If the curves, corresponding to the two sets of circles of constant absorption coefficient and constant phase jump in the  $z$  plane (see Fig. 11), are drawn in the  $M/(N+z)$  plane one can read directly from the latter graph the value of  $r$  belonging to a given point in the  $M/(N+z)$ -plane without calculation. This transformation is elucidated in Fig. 36 for arbitrary values of  $M$  and  $N$ ,  $M$  being chosen real for simplicity, however. If  $M$  were taken complex the circle-configuration in the  $M/(N+z)$  plane (lower part of the figure) should be turned through the phase angle, assigned to  $M$ , round the origin  $O$ . The two sets of circles are transformed into two identical sets, apart from a translation, rotation, and magnification. The circle of complete reflection is in the  $z$  plane the imaginary axis, in the other plane the circle with diameter  $OA$ . All  $z$  points with positive resistance are found within this circle  $OA$ . Shifting this circle  $OA$  over the complex distance  $L$  gives the transformation of the acoustical  $z$  plane into the electrical  $Z$  plane.

Now, if sample and source are placed at either end of an interferometer tube and the sample is moved in the tube, the impedance  $z$  at the source runs through a circle of constant absorption coefficient. So does the electrical impedance  $Z$  in its own plane too. It was shown by one of the authors<sup>1</sup> that the absorption coefficient of the sample bears a simple relation to the diameter of the circle in the  $Z$  plane belonging to the sample, the diameter of the circle for complete reflection and the position of the point for complete absorption in the large circle. It does not depend upon the quantity  $L$  of (5.07), i.e., upon the centre of inversion. Furthermore, the diameter for complete reflection and the position

<sup>1</sup> C. W. Kosten, *Appl. sci. Res. B*, 1 (1947) 30

<sup>2</sup> D. H. Bekkering and C. W. Kosten, *Appl. sci. Res. B*, 1 (1948) 205



of the point for complete absorption are not critically dependent on frequency, in the case of a normal loudspeaker still less than with a telephone, and may be measured once and for all. Therefore the absorption may be read from a graph like Fig. 37, giving  $a_0$  as a function of  $d/D$  and  $D/l$ , where  $d, D =$  diameter in the

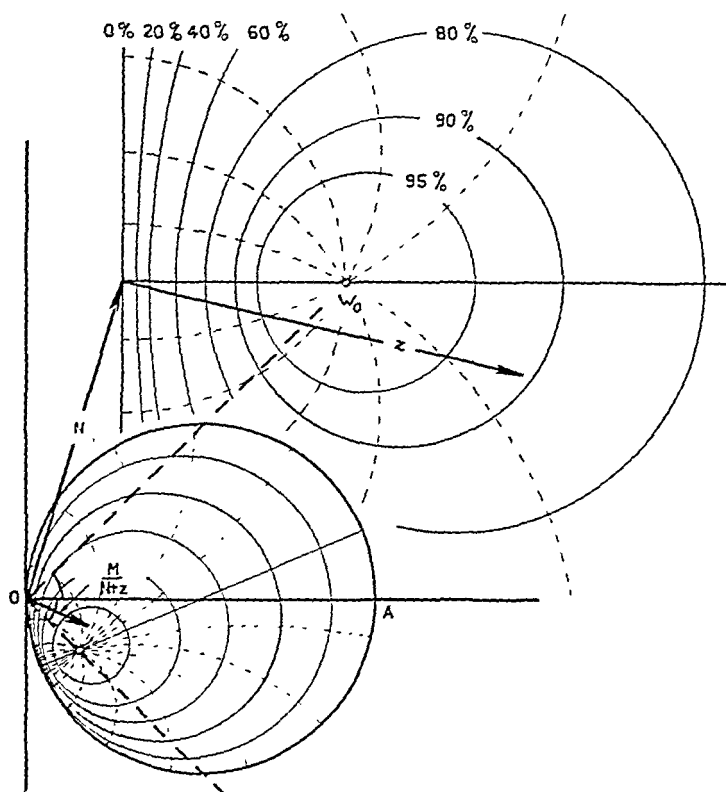


Fig. 36

The relation between the motional impedance and the acoustical impedance (reaction interferometers)

electrical impedance plane of circle belonging to the sample and a sample with 100 % reflection resp.,  $l =$  distance of the point of 100 % absorption to the 100 %-reflection-circle (see Fig. 38).  $d$  is measured and  $D$  and  $l$  are known from previous experiments. A suitable electrical set-up, with which the diameters can be meas-

ured, is shown in Fig 39. The current through the low-impedance loudspeaker is kept constant with the aid of a high series resistance. The voltage on the loudspeaker is measured with a tube

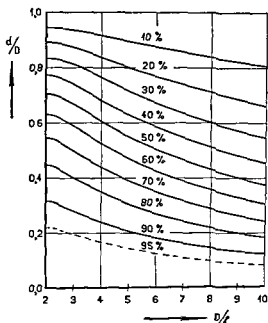


Fig 37

The absorption coefficient as a function of the diameter of electrical impedance circles and the impedance for 100 % absorption (reaction interferometer)

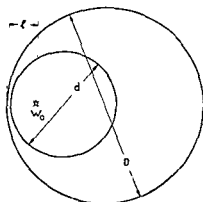


Fig 38

The meaning of the quantities  $D$ ,  $d$  and  $l$  (reaction interferometer)

voltmeter. This voltage can be compensated with an auxiliary regulated voltage. After compensation the length of the interferometer is varied till the tube voltmeter indication is a maximum. The indication is proportional to the diameter of the impedance circle.

The results are reproducible<sup>1</sup> within one unit in the second decimal of  $a_0$ . Therefore, the same accuracy seems to be obtained as with other methods, whereas the apparatus is essentially simpler.

Although this has not yet been published it is doubtless that the method can be worked out for impedance measurements, too. Phase angles can be measured if due attention is paid to the position of the sound source.

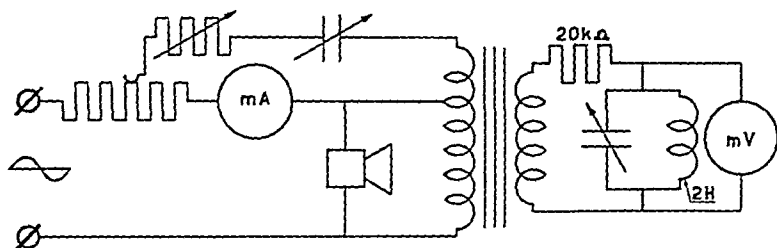


Fig. 39

Electrical set-up for reaction measurement

§ 7 GELUK'S IMPEDANCE INDICATOR<sup>2</sup>

During the last war a very remarkable and ingenious apparatus was developed by Geluk. He used the screen of a cathode ray oscilloscope as complex  $z$ -plane, on which the impedance under test was indicated automatically as to magnitude and phase, and, since his apparatus worked instantaneously, the complete  $z$ -contour, when varying the frequency, could be shown in a few seconds and photographed if desired.

A normal loudspeaker is pressed against the sample or wall under test (Fig. 40). The sound pressure between the cone and the sample is measured by a small condenser microphone, thus transforming pressures into capacity variations. The displacement of the cone is also transformed into a capacity variation. This was done by coating the cone with a thin conducting layer and placing a second conducting cone  $b$ , which remained at rest, at

<sup>1</sup> D. H. Bekkering and C. W. Kosten, *Applied sci. Research*, B, 1 (1948) 205.

<sup>2</sup> J. J. Geluk, Thesis Delft, 1946.

a small distance of the actual cone of the speaker. This second cone is called the anti cone and is amply perforated in order not to hinder the vibrating cone in its vibrations. The capacity variations proportional to pressure and displacement respectively are changed into electric voltages with the aid of two similar high frequency devices. The displacement voltage is multiplied by  $j$  (turning the phase by  $90^\circ$ ) thus providing us with a voltage proportional to the velocity of the cone. The velocity was automatically kept constant by controlling the output voltage of the generator with the aid of a sound level recorder of the Neumann type. The pressure voltage is then proportional to the ratio  $p/v$  and if we succeed in indicating that voltage on the screen of the oscilloscope as to magnitude and phase an impedance indication is obtained. In order to solve this problem an auxiliary

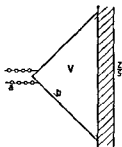


Fig 40

The sound source with anti-cone of Geluks impedance indicator

voltage of equal magnitude as the pressure voltage differing  $90^\circ$  in phase was derived by electric means. The two voltages are supplied to the two pairs of plates of the oscilloscope leading to a circular image on the screen of radius proportional to the pressure i.e. to the impedance  $z$ . Finally the electron beam is suppressed during the whole circle except for the moment the velocity passes through zero in the positive direction. So one single spot is indicated on the screen giving the impedance as to magnitude and phase.

The disadvantages are obvious. The accuracy can hardly be expected to be as high as with interferometers. Moreover the apparatus is very complicated and needs calibration as to the magnitude. In those cases however where rapid comparison of

impedance contours is wanted, e.g., in developing materials or when checking the properties of an absorbing layer in a completed building, the method may turn out to be valuable.

Before entering into some of the details of the apparatus something should be said about what is actually indicated on the screen. The velocity indication is obviously proportional to the mean velocity of the cone and does not depend upon the velocity distribution along the cone. The condenser microphone measuring the pressure is placed quite near to the cone surface, so the indicated ratio  $p/v$  is approximately the impedance at the source. The volume between cone and sample may be treated as a short interferometer tube of effective length  $l$  equal to volume divided by surface. Since the influence on the impedance of a column of air is a clockwise turning of the impedance along a circle of constant absorption (Fig. 11), the change in phase jump  $\Delta$  being  $2\pi$  for every half wave length  $\lambda$ , the correction due to the effective length  $l$  is a counter-clockwise shifting of  $z$  along a circle of constant absorption, the correction in  $\Delta$  amounting to  $2\pi l/\frac{1}{2}\lambda$ . One sees that this correction decreases in importance with decreasing frequency as was to be expected. Moreover it does not affect the absorption coefficient.

#### § 8 DETAILS OF GELUK'S IMPEDANCE INDICATOR

Both sound pressure and velocity are measured through the intermediary of capacity variations. The latter are transformed into current variations by a modification of a method described by Zakarias<sup>1</sup>. Since this method deviates considerably from the commonly used Riegger scheme<sup>2</sup> it may be outlined here (Fig. 41). The varying capacity  $C_m$  forms part of the capacity of a high frequency  $LC$ -circuit in a high frequency generator using the oscillator part of the Philips octode AK 2 as generator tube. To the fourth grid of the AK2 a circuit is connected tuned to the frequency of the generator with  $C_m$  having its equilibrium value. The Philips tube AF 7 is used as amplifier. Calculations show that the plate current of the generator tube depends upon the capacity of the  $LC$ -circuit according to Fig. 42. The apparatus

<sup>1</sup> Zakarias, *Tech. Mitt. Tungsram*, 39 (1938) 103.

<sup>2</sup> H. Riegger, *Wiss. Veröffentl. Siemens-Werken*, 3 (1924) 67.



to the velocity with an  $RC$ -connection (Fig. 43) in which  $RC = 10^{-5}$ , giving an acceptable transformation up to 1000 Hz.

The calibration of the condenser microphone in a *relative* way is usually performed by applying an alternating voltage of the same frequency as that of the sound to the condenser plates, superposed upon a constant voltage:  $u = u_0 + u_1 \cos \omega t$ , in which  $u_1 \ll u_0$ . The attractive force between the plates varies with the square of the voltage. The equivalent sound pressure is therefore

$$f_k 2 u_0 u_1 \cos \omega t.$$

The term in  $u_0^2$  cancels out since it is constant, whereas the term in  $u_1^2$  may be neglected; the Kelvin constant  $f_k$  in this equation does not depend upon the frequency. The alternating plate current of the generator now takes the form

$$i = f \omega f_k \cdot 2 u_0 u_1 \cos \omega t,$$

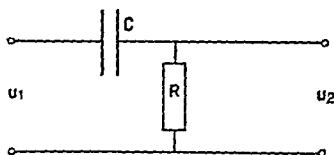


Fig. 43  
Turning the phase by  $90^\circ$

$f \omega$  being a function of frequency depending upon the mechanical behaviour of the microphone and the electrical behaviour of the measuring apparatus. Measuring the amplitude of  $i$  as a function of  $\omega$  with  $u_0$  and  $u_1$  constant gives us  $f \omega$  apart from a constant factor. For the *absolute* calibration measurements were made of the change in direct current caused by a very small static excess pressure, which, again, was measured with a sensitive micro-manometer.

The pressure voltage is applied to one pair of plates of the oscilloscope. The same voltage, shifted through  $90^\circ$  in phase, is applied to the other pair. This voltage is made with the aid of the arrangement of Fig. 44 (see also the vector diagram Fig. 45). At every frequency  $R(\omega)$  should have the appropriate value; it varies inversely proportional to the frequency. This was performed

automatically by coupling the shaft of the variable condenser of the audiofrequency generator to the shaft of the metal wire resistance  $R(\omega)$  that was constructed especially to fit the purpose

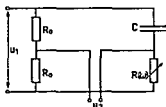


Fig 44

Turning the phase by  $90^\circ$  independent of frequency without changing the magnitude of the output voltage

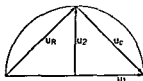


Fig 45

Vector diagram to Fig 44

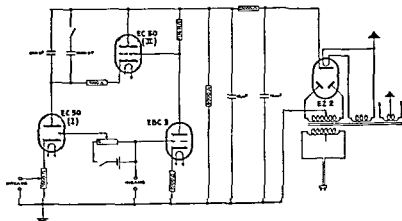


Fig 46

Impulse generator

In order to suppress the image on the screen, except for one single point, the synchronous pulse generator of Fig 46 was made. The two thyratrons EC 50 divide the d.c. voltage of the rectifier



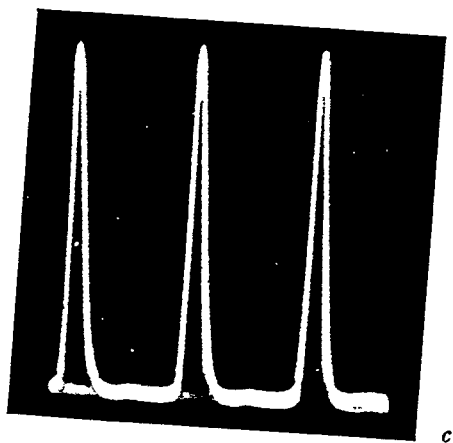
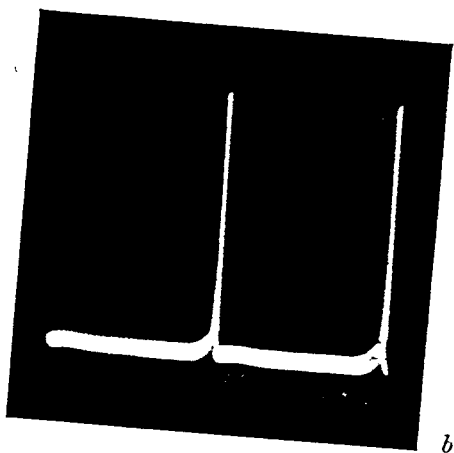
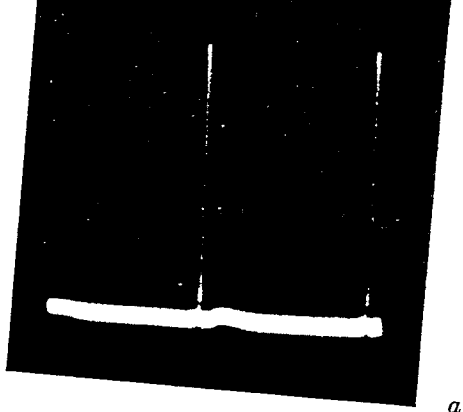


Fig. 47

Periodic pulses: *a* 100 Hz, *b* 1000 Hz, *c* 10000 Hz

The first (left) starts when the input voltage just becomes positive charging the condenser in its anode circuit in a very short time thus giving a short pulse to the output. This situation lasts until about  $\frac{3}{4}$  of the period later the second thyatron discharges initiated by the increasing negative voltage on the

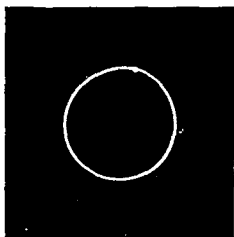


Fig 48

Reinforcing the image on the screen with pulses

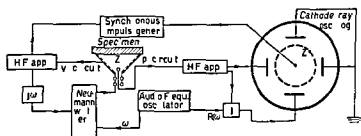


Fig 49

Functional scheme of Geluks impedance indicator

grid of the EBC3. This brings the arrangement back to the initial situation. Form and speed of the pulses may be seen from the photographs Fig 47 a b and c.

The pulse is applied to the Wehnelt cylinder of the oscilloscope thus making the image brighter at the moment of the pulse.

A functional diagram of the complete set up is given in Fig 49.

## CHAPTER VI

### EXPERIMENTAL RESULTS; COMPARISON WITH THEORY

#### § 1 INTRODUCTION

In this chapter a summary will be given of measurements carried out on characteristic samples. We should like to emphasize the great value of plotting the results in the complex  $z$ -plane, as we shall do in this chapter, as a rule. The behaviour is given by the  $z$ -contour, to which a frequency scale is added, generally in hundreds of Hz. One reads at a glance from the graph the frequencies of resonance and anti-resonance, the degree of damping, the absorption coefficient as a function of frequency; moreover irregularities in the sample manifest themselves directly in irregular contours. Plotting real and imaginary part as a function of frequency, as frequently done in the literature, turns out to be less surveyable.

A difficulty encountered in all impedance measurements is a certain vagueness as to the phase jump  $\Delta$ . The resulting  $\Delta$  depends upon what is defined as the front surface of the sample. With a rough front surface there may be an uncertainty of 1 or 2 mm in this respect. If one chooses the front surface more outside the sample by an amount  $\Delta x$ , the measured phase jump decreases by the amount  $2\pi(2\Delta x/\lambda)$  which is the angle over which the phase shifts in passing twice the distance  $\Delta x$ . In the impedance diagram this means a clockwise shifting along a circle of constant absorption for all measured impedances. Especially for impedances high compared with  $W_0$  such a shift in  $\Delta$  may mean a considerable change in impedance and, therefore, in the apparent character of the contour. This should be borne in mind by studying contours in the  $z$ -plane.

Since the concept of the structure factor  $k$ , as introduced by the authors, is still not generally in use, it seems worth while to give firstly a few results demonstrating its *raison d'être*, nature, and importance. We shall then give results of more practical

samples which can serve for elucidating our theoretical considerations, in doing this we shall follow the same division as was used in the theoretical chapters. Most of the results given have been obtained with an old interferometer, a prototype of Fig 33, which did not give very accurate results, especially as to the phase jump  $\Delta$ . As was said in Chapter I, we smoothed the curves when necessary without changing their character. Beranek's results (§ 4) are of course the original ones.

## § 2 EXPERIMENTS ON ARTIFICIAL SAMPLES

Experiments have been carried out on samples made of glass tubes stacked in the manner of a honeycomb, with the axis perpendicular to the front surface of the model. In this case  $k=1$  and the resistance can be expected to agree with Kirchhoff's theory. Placing the same tubes inclined with respect to the normal towards the front surface provides us of a sample with a structure factor  $k$  greater than unity. If the inclination is  $60^\circ$ , we must expect  $k=4$ . Using the same tubes the thickness of the sample is two times smaller. The sound velocity in the direction of the normal is, however, proportional to  $\sqrt{k}$ , i.e., is decreased by a factor 2, too. Therefore the same resonance frequencies should be found. This complicated reasoning may be omitted, of course. The resonance frequency of a single tube does not depend upon its inclination. However the result is that the resonance frequency for a given thickness of the sample depends upon the inclination, it is explained without having recourse to the concept of an increased air density "by vibrating fibres" as has repeatedly been done.

Fig 50 gives a view of the sample with slanting tubes (dimensions of sample approx  $20 \times 20 \text{ cm}^2$ , length of tubes approx 20 cm). The impedance contours are given in Fig 51. The absorption as a function of frequency is shown in Fig 52. The resonance frequencies are about the same. One may easily verify that the impedance of both samples only differs by a factor  $\sqrt{k}$  i.e., 2 in our case, the slanting tubes giving rise to the greater impedance. This may be seen directly from the fact that a close packing of tubes with  $60^\circ$  inclination only contains half as many tubes as a close normal packing. In a formal way this may

be derived from the general equation (1.14).  $K$  is unchanged;  $\rho = k\rho_0 + \sigma/j\omega$  is  $k$  times greater since  $\sigma$  is proportional to  $k$ ;

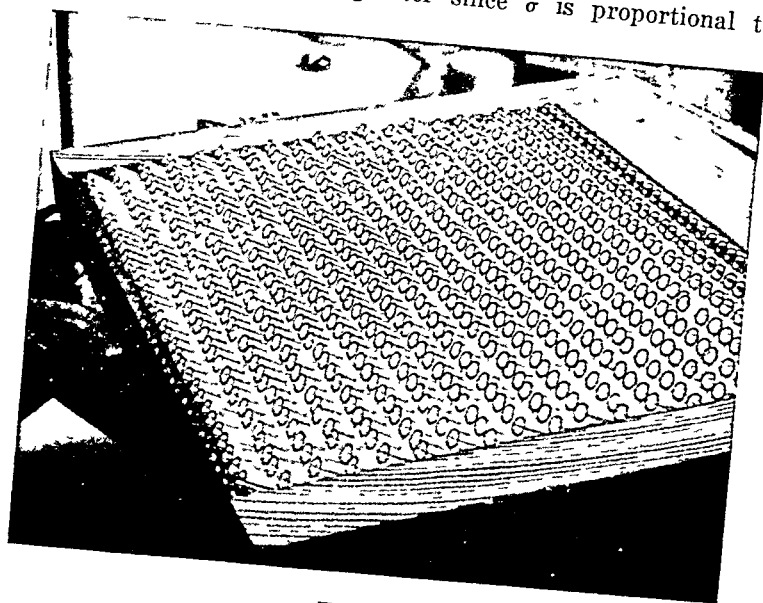


Fig. 50  
Sample with glass tubes under 60° slope

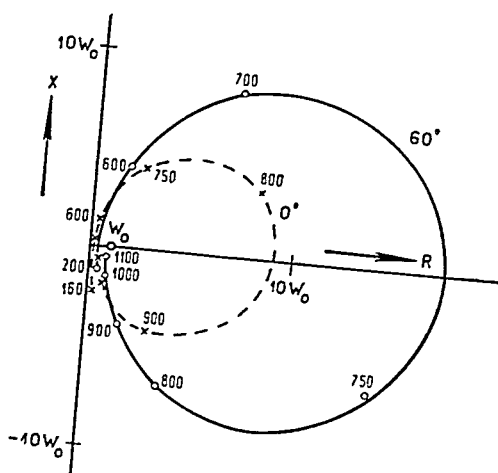


Fig. 51  
Impedance contours of the glass tubes samples at 0° and 60° slope

$l$  is  $\sqrt{k}$  times smaller Fig 51 is quite in agreement herewith Quantitatively the value of the resistance was greater than according to Kirchhoff's theory by about a factor 3 This turned

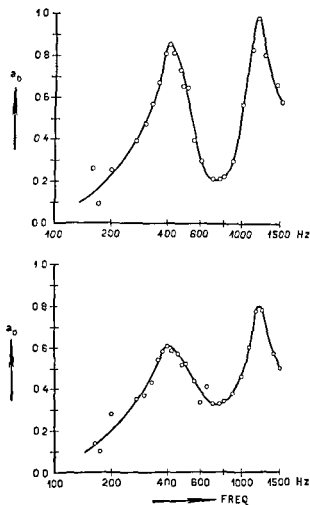


Fig 52

Absorption characteristics to Fig 51



Fig 53

Sample with artificial side holes

out to be due to the contribution of the interstices between the tubes, as further experiments have shown. For further details we refer to the original publications<sup>1</sup>. Another interesting sample is shown in Fig. 53. It consists of five layers of perforated "non-porous" materials (wood), 4 mm thick, at mutual distances of  $\frac{1}{4}$  mm. The holes are 3.8 mm in diameter; 232 of them are made in the sample of  $20 \times 20$  cm<sup>2</sup>. Part of the interstices between the planks is occupied by the supports of the construction. Taking this into account the geometrical value of  $k$  (i.e., the total volume of air divided by the volume of the canals passing through the planks) was computed to be 7.84. The resonance-frequency was 750 Hz. Taking into account the correction for the open end at the entrance of the canals, this points to a sound velocity of  $\pm 0.041 \cdot 750 = 123$  m/sec, giving a  $k$ -value of  $(348.5/123)^2 = 8.0$ , agreeing very satisfactorily with the geometrically computed value 7.84. Again, vibrating fibres cannot be made responsible for this high value of  $k$ . The origin must be sought in the structure itself.

### § 3 IMPERVIOUS MATERIALS OF HIGH ELASTICITY

The best material of this kind is cellular rubber. The results have already been given in Chapter I § 7 (Figs 12 and 13). The density of the material was 116 kg/m<sup>3</sup>, the static rigidity modulus  $G = 0.17 \cdot 10^5$  newton/m<sup>2</sup> (0.17 kg/cm<sup>2</sup>). From the resonance frequency one computes  $3.3 \cdot 10^5$  for the dynamic value of the *total* stiffness. Since the air content is circa 88 % (derived from the density 116) the *air* stiffness is about  $1.4 \cdot 10^5 / 0.88 = 1.6 \cdot 10^5$ . Therefore the dynamic *rubber* stiffness is  $1.7 \cdot 10^5$ , i.e., 10 times greater than  $G$ . Assuming arbitrarily Poisson's ratio  $m = 4$  gives  $K_{1 \text{ stat.}}/G = 3$ , leading to  $K_{1 \text{ dyn.}}/K_{1 \text{ stat.}} = 10/3$ .

Materials of this type are obviously very bad for normal use owing to the strong selective absorption. Only in cases where selective absorption is wanted should they be employed.

---

<sup>1</sup> C. Zwikker, J. vanden Eijk, and C. W. Kosten, *Physica*, 8 (1941) 1094; 10 (1943) 239.

## § 4 POROUS MATERIALS WITH RIGID FRAME

With a view to the theory of elastic layers it needs verification whether materials like felt, rock wool, wood fibre plates, etc may be regarded as rigid, since their air resistance is usually considerable. Acoustic plasters are of course good examples of rigid materials. The contours of the former flexible materials,

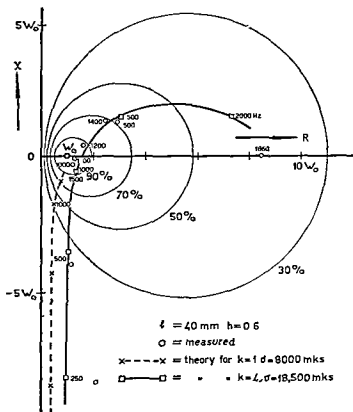


Fig 54

Measurements and theoretical curves of a sample of acoustic plaster,  
necessity of the structure factor concept

even that of soft sponge rubber layers, with porous front surface (see § 5) are however, of the same kind as that of plasters. A typical contour for an acoustic plaster is given in Fig 54. The theoretical curves show clearly the necessity of a structure factor of about 4. One sees that a higher air resistance is very likely to increase the absorption coefficient at least at the lower





frequencies At low frequencies the structure factor should, as a rule, be taken higher This indicates that, at least in these materials part of the air contents can no longer take part in the dynamic process at frequencies of, say, 800 Hz and higher

Ber anek also gives the impedance contour for Celotex C-4 (125 meh) Here the general theoretical expression for homogeneous materials fails which is not surprising (see § 8)

Fig 56 finally gives us an idea of the absorption characteristics of this class of materials Low absorption at low frequencies is a general feature

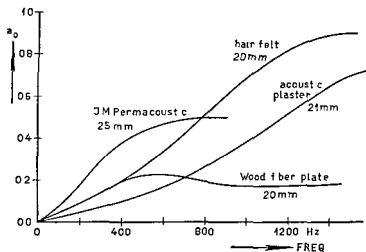


Fig 56

Absorption characteristics of normal porous materials

#### § 5 POROUS MATERIAL ELASTIC FRAME OPEN FRONT SURFACE

Fig 57 shows the absorption characteristics for three specimens of sponge rubber For Latteel the air resistance is obviously so low that no coupling effect is noticeable ( $\sigma \approx 20000$  mks), this is corroborated by the  $z$  contour which resembles very much that of hair felt (Fig 55a) Quantitatively the contour can be described with the static value of  $\sigma$  and a structure factor of 7 The air resistance of the Dunlopillo sample is about 10 times higher, giving rise to more or less coupled vibrations and the accompanying selective absorption at the frequencies of resonance of the 'frame wave'

It is a well-known fact that the absorption coefficient as determined in the reverberation room is, as a rule, higher than that obtained at normal incidence in an interferometer. In Fig. 58

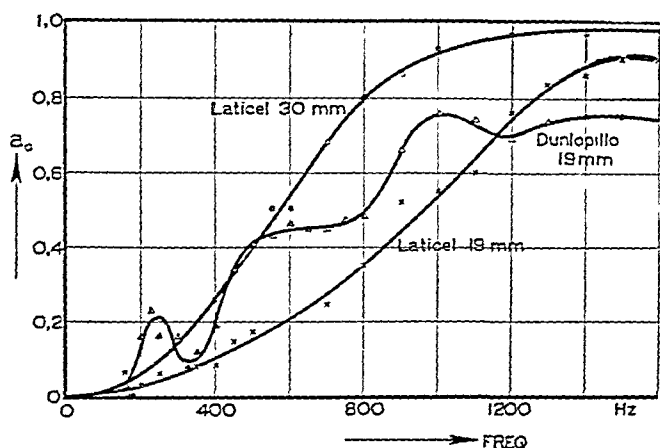


Fig. 57

Absorption by sponge rubber layers with open front surface

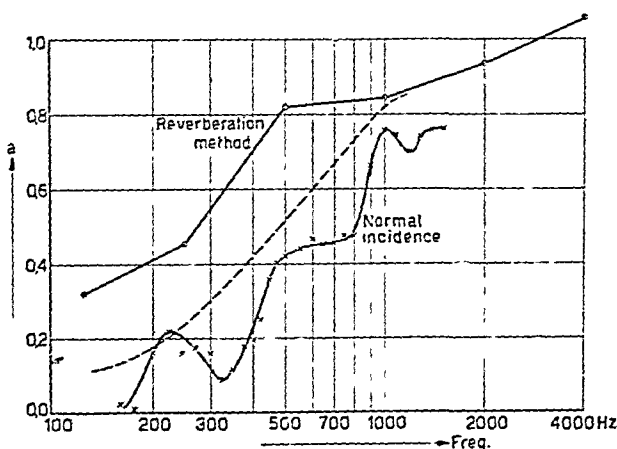


Fig. 58

Measurements in the interferometer as compared to those with the reverberation method

a comparison is given. The reverberation results were obtained in a room of 165 m<sup>2</sup> with 10.3 m<sup>2</sup> Dunlopillo on the floor. The dotted line is computed from the interferometer results by

assuming the impedance to be real (which certainly is not the case as a matter of fact) and independent of the angle of incidence and averaging the absorption coefficient for random incidence

#### § 6 POROUS MATERIAL ELASTIC FRAME COATED SURFACE

Figs 59 60 and 61 show absorption characteristics of similar layers as described in § 5, this time coated with a thin impervious

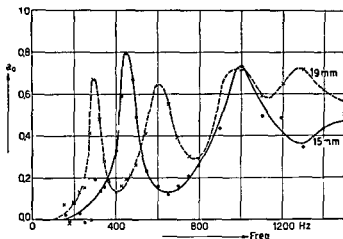


Fig 59

Absorption by sponge rubber (laticel) layers with coated surface

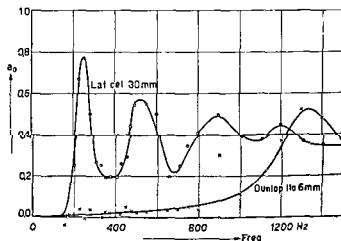


Fig 60

Absorption by coated sponge rubber layers

layer of  $0.1 \text{ kg/m}^2$ . These materials have been developed on a laboratory scale only. The coating layer was of the cellophane type. They may be considered, however, as typical of the class of materials owing their behaviour to high elasticity and porosity. The influence of the coating can be seen from Fig. 62 (smoothed curves).

In order to obtain a more practical material a layer of Dunlopillo was coated with a thin impervious layer of cotton, latex, and paint. This layer is rather heavy and will impair the absorption at high frequencies. Careful reverberation measure-

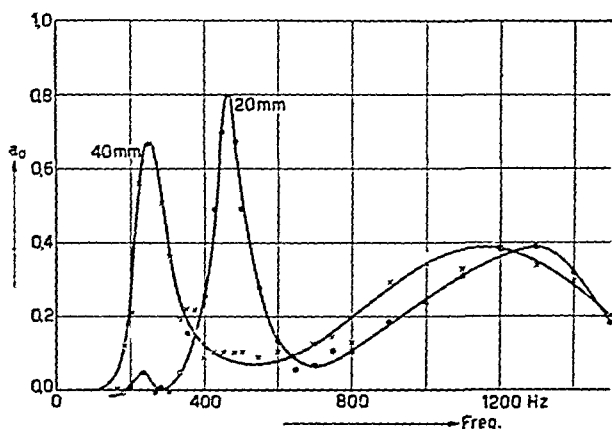


Fig. 61

Absorption by coated sponge rubber layers

ments with  $8.4 \text{ m}^2$  of this material in a room of  $165 \text{ m}^3$  were carried out<sup>1</sup>, the result of which is shown in Fig. 63. A pure tone was used; every measuring point is an average of 100 measurements. For comparison a small sample was subsequently measured in the interferometer (Fig. 64). The general shape of both curves is the same. In accordance with the general practice the reverberation method yields higher absorption coefficients.

The results of this and the foregoing section could be used

<sup>1</sup> C. W. Kosten and C. Zwicker, *Physica*, 8 (1941) 947.

This impedance terminates the absorbing layer of thickness  $d$ . If wave impedance  $W$  and propagation constant  $\gamma$  of the absorbing material are known, the impedance at the front surface of the construction is readily computed from the general equation (104), giving the impedance of a layer of given  $W$  and  $\gamma$  backed by a known impedance. In general  $W$  and  $\gamma$  are complex, in which case computation is tiresome. It is however easy to find approximately the frequencies at which resonance occurs, i.e., where the absorption coefficient will be maximum. To this end we neglect damping of the waves in the material, the impedance is then purely imaginary, resonance taking place when the impedance is zero. The computa-

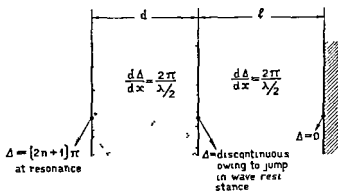


Fig. 65

Scheme indicating the general line along which the resonance frequencies of a porous material on a layer of air can be computed

tion of the impedance may be replaced by a construction along the imaginary axis of the circle-diagram. This will be elucidated with the aid of Fig. 65.

The phase angle  $\Delta$  of the complex reflection coefficient  $r$  is zero at the rigid wall; it changes by  $2\pi$  for every half wave length through the air. The phase angle in the air, just to the right of the material is therefore  $l(4\pi/\lambda)$ . The impedance can be indicated at once in Fig. 11. Now on passing from the air just into the material the impedance is unchanged; the wave impedance makes a jump by a factor  $\sqrt{k}/h$ , however. This means that the sets of circles of Fig. 11 are multiplied by  $\sqrt{k}/h$ . The phase angle just inside the material therefore, may be read from the multiplied circle diagram from the known value of the imaginary impedance.

or, what comes to the same thing but is much more convenient, we may divide the impedance by  $\sqrt{k}/h$  and read the phase angle from the same circle-diagram. On passing further to the left in the material another contribution of the amount  $d$  ( $\pm \pi/\lambda'$ ) is added to  $\Delta$ , if  $\lambda'$  denotes the wave length in the material. We then find the phase angle  $\Delta$  at the front surface which should be  $(2n+1)\pi$  for resonance. Fig. 11 is merely used for a convenient explanation. The procedure may now be put in the form of simple formulae.

The connection between an imaginary impedance  $z$  and the corresponding  $\Delta$ -value is read from Fig. 10 to be

$$z = jW \cot \frac{1}{2} \Delta.$$

At the right boundary of material and air the impedance is continuous, therefore

$$W \cot \frac{1}{2} \Delta_{\text{mat.}} = W_0 \cot \frac{1}{2} \Delta_{\text{air}}$$

from which  $\Delta_{\text{mat.}}$  is readily computed since all other quantities are known. Adding  $d$  ( $\pm \pi/\lambda'$ ) and putting the resulting  $\Delta$  equal to  $(2n+1)\pi$  gives as the resulting transcendental equation from which the resonance frequencies are obtained<sup>1</sup>

$$\tan \omega l/c_0 \tan \omega d \sqrt{k}/c_0 = h/\sqrt{k}.$$

The influence of thin layers of air is sometimes very considerable (Fig. 66) which explains the discrepancies frequently found.

The same procedure may be used for finding the impedance in the case that the damping is not neglected<sup>2</sup>. The result can then be obtained most conveniently by a combined graphical and calculation method. This will be elucidated for a two-layer system backed by a layer of air (Fig. 67). The impedance is constructed in the  $z/W$ -plane, whereby it should be borne in mind that  $W$  changes on passing from one layer to another. The value of  $z/W_0$  at the point 1 of the structure may be indicated at once in the  $z/W$ -plane, since  $\Delta$  is known in this point ( $l \pm \pi/\lambda_0$ ). From points 1 to 2  $W$  is discontinuous corresponding to the 1—2-jump in the

<sup>1</sup> J. van den Eijk, C. W. Kosten, and W. Kok. *Applied sci. Research*, B, 1 (1947) 50.

<sup>2</sup> C. W. Kosten, *Nederlands Tijdschr. Natuurk.* 14 (1948) 309.





$z/W$ -contour passes through a part of a spiral, the end-points of which part are related by

$$r_3 = r_2 \exp(-2 \gamma_{\text{mat. 1}} l_{\text{mat. 1}})$$

from which  $r_3$  must be calculated in order to find point 3. The jump 3—4 in the  $z/W$ -plane again corresponds to the discontinuity in  $W$  at the boundary 3—4, etc.

Experiments with the sample on a layer of air have also been carried out with a special Laticel (sponge rubber) sample with coated surface. In order to provide free passage to the outflowing air the sample was amply perforated. In Fig. 68 curve 1 gives

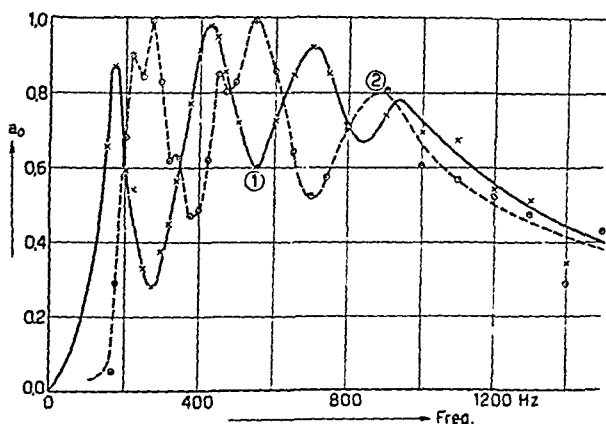


Fig. 68

Sponge rubber sample with coated surface on a 78 mm layer of air:  
1 free hanging, 2 on a sheet iron perforated support (Fig. 69a)

results of the free hanging sample. In order to meet more practical conditions it was then supported by the sheet iron gauze of Fig. 69a, yielding curve 2 of Fig. 68. The resonance frequencies are obviously shifted, explained by the radical change in the back side situation of the sponge rubber frame (free end  $\rightarrow$  fixed end). To counteract the selective absorption the same sample was stuck to a support of Fig. 69b, yielding Fig. 70. Owing to the irregularity of the sample plus support no resonance bands can be distinguished in this case; the measuring points suggest a very complicated absorption spectrum to be present. The average absorption is, however, very satisfactory.

## § 8 CELOTEX C 4

The behaviour of Celotex C 4 deserves a special treatment. The impedance contour for this material as given by Beranek<sup>1</sup> is shown in Fig 71. Morse et al showed the impossibility of explaining this curve with the theory of homogeneous porous

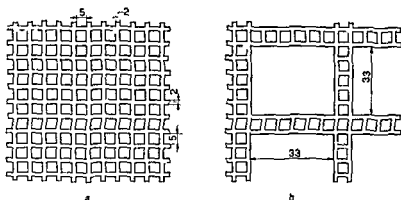


Fig 69

Sheet iron supports for the mounting of the sponge rubber samples on a layer of air

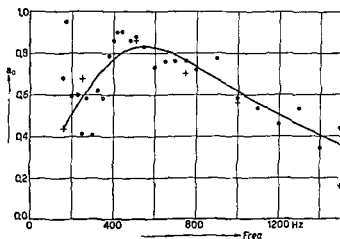


Fig 70

As Fig 68 with sheet iron support of Fig 69b

<sup>1</sup> L L Beranek *J Acoust Soc Am* 12 (1940) 14

media. The structure factor (their "effective density") should be taken rapidly decreasing with increasing frequency in order to meet the measured contour. Remembering the influence of side holes on the structure factor this is not surprising. The behaviour may be understood as follows.

The main pores, in which the sound propagation takes place, are the macroscopic holes of 6 mm diameter distributed in a regular pattern all over the material. The rest of the material

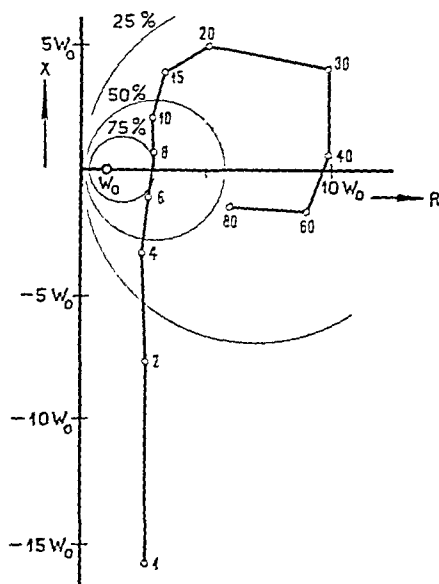


Fig. 71

Impedance contour of Celotex C-4 (Beranek, frequencies in 100 Hz)

is fibrous and porous; the air contents of this porous medium takes the place of side holes to the main pores, which are only accessible through a certain resistance, viz., the resistance of air flow through the porous material. Now this resistance is very likely to be so high that at high frequencies there is no longer a possibility of air exchange between main pores and side holes. In Fig. 72 the approximate electrical analogue of a small part of a main pore is shown. The whole material is to be considered as a long electric line with distributed self-inductance (mass in the main pores), distributed capacity (compliance in the main

pores) and distributed capacity with series resistance (compliance of the side holes with entrance resistance). The ratio  $C_2/C_1$  is equivalent to the structure factor of the main pores i.e., total air contents divided by air contents in the main pores. It is of the order 15 to 20. This agrees fairly well with the measurements

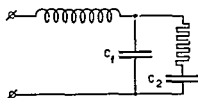


Fig. 7.  
Electrical analogon to Celotex C—4

In order to meet the measured curve Morse et al assume  $k = 38$  at about 200 Hz 12 at about 2000 Hz. From the resonance frequencies one computes 16 at about 700 Hz and 2.5 at about 3000 Hz. Calculations have shown that indeed an element as shown in Fig. 72 satisfies the measurements reasonably.

## CHAPTER VII

### ABSORPTION BY RESONATORS

#### § 1 INTRODUCTION

In this chapter we shall deal with the absorption by resonators of the Helmholtz type. A great number of publications<sup>1</sup> on this subject have appeared. Especially in the case of the single resonator the confusion is astonishing — the more so since Rayleigh has already given all fundamental knowledge that is wanted — so that a treatment of this problem at some length seems worth while. The case of perforated panels before a rigid wall can be treated with the theory of resonators. It is much more important and simpler than that of the single resonator and is given in a short cut by W. Willms<sup>1</sup> and V. L. Jordan<sup>1</sup> (*Akust. Z.*). The development of adequate constructions for any particular case has remained, however, a question that belonged to the domain of the acoustical expert. In this chapter graphs will be given that enable one to make a good choice, even without understanding the principles underlying them.

In principle a resonator consists of a vessel with volume  $V$ , the interior of which is in communication with the external medium through a channel, which may be narrow or rather wide, short or rather long, circular in cross-section or not. If an external

---

<sup>1</sup> Rayleigh, *Theory of sound II*, 2nd ed., p. 170, Cambridge 1896; E. C. Wente and E. H. Bedell, *Bell System Techn. J.*, 7 (1928) 1; E. Wintergerst, *Z. tech. Phys.*, 16 (1935) 569; Rschewkin, *Tech. Phys. USSR*, 3 (1936) no. 6; E. Meyer, *Elek. Nachr.-Tech.*, 13 (1936) 95; W. Zeller, *Akust. Z.*, 3 (1938) 32; W. Willms, *Akust. Z.*, 4 (1939) 29; V. L. Jordan, *Akust. Z.*, 5 (1940) 77; P. O. Pedersen, *Ingeniørvidenskab. Skrifter*, no. 5, Copenhagen 1940; P. V. Brüel, *Lydisolation og Rumakustik*, p. 104, Göteborg 1946; F. Ingerslev and A. K. Nielsen, *Ingeniørvidenskab. Skrifter*, no. 5, Copenhagen 1944; P. V. Brüel, *Summer Symposium of the Acoustics Group of the Physical Society* 1947, London 1949; A. Gigli, *J. Acoust. Soc. Am.*, 20 (1948) 839; V. L. Jordan, *J. Acoust. Soc. Am.*, 19 (1947) 972.

source of sound provides a sound pressure at the aperture of the channel, the air in the channel will be set into vibration, by which the interior is periodically compressed and expanded and acts like a spring. The kinetic energy is concentrated in the region of vigorous motion, i.e. in the channel. The potential energy, on the contrary, is to be sought in the interior. The system is closely analogous to a mass  $m$  mounted on a spring of compliance  $C$  (displacement/force).

The "mass" of the resonator is that of the air in the channel; it vibrates approximately with the same velocity throughout the whole channel. If the channel has the length  $l$  and the cross section  $S$ , the mass amounts to

$$m = \rho_0 l S$$

The compliance is computed from the definition

$$C = dx/dF,$$

if  $dx$  is a small displacement of the air in the channel due to a small driving force  $dF$ . Now

$$dx = -dV/S, \quad dF = S dp, \quad K_0 = -V dp/dV$$

if  $dV$  denotes the volume of air added to the internal air,  $dp$  the excess pressure inside that is approximately constant throughout the vessel, and  $K_0$  the compression modulus of air. Therefore

$$C = \frac{1}{S^2} \frac{V}{K_0}$$

The resonance frequency of the resonator is found from the familiar formula  $\omega_{res} = 1/\sqrt{mC}$ , to be

$$2\pi \nu_{res} = \omega_{res} = c_0 \sqrt{\frac{G}{V}} \quad (7.01)$$

if  $G = S/l$  and  $c_0 = \sqrt{K_0/\rho_0}$  = the normal velocity of sound in free air.

The channel will seldom be of such a simple form that it can be treated as a cylinder with a certain length, and even in this case our treatment is only an approximate one, since there is also a contribution to the kinetic energy, and, therefore, to the effective mass, at the beginning and the end of the channel, where

the flow of air widens into the free air and the interior of the vessel. Therefore we have to add to  $l$  a small length due to these end corrections. For channels with circular cross section the total correction for both ends amounts to 0.8 times the diameter  $D$ . If  $l$  is reduced to zero by taking as "channel" a single aperture in the thin wall of the vessel the mass is even completely governed by these end corrections. In this case  $G$  is exactly equal to  $D$ . For full details we refer to Rayleigh<sup>1</sup>.

The equation (7.01), giving  $\nu_{\text{res.}}$  as a function of  $G$  and  $V$  is illustrated in Fig. 73. Since for holes in a thin wall  $G \approx D$ ,

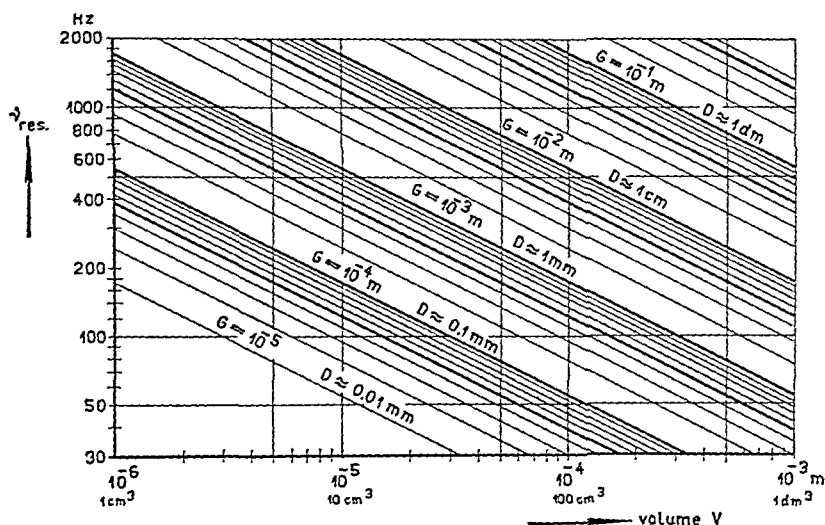


Fig. 73

The resonance frequency of a resonator as a function of conductivity  $G$  and volume  $V$ . For a circular hole in a thin panel  $G$  is equal to the diameter of the hole (see Fig. 83 for thick panels).

indications of  $D$  are also given in Fig. 73. One should bear in mind, however, that this is only an approximation for *thin* walls. Walls are thin in this respect if the thickness is very small in comparison with the diameter of the hole.

A most valuable picture is the following.  $G = S/l$  is obviously the electrical conductivity of a conducting body of the same shape

<sup>1</sup> Rayleigh, *Theory of sound II*, 2nd ed., §§ 303 a.f., Cambridge 1896.

as the channel, if the specific conductivity of the conductor is taken unity. This scheme is of quite general validity<sup>1</sup>, and can help us to estimate  $G$  in complicated cases. If the vessel is perforated at several places at considerable distances apart the conductivities  $G$  can simply be added. Taking 4 apertures of diameter  $D$  in a very thin vessel gives  $G=4D$ . If the apertures are as near to each other as possible they mutually affect their end corrections, since the passage to the free air is restricted, thus decreasing the conductivity of each aperture. The minimum, however, is  $G=2D$ , the conductivity of one aperture of a surface of the four apertures together.

For a cylindrical channel of nearly circular cross-section we have approximately, as mentioned above

$$G=S/(1+0.8D) \quad (7.02)$$

Another rather simple case for which the conductivity can be given is that of one single slit of breadth  $b$  in an infinite panel of thickness  $d$  (Pedersen<sup>2</sup>). Per unit length of the slit we have

$$1/G=d/b+0.7+(2/-)\ln 2c_0/\omega b \quad (7.03)$$

Even when the end corrections in  $G$  are taken into due account our description of the physical behaviour of the resonator remains an approximate one. The kinetic energy is not restricted fully to the channel and its direct environment, the potential energy in the channel is not completely negligible. In fact, the description is based on the assumption that the wave length is very great in comparison with all dimensions of the resonator, a condition which is fulfilled to a sufficient degree with normal resonators with a view to other approximations that have to be made if the damping is artificially increased. Those who are interested in a further refinement of the usual description given above are referred to a recent excellent article of Uno Ingård<sup>3</sup>, dealing with cylindrical resonators with one circular perforation.

<sup>1</sup> Rayleigh, *Theory of sound II*, 2nd ed., § 303 a.f., Cambridge 1906

<sup>2</sup> P. O. Pedersen, *Lydtekniske Undersøgelser, Ingeniørvidenskab Skrifter*, p. 72, Copenhagen 1940, see also Ingerslev and Nielsen (note 1 page 127) and H. Lamb, *Hydrodynamics*, p. 531, 6th ed., Cambridge 1932

<sup>3</sup> U. Ingård, *J. Acoust. Soc. Am.*, 20 (1948) 665



It will turn out to be necessary to provide the resonator with a reasonable damping in order to avoid strong selective absorption at resonance only. If this damping is performed by filling the volume with some porous material we must bear in mind that this influences both the volume of the spring (since part of the volume is occupied by incompressible material) and the conductivity. The latter influence is linked up with the structure of the porous material. Displacement of the air through the porous medium (which takes place at the site of the inner end correction) is only possible through the main pores of the material, i. e. through a fraction  $h/k$  of the space, where  $h$  is the porosity and  $k$  is the structure factor (see Chapter I § 8). This means that the apparent air density in this region *may* be as much as 5 to 10 times greater than the normal value, which can be taken account of by supposing the inner end correction to be 5 or 10 times greater than according to the diameter of the hole. For thin panels this amounts to a 3 to 5 times smaller conductivity, leading to a 1.7 to 2.2 times lower resonance frequency than expected. In comparison with this effect the increase of the resonance frequency due to the decreased volume will be small.

A resonator has three functions acoustically:

- a. it absorbs energy by friction in or near the channel,
- b. it acts as a second source of sound due to radiation from the channel mouth and therefore is a means for diffusing the incident sound,
- c. it stores energy by its resonance, which energy is partly restored to the room after the incident sound has ceased, thus prolonging the reverberation time of the room under certain circumstances; this effect is governed by the reverberation time of the resonator itself, which, again, depends upon its damping.

It will be clear that, if the resonator has little damping, it will only respond to frequencies to which it is exactly tuned. Then, however, it will be set into vigorous action and will absorb much energy. Its storing capacity is great in this case, its reverberation time long. Out of resonance it will practically do nothing, so as an absorber it will be unsuitable for most purposes.

In order to make it absorb in a reasonable frequency range the

damping must be materially increased. But then it is much less suitable for storing the energy and its reverberation effect is of no importance.

Since we direct our attention to the absorption properties we are in search of constructions that absorb to a reasonable degree at reasonable frequencies in a frequency range of reasonable breadth, and may, therefore, neglect the reverberation effect for the room in which it will be applied.

We shall now proceed to the computation of the absorbing qualities of resonators and shall deal with the following cases

- a the single resonator in an infinite wall,
- b perforated panels before a rigid wall,
- c multiple resonators in panel form

## § 2 THE SINGLE RESONATOR IN AN INFINITE WALL

Let us postulate a plane travelling wave, impinging normally to a rigid wall of infinite dimensions, in which one single resonator is incorporated of conductivity  $G$ , volume  $V$  and resistance  $R$  (Fig. 74). The resistance is a measure for the damping of the resonator and will be defined next.

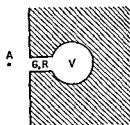


Fig. 74  
The single resonator

As regards the absorption and the diffusing effect the resonator is fully described by its impedance  $Z$  as a function of frequency.  $Z$  is defined as the ratio of excess pressure at the site of the entrance  $p$  over the velocity of volume displacement  $v$ . It can easily be expressed in terms of  $G$ ,  $R$  and  $V$ , viz

$$Z = \frac{j\omega\rho_0}{G} + R + \frac{\kappa p_0}{j\omega V} \quad (7.04)$$

This equation expresses the fact that part of the external pressure is needed for overcoming the inertia of the air mass in the channel which can only move with friction, the remaining part of the pressure serving for the adiabatic compression of the interior. The system, therefore, resembles an electrical series connection. The inertia term for a cylindrical channel equals, apart from the end corrections,  $j\omega\rho_0 l/S$  and must according to Rayleigh be written in the general form  $j\omega\rho_0/G$  if the channel is not cylindrical and end corrections are taken into account. To be precise: if we write  $G$  for  $S/l$  in the expression for  $Z$  also the end correction at the outside of the channel is included;  $p$  contains an inertia term owing to that external mass, i.e.,  $p$  is not exactly the pressure in the mouth of the channel but the pressure in front of the external mass, say at a distance equal to the diameter of the channel before the plane of the mouth (point  $A$  in Fig. 74). The stiffness term of  $Z$  follows at once from the definition of the compression modulus that equals  $\kappa p_0$ ,  $j\omega$  originating in a differentiation in order to derive the velocity from the displacement (electrical analogy  $1/j\omega C$ ).

Obviously  $R$  is the component of the sound pressure  $p$  at  $A$  which is in phase with the velocity of volume displacement divided by the velocity of volume displacement  $v$ .

If the sound pressure  $p$  at  $A$  has an amplitude  $\hat{p}$ , giving a velocity of volume displacement of amplitude  $\hat{v}$ , the absorbed power is  $\frac{1}{2} \hat{v}^2 R$ , analogous to the electrical expression  $I^2 R = \frac{1}{2} \hat{i}^2 R$ .  $\hat{v}$  can be calculated from  $\hat{p}$  by

$$\hat{p} = |Z| \hat{v},$$

so that we only want the value of  $\hat{p}$  in order to find the absorbed power.

Now this is the point that frequently gives rise to confusion. If a plane wave of amplitude  $\hat{p}_i$  is impinging upon the wall, the pressure at  $A$  has neither an amplitude  $2\hat{p}_i$ , as is found just in front of a rigid wall, nor  $\hat{p}_i$ , as assumed by several authors, but depends also upon the radiation impedance of the mouth. In order to find this sound pressure assume a massless piston to be present in the mouth of the channel that can move without friction in the aperture. This piston is virtually subjected to a velocity of volume displacement  $v$  with the aid of an *auxiliary* external force.

Furthermore the incident plane wave is supposed to be present. The pressure at the outside of the piston consists of two parts, viz.,  $2p$ , due to the incoming wave and  $Z_{\text{rad}} v$  due to the radiation, if  $Z_{\text{rad}}$  is the radiation impedance of the piston. The pressure at the inside is simply  $Z'v$ , where  $Z'$  obviously is  $Z$  minus the impedance due to the external mass ( $j\omega\rho_0\Delta l_{\text{ext}}/S$ ). Therefore the condition for equivalence of pressure on either side is

$$2p - Z_{\text{rad}} v = Z'v, \quad (7.05)$$

the minus sign on the left hand side being due to the velocity being taken positive inwards into the resonator. If  $v$  is given a value fulfilling this equation there is no external force needed to maintain the motion of the piston and the piston may be removed without, to a first approximation, changing the situation. There

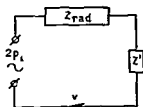


Fig. 75

The electrical analogue of the single resonator

fore (7.05) is the relation between the velocity  $v$  and the pressure of the incoming wave for a resonator without a piston. Obviously Fig. 75 is the corresponding electrical scheme. The e.m.f.  $2p$ , acts upon the series connection of  $Z_{\text{rad}}$  and  $Z'$ . This can be derived from the electrical theorem: the current in any branch of any electrical network is equal to the current that is found through that branch if it were connected to the terminals of a source with an e.m.f., equal to the voltage on the terminals of the branch in the network if its impedance is increased to infinity, and an internal source impedance equal to the impedance measured at the terminals of the branch in the network, if the branch and all e.m.f.'s in the network are removed.

The acoustical "e.m.f." in our case is the pressure  $p$  for  $Z' = \infty$ , i.e.,  $2p$ . The internal impedance of the source is obviously the radiation impedance, since this is the impedance that is found if

the resonator is removed and the impinging wave is stopped.

From Fig. 75 we see

$$v = 2 p_i / (Z_{\text{rad.}} + Z'),$$

giving as an expression for the absorbed power

$$\text{abs. power} = \frac{1}{2} \left| \frac{2 p_i}{Z_{\text{rad.}} + Z'} \right|^2 \text{Re} (Z')$$

if  $\text{Re}$  denotes "real part".

A better indication for the value of the resonator as an absorber is found by dividing the absorbed power by the incident intensity  $\frac{1}{2} |p_i|^2 / W_0$ , thus giving the total absorbing power  $A$  in  $\text{m}^2$  Sabine of the resonator

$$A = \frac{4 W_0 \text{Re} (Z')}{|Z_{\text{rad.}} + Z'|^2}. \quad (7.06)$$

$Z_{\text{rad.}}$  consists of an imaginary part due to the external end correction, which, added to  $Z'$  transforms  $Z'$  into  $Z$ , and a real part, which will be called the radiation resistance. The latter real part is, owing to the wave length being very great in comparison to the dimensions of the cross-section, equal to<sup>1</sup>

$$\text{Re} (Z_{\text{rad.}}) = 2 \pi W_0 / \lambda^2 = R_{\text{rad.}}. \quad (7.07)$$

It is clear from (7.06) that we may replace  $Z'$  by  $Z$ , if the imaginary part of  $Z_{\text{rad.}}$  is left out of consideration.

$A$  will be a maximum in the neighbourhood of resonance, i. e., when  $Z = R = \text{real}$ . Varying  $R$  in order to obtain maximum absorption at that frequency (i. e., at  $\lambda = \text{constant}$ ) we are obviously to take

$$R = R_{\text{rad.}}$$

and find

$$A_{\text{max.}} = \lambda_{\text{res.}}^2 / 2 \pi. \quad (7.08)$$

E. g., if the resonance frequency be 345 Hz, i. e.,  $\lambda_{\text{res.}} = 1 \text{ m}$ , about  $\frac{1}{6} \text{ m}^2$  of incident energy is absorbed.

Another feature of the resonator, its diffusing effect<sup>1</sup>, may readily be estimated. Interchanging  $Z'$  and  $Z_{\text{rad.}}$  (7.06) immediately

<sup>1</sup> Rayleigh, *Theory of sound* II, 2nd ed., § 319, Cambridge 1896.

gives the amount of power that is radiated from the mouth in all directions, measured in terms of the incident intensity (7.08) gives the amount of diffused power if  $R = R_{\text{rad}}$  and the resonator is in resonance. The maximum of diffused power is however 4 times as great. This can be shown by interchanging  $Z'$  and  $Z_{\text{rad}}$  in (7.06) and considering the case of resonance with  $R = 0$ .

The result of (7.08) looks very promising. We should bear in mind however, that we generally want to absorb in a rather broad frequency range of, say, two octaves at least. If the resonator has so little damping as to give (7.08) it absorbs strongly selectively and shows very little absorption outside resonance. In order to get an insight into the effect of the resonator it is, therefore, necessary to study the absorption outside resonance.

The equation (7.06) also applies in this case. If we introduce  $f = \text{frequency/resonance frequency} = \nu/\nu_{\text{res}}$ ,

$\mu = \text{resistance of resonator/radiation resistance at resonance}$   
 $= R\lambda_{\text{res}}^2/2\pi W_0$  (see 7.07),

$g = G/\lambda_{\text{res}}$ ,

(7.06) can be shown to assume the form

$$A = \frac{\lambda_{\text{res}}^2}{2\pi} \frac{4\mu}{(f^2 + \mu)^2 + \left(f - \frac{1}{f}\right)^2/g^2} \quad (7.09)$$

At resonance we have ( $f = 1$ )

$$A_{\text{res}} = \frac{\lambda_{\text{res}}^2}{2\pi} \frac{4\mu}{(1 + \mu)^2}, \quad (7.10)$$

which equals (7.08) for  $\mu = 1$ .

Outside resonance ( $f \neq 1$ )  $A$  will be smaller than  $A_{\text{res}}$ .  $A$  will be  $A_{\text{res}}/2$  for

$$(f^2 + \mu)^2 + (f - 1/f)^2/g^2 = 2(1 + \mu)^2 \quad (7.11)$$

From this equation we can compute two frequencies  $f_1$  and  $f_2$ , the number of octaves  $O$  between  $f_1$  and  $f_2$  being an adequate measure for the curve width.

There are five quantities that can be looked upon as measures for the efficiency of the resonator, viz.,

$A_{\text{res.}}/\lambda_{\text{res.}}^2 =$  a function of  $\mu$  only (see Fig. 76) that is maximum for  $\mu=1$  (the part of the curve for  $\mu < 1$  is not shown in Fig. 76),

$O =$  the number of octaves between the frequencies where the absorption is  $A_{\text{res.}}/2$  (see Fig. 77 and 78, dotted lines);  $O$  is a function of  $\mu$  and  $g$ ,

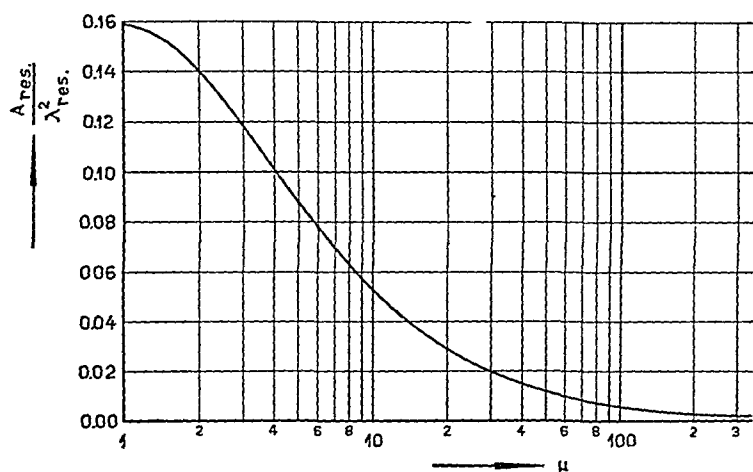


Fig. 76

The number of  $\text{m}^2$  Sabine ( $\text{m}^2$  "open window") absorbed at resonance by a single resonator, divided by the square of the wave length at resonance, as a function of the ratio internal resistance/radiation resistance ( $>1$ )

$A_{\text{res.}} O/\lambda_{\text{res.}}^2 =$  a function of  $\mu$  and  $g$  (see Fig. 77 lower part); it increases with  $g$ , i.e., with  $G$ ; this quantity measures the effect of the resonator in an absolute way,

$A_{\text{res.}} O/G^2 =$  a function of  $\mu$  and  $g$ ;  $G^2$  is a rough measure for the surface of the mouth (for thin vessels  $G=D$ ); this quantity, therefore, is of some value *aesthetically*, since it gives the effect in comparison with the surface of the perforation of the wall; this quantity is not given in a graph, but it increases with decreasing conductivity (diameter of the mouth),

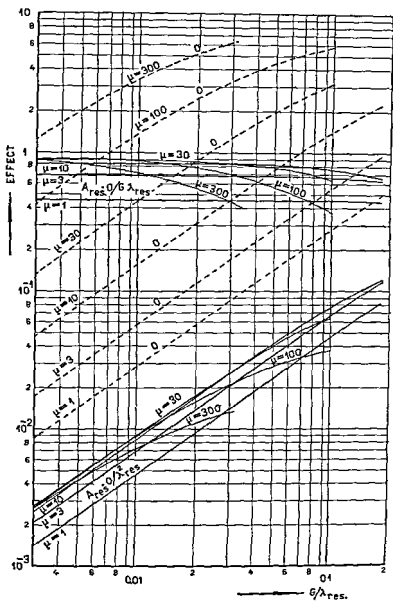


Fig 77

Various criteria for the effectiveness of a single resonator as a function of internal resistance (relative measure  $\mu$ ) and conductivity  $G$



$A_{\text{res.}} \cdot O / \lambda_{\text{res.}} G = a$  function of  $\mu$  and  $g$ ; at low values of  $\mu$  and/or  $g$  of  $\mu$  only (see the band of flat curves in the upper part of Fig. 77); this quantity is, like the foregoing two quantities, a measure for the absorbed area of "open window" times the number of octaves for which the "window is open"; the unit surface with which it is compared, is this time  $\lambda_{\text{res.}} G$ ; expressed in this unit its magnitude is approximately 1 for  $\mu$  adequate and  $g$  not too great. The latter fact

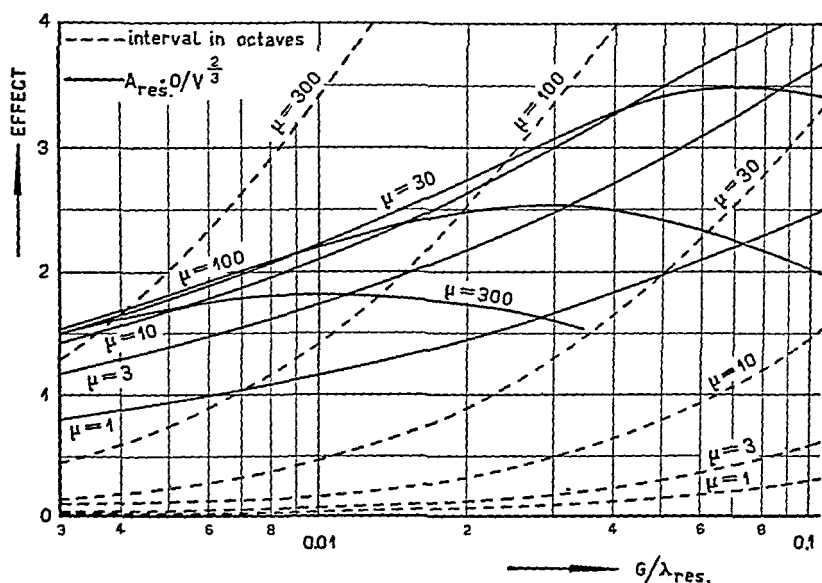


Fig. 78

Wall economy and selectivity of a single resonator as a function of internal resistance (relative measure  $\mu$ ) and conductivity  $G$

is illustrated in Fig. 79, a figure worth while remembering, since it tells us practically everything.  $A_{\text{res.}} \cdot O / \lambda_{\text{res.}} G$  is proportional to  $A_{\text{res.}} \cdot O \cdot \lambda_{\text{res.}} / V$ , i.e., to the ratio of the effect  $A_{\text{res.}} \cdot O$  and the volume of the resonator and may for this reason be looked upon as measuring the effect from the *economical aspect*; since the quantity under consideration is nearly unity for  $\mu$  adequate and  $g$  not too great, we may conclude that *all resonators are equally economical* ( $\mu$  adequate,  $g$  small),

$A_{res}$   $O/V^{2/3} =$  a function of  $\mu$  and  $g$  An estimation of the effect of a resonator with respect to the wall economy can perhaps best be given by expression the product open window  $\times$  interval in units of the area of the wall occupied by the resonator,  $V^{2/3}$  is a rough measure for this resonator surface (see Fig 78)

Fig 78 shows that, in order to have the resonator absorb with high wall economy in a frequency band of one octave or more,  $\mu$  should be 10 to 30, whereas  $G/\lambda_{res}$  should be possibly 0.04 or more If the most economical resonator that is practicable is found from this figure, we can compute the effect, or use Fig 77 for convenience

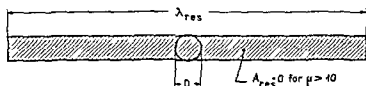


Fig 79

The absorbed area at resonance  $A_{res}$  times the number of octaves  $O$  for which the absorbed area exceeds  $A_{res}/2$  is approximately equal to  $G\lambda_{res}$ , if  $\mu$  and  $g$  are reasonable For a circular hole in a thin panel  $G \approx D$

All curves in Fig 77 are straight for small values of  $G/\lambda_{res}$  Mathematical expressions for them can easily be derived from (7.11) assuming  $f$  to be approximately 1 and  $g$  very small in comparison with 1 We obtain

$$\left. \begin{aligned} O &= 1.442 (1 + \mu) g \\ A_{res} \quad O/\lambda_{res}^2 &= 0.918 \mu g / (1 + \mu) \\ A_{res} \quad O/G^2 &= 0.918 \mu / g (1 + \mu) \\ A_{res} \quad O/\lambda_{res} G &= 0.918 \mu / (1 + \mu) \\ A_{res} \quad O/V^{2/3} &= 10.64 \mu V^{1/3} g / (1 + \mu) \end{aligned} \right\} \quad (7.12)$$

1.442 is the decimal value of  $1/\ln 2$ , 0.918 of  $2/\pi \ln 2$

It is surprising that these formulae hold with sufficient accuracy up to intervals of about an octave.

### § 3 THE USE OF SINGLE RESONATORS IN PRACTICE

The data of § 2 will be elucidated by a practical example. Suppose a room of about 1000 m<sup>3</sup> to have brick walls and a few windows. The room is to be used for meetings of about 20 people. The overall-boundary surface will be about 600 m<sup>2</sup>, the average absorption coefficient about 5 %. The optimum average absorption coefficient can be calculated from Sabine's law (say reverberation time wanted 1 sec) to be 28 %, so some 23 % has to be provided for. Resonators are supposed to be prescribed for aesthetical reasons.

In order to keep the costs as low as possible the most annoying frequencies, say 150—600 Hz, will be most absorbed. Let us try to find suitable resonators of one single kind, resonance frequency 300 Hz, interval 2 octaves. We calculate:

$$\lambda_{\text{res.}} = 340/300 = 1.1 \text{ m,}$$

$$G = 3 \text{ cm (high, but tolerable),}$$

$$G/\lambda_{\text{res.}} = 0.027 \text{ (reasonable wall economy, Fig. 78),}$$

$$\mu \approx 50 \text{ (Fig. 77 or 78 for 2 octaves wanted),}$$

$$A_{\text{res.}} \cdot O/\lambda_{\text{res.}}^2 = 0.0215 \text{ (Fig. 77 for } g = 0.027, \mu = 50),}$$

$$A_{\text{res.}} = 0.0215 \times 1.1^2/2 = 0.013 \text{ m}^2,$$

$$\text{number of resonators wanted /m}^2 = 23/1.3 = 17.7,$$

$$V \approx 1000 \text{ cm}^3 \text{ (eq. (7.01) or Fig. 73).}$$

There are several reasons for decreasing the number of resonators. The first one is that the theory of § 2 applies to normal incidence, whereas in practice the incidence is more or less at random. Now the acoustical "e.m.f." is  $2p$ , independent of the angle of incidence  $\theta$ . The absorbed power is therefore also independent of  $\theta$ , whilst the absorption coefficient of the wall is proportional to  $1/\cos \theta$ . At  $\theta = 60^\circ$  the absorption coefficient is doubled, whereas

for  $\theta$  approaching  $90^\circ$  the absorption coefficient increases without limit. Even the effect averaged over the solid angle (see Chapter VIII § 2 equation (8.03)) is infinitely high. We therefore think that in practice the effect will be at least a factor 2 greater than according to § 2.

A second advantageous circumstance is that the impedance contour of a resonator is not exactly a straight vertical line in the complex impedance plane, as is assumed in equation (7.04). It is sometimes curved, the resistance being approximately minimum at resonance. This means that the resonance peaks are to be expected broader than according to the theory of § 2.

It therefore seems justified to assume that in the case mentioned 8 resonators per  $\text{m}^2$  have a reasonable effect. Of course several surfaces are unsuitable for mounting resonators (doors, windows, the floor), so that the number of resonators per  $\text{m}^2$  of the remaining surface should be increased accordingly.

Although the solution of the practical problem of this § seems correct there is a reason to make another choice.  $\mu$  should be 50, which will be difficult to achieve without measurement of resistances, e.g. by impedance measurement. An alternative is to take about the same number of resonators but to use a certain spread in resonance frequencies.  $\mu$  can then be taken smaller. This will even slightly augment the wall economy (Fig. 78). We then use resonators of  $\mu = 10$  to 50. The effect will now be rather independent of  $\mu$ .

Finally we should like to emphasize that in order to act as absorber the resonator should have a reverberation time much shorter than that of the room where the resonators are used. In most cases this condition is easily fulfilled. In case of doubt it should be checked. Without giving the derivation we give the formula for the reverberation time

$$\tau = 13.82 \frac{\rho_0}{(R_{\text{rad}} + R)G} = 0.0064 \frac{1}{1 + \mu} \frac{\lambda_{\text{res}}}{G/\lambda_{\text{res}}}$$

Requiring  $\tau$  not to exceed 0.1 sec and putting  $\mu$  for reasons of economy at the minimum value 10, we can compute the minimum permissible conductivity (approx. diameter of the mouth) as a function of the resonance frequency (see Table 9). At low frequencies it seems advantageous to choose  $\mu$  greater than 10.

TABLE 9

MINIMUM CONDUCTIVITY  $G$  AT VARIOUS RESONANCE FREQUENCIES  
FOR  $\tau < 0.1$  SEC AND  $\mu > 10$

$\nu$	$G_{\min}$
100 Hz	0.069 m
200	0.017
400	0.004
800	0.001

#### § 4 PERFORATED PANELS BEFORE A RIGID WALL

We now proceed to the more important case of perforated panels, mounted at some distance before a rigid wall and similar constructions that can be treated as a system consisting of an infinite number of resonators, all channels ending in a rigid plane wall. The resonators will be supposed to be distributed in some regular way over the surface, the number per  $\text{m}^2$  being  $n$ . This case indeed is more important than that of the single resonator since it turns out feasible to make in a more economical way constructions that absorb very satisfactorily in a wide frequency range. As a matter of fact absorbers of this type are in widespread use. They usually contain some porous medium (e.g., glass silk) between panel and wall.

Now from a theoretical point of view it is much easier to suppose the air resistance concentrated in the channels, i.e., near the perforations, which will, therefore, be assumed presently. There is much evidence, however, that the theoretical results will be applicable to practical constructions with a porous medium in the entire volume behind the perforated panels. Frictional losses will be maximum where the velocities are maximum, i.e., near the perforations. The bulk of the porous medium is present in the regions where the air essentially is at rest and acts as a spring. This part of the porous medium only manifests its presence by reducing the air volume, thus increasing the resonance frequency a little. Indeed, the experimental results will be shown to agree fairly well with the theoretical formulae based on the assumption of concentrated air resistance.

The quantities governing the problem are (see Fig. 80)

$V$  = the volume per perforation,

$n$  = the number of perforations per unit surface,

$G$  = the conductivity of one hole ( $S/l$  for a long cylindrical channel),

$R$  = the air resistance of one hole (pressure difference divided by velocity of volume displacement through one hole disregarding inertia effects)

If the dimensions of  $V$ , and, therefore, the mutual distances of the holes, are very small in comparison to the wave length, a *specific* acoustic impedance can be defined as  $z$  = pressure/velocity of volume displacement per  $m^2$ , from which the absorption coeffi-

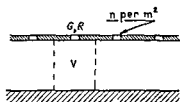


Fig 80

Quantities governing the behaviour of perforated panels

cient  $a_0$  of the construction can be computed with the aid of the usual relation

$$a_0 = 1 - \left| \frac{z - W_0}{z + W_0} \right|^2 \quad (7.13)$$

This expression can be obtained along the same lines as in the preceding section. We then are to take the acoustical "e.m.f." equal to  $2p_i$ , as before, the internal impedance or radiation impedance being  $W_0$ . It is clear that the external end correction has to be incorporated in  $z$ .

Since the volume displacement per  $m^2$  is  $n$  times that of one hole we can put immediately (see (7.04))

$$z = \frac{1}{n} [R + j\omega\rho_0/G + \kappa p_0/j\omega V] \quad (7.14)$$

It is not advantageous to substitute (7.14) in (7.13) in order to find  $a_0$ . We can better have recourse to the circle diagram (Fig 11), from which  $a_0$  can be read if  $z$  is known. In resonance the impedance is  $R/n$ , a real quantity that can be varied at will

for the same construction by adequately choosing the air resistance  $R$  of the perforations. If the frequency is varied around resonance,  $R$  can be considered as a constant and an impedance contour parallel to the imaginary axis is found. The frequency scale along this contour only depends upon  $n$ ,  $G$  and  $V$  (see the imaginary part of  $z$  in (7.14)) and is independent of  $R$ . One sees at a glance from Fig. 11 that, if  $R$  is increased for a given construction ( $n$ ,  $G$  and  $V$  constant), the frequency range of absorption is extended. But, simultaneously, the absorption coefficient at resonance decreases with increasing  $R$ . Therefore, increased  $R$  means decreased selectivity (in most cases a great advantage), but decreased maximum absorption coefficient (in most cases a disadvantage). The problem is, therefore, to find for every case the most adequate compromise between these two features.

An adequate measure for the selectivity of the construction is the frequency range in which the absorption coefficient is more than 50 % of the maximum value (resonance). Putting  $z = r + jx$  in (7.13), where  $x$  is a function of frequency,  $a_{0\text{res.}}$  is obtained by inserting  $z = r$  (i. e.,  $x = 0$ ). The critical value of  $x$  for which  $a_0$  is equal to  $\frac{1}{2} a_{0\text{res.}}$  is easily found from (7.13) to be

$$x = \pm (r + W_0). \quad (7.15)$$

The critical  $x$ -value as a function of  $r$  can obviously be represented in the complex impedance plane by the two lines at  $45^\circ$  slope through the point  $-W_0$  (see Fig. 81), from which it is clear that the selectivity is only small for not too small values of  $r$  ( $= R/n$ ). Taking 40 % and 75 % as reasonable limits for  $a_{0\text{res.}}$  in practice, one sees from Fig. 11 and 81 that  $R/n$  should be somewhere in between  $3 W_0$  and  $8 W_0$ , say between 1300 and 3500 mks-units.

Inserting the expressions for  $x$  and  $r$ , as read from (7.14), in (7.15) gives an equation from which the two critical frequencies that determine the width of the absorption characteristic can be computed. As in § 2 the ratio's of these frequencies and the resonance frequency will be labelled  $f_1$  and  $f_2$ . They can be called the relative critical frequencies. Bearing in mind that  $\omega_{\text{res.}} = c_0 \sqrt{G/V}$ , one easily verifies that  $f_1$  and  $f_2$  satisfy the equation

$$f - \frac{1}{f} = \pm n \sqrt{GV} \left( \frac{R}{nW_0} + 1 \right) \quad (7.16)$$

This equation is the parallel of (7.11) of the single resonator theory (7.16) is, however, much simpler. All quantities except  $f$  are combined in one single variable the right hand side of (7.16). This is due to the simpler radiation impedance in this case, that is independent of frequency. One simple feature of (7.16) is, that  $f_1 f_2 = 1$ , i.e.  $f_1$  and  $f_2$  are situated symmetrically with respect to 1 on a logarithmic frequency scale.

If the number of octaves  $O$  between  $f_1$  and  $f_2$  is small simple

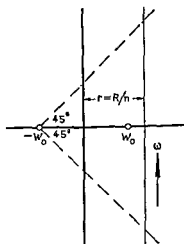


Fig. 81

To the selectivity of perforated panels

relations hold as in § 2. There is even a close analogy in the formulae if analogous variables are introduced

Labelling

$$R/nW_0 = \mu',$$

$$nG = G' \text{ (conductivity per m}^2\text{),}$$

$$nV = V' \text{ (volume per m}^2 \approx \text{width of the air gap between panel and wall),}$$

$$G'/\lambda_{\text{res}} = g',$$

the following equations can be shown to be valid



$$\left. \begin{aligned}
 a_{0_{\text{res.}}} &= 4 \mu' / (1 + \mu')^2 \\
 O &= \frac{\lambda_{\text{res.}}^2}{2} 1.442 (1 + \mu') g' \\
 a_{0_{\text{res.}}} \cdot O / \lambda_{\text{res.}}^2 &= 0.918 \mu' g' / (1 + \mu') \\
 a_{0_{\text{res.}}} \cdot O / G'^2 &= 0.918 \mu' / g' (1 + \mu') \\
 a_{0_{\text{res.}}} \cdot O / \lambda_{\text{res.}} G' &= 0.918 \mu' / (1 + \mu'),
 \end{aligned} \right\} \quad (7.17)$$

i. e., analogous formulae hold but for the factor  $\lambda_{\text{res.}}^2/2$  that has disappeared from the equation of  $a_{0_{\text{res.}}}$  and now enters in  $O$ . The equations in which the product  $a_{0_{\text{res.}}} \cdot O$  is involved are the same, i. e., also in this case high values of  $\mu'$  and  $g'$  are advantageous. It should be borne in mind, however, that (7.17) only holds for rather small values of  $O$ , thus limiting the validity of (7.17) to certain maximum values of  $\mu'$  and  $g'$ .

If  $O$  is no longer supposed to be small, graphs have to be used for exact design which this time are simpler however, since  $a_{0_{\text{res.}}}$  as well as  $O$  are functions of one independent variable only.

The design is then based upon the formulae

$$\left. \begin{aligned}
 a_{0_{\text{res.}}} &= 4 \mu' / (1 + \mu')^2 \\
 O &= \text{a known function of the product } \lambda_{\text{res.}} G' (1 + \mu')
 \end{aligned} \right\} \quad (7.18)$$

The following way of developing a construction seems suitable

1. choose  $a_{0_{\text{res.}}}$ ,  $O$ ,  $\lambda_{\text{res.}}$ ,
2.  $\mu'$  and  $\lambda_{\text{res.}} G'$  then follow from (7.18) or from the graphs representing these formulae,
3.  $\mu'$  yields  $R/n$ ,
4.  $\lambda_{\text{res.}} G'$  and  $\lambda_{\text{res.}}$  yield  $G' = nG$  and  $V' = G' \lambda_{\text{res.}}^2 / 4 \pi^2$ ,  
i. e., the gap between panel and wall,
5. the amount  $nG$  can be achieved with many small holes or with a smaller number of big holes. An approximate practical solution may be obtained from  $nG \approx nD$ , where  $D$  is the diameter of one hole.

## § 5 RULES FOR DESIGNING PERFORATED PANEL ABSORBENTS

In this section we shall give some graphs for the design of practical constructions, based upon the theory of § 4, but adapted to the use without understanding this theory.

Fig 82 shows what can be achieved with perforated panels

If  $a_{0_{res}}$ , i.e., the absorption coefficient at resonance (maximum value of  $a_0$ ) and the number of octaves  $O$  in which the absorption coefficient is greater than  $a_{0_{res}}/2$  are given, Fig 82 immediately yields the necessary values of  $R/nW_0$  (right scale on the ordinate axis), the ratio  $V'/\lambda_{res}$  of the thickness of the air space  $V'$  and the wave length at resonance  $\lambda_{res}$ , and the product  $\lambda_{res} nG = \lambda_{res} G'$ ,

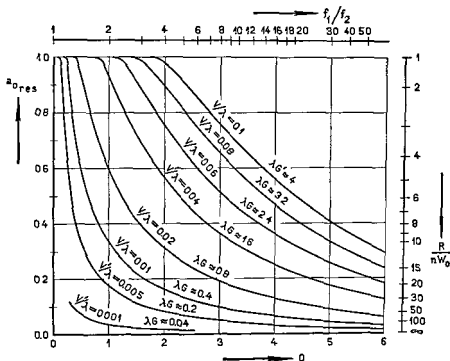


Fig 82

Design chart for perforated panels

where  $n$  is the number of holes per  $m^2$ ,  $G$  the conductivity of one hole and, therefore,  $G'$  is the conductivity per  $m^2$

Owing to the relation  $\omega_{res} = c_0 \sqrt{G'/V'}$  the ratio  $V'/\lambda_{res}$  is equal to  $\lambda_{res} G'/4\pi^2$  so that the curves of constant  $V'/\lambda_{res}$  in Fig 82 are also curves of constant  $\lambda_{res} G'$  (constant values approx 40 times greater)

In order to give another idea of the frequency band in which the absorption is reasonable also the abscissa axis has a double

scale. The main scale gives the number of octaves between the two critical frequencies  $f_1$  and  $f_2$ , the supplementary scale the ratio between these frequencies.

As a rule the frequency at which the absorption is maximum is also specified, so that from  $V'/\lambda_{\text{res.}}$  the air space  $V'$  between panel and wall can be computed. If the resonance frequency is 340 Hz  $\lambda_{\text{res.}}$  is one meter and  $V'/\lambda_{\text{res.}}$  is equal to the air space in meters. One sees that for 75 % maximum absorption in 3 octaves (150—1200 Hz)  $V'/\lambda_{\text{res.}}$  should be about 0.1, i. e.,  $V'$  should be about 5 to 10 cm.

The numerical value of  $\lambda_{\text{res.}}nG$ , found from the requirements, can be obtained in many ways. If the perforation consists of cylindrical holes of cross-sectional area  $S$  in a panel of thickness  $l$

$$G = S/(l + 0.8 D), \quad (7.19)$$

where  $D$  = diameter of a hole. If the damping of the resonator is provided by a thin air resisting layer in or quite near to the channel this expression holds. If, however, the entire volume of the resonator is filled with porous material or the air resisting layer near the channel is of a thickness equal to the radius of the hole or more,  $G$  is decreased. We then have to replace  $0.8 D$  in (7.19) by  $0.4 (1 + k/h) D$ , where  $k$  is the structure factor and  $h$  the porosity of the porous material. As a rule  $k/h$  may be assumed to amount to 2 for generally used filling materials. If the panel is of small thickness in comparison to the diameter of the perforations, (7.19) reduces to

$$G = D \quad (7.20)$$

or to

$$G = 2 D/(1 + k/h) \quad (7.21)$$

if the entire resonator is filled with porous material. In practical cases (7.20) may be a rough approximation, very helpful in the design. If the thickness is not negligible and if  $k$  can be put equal to unity (air resistance concentrated in a thin layer or unfilled resonators) an adequate couple of  $l, D$  values can be read from Fig. 83, giving  $G$  as a function of  $l$  and  $D$ . E. g., the conductivity  $G = 3$  mm may be obtained with holes of 5 mm diameter in a panel of 2.5 mm thickness.

*Example* Design a construction with resonance frequency 300 Hz, absorbing 60 % at 300 Hz and 30 % at 100 Hz and 900 Hz

From Fig 82 we find that, in order to fulfil the requirements ( $a_{\text{res}} = 0.6$ ,  $f_1/f_2 = 9$ ) we are to take

$$V'/\lambda_{\text{res}} = 0.03,$$

$$\lambda_{\text{res}} G' = 3.2,$$

$$R/nW_0 = 4.5$$

Since  $\lambda_{\text{res}} = 345/300 = 1.15$  m we obtain

$$V' = 0.09 \text{ m} = 9 \text{ cm}$$

$$G' = nG = 2.8 \text{ m}^{-1}.$$

The air space is, therefore, fixed and should be 9 cm. A few solutions that fulfil  $G' = 2.8 \text{ m}^{-1}$  are

$n$	$G$	$D$	$l$	% perf
250 $\text{m}^{-2}$	11.2 mm	14 mm	1 mm	4 %
		20	10	8
500	5.6	7	1	2
		12	10	5.5
1000	2.8	3.5	1	1
		8	10	5
2000	1.4	2	1	0.6
		5	10	4

These results are directly read from Fig 83. The last column gives the *percentage perforation*. In order to keep this low many small holes in thin panels are required. If aesthetic requirements do not play a part a solution with a small number of big holes might be much more economical and equally effective.

The real difficulty of the design is to adjust  $R$  to the required value by means of some practical construction. This may be done by filling the whole gap with some porous medium (e.g., glass silk) of the required air resistance.

For thin panels (thickness small in comparison to the diameter of the holes) the resistance  $R$  can be expressed in the conductivity  $G$  of one hole and the specific air resistance of the filling material. This relation holds even for non circular perforation owing to the

close analogy of the two concepts.  $1/G$  is, according to its definition,

$$\frac{1}{G} = \int \frac{dl}{S}$$

the integral being taken over the channel, end corrections included. One should bear in mind that the effective area  $S$  through which the flow of air takes place is  $k/h$  times smaller if porous material

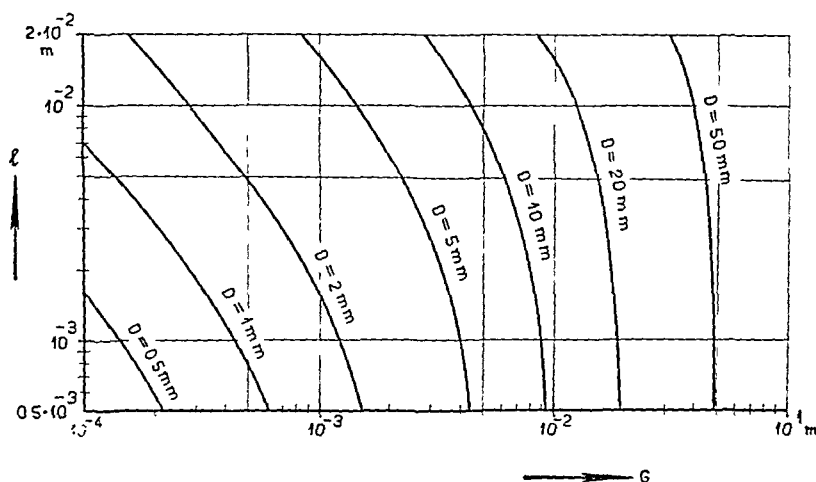


Fig. 83  
The conductivity  $G$  of a circular cylindrical channel  
of diameter  $D$  in a panel of thickness  $l$

is present at the site under consideration.  $R$  is, also according to its definition,

$$R = \int \frac{(dp/dl)dl}{v \cdot S},$$

if  $v$  = specific velocity of volume displacement, the integral being taken over the same path. Now  $(dp/dl)/v$  is the specific air resistance  $\sigma$  of the medium. If  $\sigma$  is great at the site of the internal end correction only, the  $R$ -integral can be restricted to that part of the channel; if the panel is very thin, the  $G$ -integral is taken over exactly the double length, and owing to the symmetry

$$R = \sigma \cdot 1/G (1 + k/h) \quad (7.22)$$

Now  $G$  and  $R$  are found from the requirements, so  $\sigma$  can be computed if  $l/h$  is put equal to, say, 2

Therefore, if the whole gap is filled with porous medium, its specific air resistance should be

$$\sigma = (1 + l/h) RG \quad (7.23)$$

Since resonators are generally used at low frequencies, the steady flow value of  $\sigma$  can be taken as an approximation. For higher precision the dynamical value at the corresponding frequency must be used, which can be greater (see Chapter I § 9)

With practical constructions the product  $RG = G'R/n$  only varies in a limited range (see Fig. 82) from which values for  $\sigma$  can be computed lying in the neighbourhood of that of hair felt or lower (Chapter II § 5). If the panel is thick in comparison to the diameter of the holes  $\sigma$  should be higher than according to (7.23) in the ratio

$$\{1 + 0.4(1 + l/h)D\} / 0.4(1 + l/h)D$$

A simpler way of adjusting  $R$  to the required value is the coating of the panel at the outside or the inside with a thin layer of adequate air resistance, e.g. a high resistance textile coating, blotting paper, etc. Now there is no objection against measuring the resistance under steady flow, since such high resistance layers are certainly governed, even in the dynamical case, by the Poiseuille law. Moreover the quantities  $l$  and  $h$  do not enter into  $G$  in this case.

An advantage of filling the entire gap with porous material is probably that we then obtain constructions that also absorb reasonably in the frequency range where the resonator conception fails, i.e., far above resonance.

#### § 6 RULES FOR DESIGNING PANEL ABSORBENTS WITH SLITS

If the perforations are not circular in cross-section, but have the form of infinite or very long slits in the panel the rules of § 5 can be used as well. We then have to consider  $V$ ,  $G$  and  $R$  as the volume, conductivity and air resistance per m length of a slit. A rough approximation for the conductivity  $G$  might

be computed from the formula for a single slit, according to Pedersen (see § 1 of this chapter)

$$1/G = d/b + 0.7 + (2/\pi) \ln 2 c_0/\omega b,$$

although there is some evidence that this expression lacks accuracy in the case of panels with many slits.

For thin panels and gaps completely filled with porous material we, again, have

$$\sigma = (1 + k/h) RG.$$

## § 7 EXPERIMENTAL RESULTS

The literature does not provide us with many adequate data corroborating the theory. In this section results of a few fundamental experiments will be described<sup>1</sup>.

Impedance measurements have been carried out on simple resonators; they merely consisted of a circular metal plate of 5 mm thickness, provided with a circular hole of 4 or 8 mm diameter in the middle, which plate was fixed in the sample holder of the interferometer of Fig. 33 (diameter of the tube 90 mm) at an appropriate distance before the rigid back plate of the holder. In this way resonators of two conductivities and adjustable volume could be built.

Experiments of this kind yield results that should comply with the theory of perforated panels (§ § 4, 5), not with that of a single resonator (§ 3). As a matter of fact the reflected wave is plane at a reasonable distance from the resonator, as is the case with perforated panels. The behaviour is the same as that of a wall completely occupied by resonators of the same kind, i.e., with a number  $n$  per  $m^2$  equal to 1 divided by the surface of the interferometer tube in  $m^2$ . It makes no difference that the interferometer tube is circular in cross-section. It is merely not feasible to cover a wall with  $n$  round resonators of the described form.

In Fig. 84 three impedance contours are given drawn in full, the data of which are

$$D = 4 \text{ mm}, V' = 1.8 \text{ mm}, 8.1 \text{ mm}, 11.3 \text{ mm resp.}$$

---

<sup>1</sup> We thank Mr. E. G. de Bruyn, phys. cand., for carrying out the experiments.

The measuring frequencies are added near the measured impedances. The corresponding absorption characteristics are given drawn in full in Fig S5. The experimentally found resonance frequencies

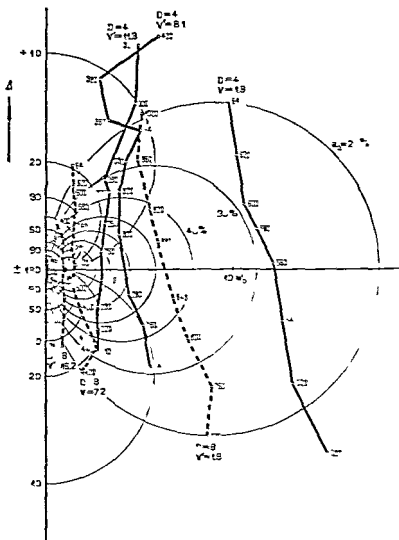


Fig S4  
Impedance contours of six simple cylindrical resonators  
(to the theory of pages)

are 575, 290 and 240 Hz resp. whereas from diameter  $D$  and volume  $V$  one computes 627, 290 and 252 Hz (approximate values may readily be found with the aid of Figs S3 and 73). One sees



that the agreement is very good except for the resonator of 2 mm depth ( $V' = 1.8$  mm as a consequence of the thickness of the sample holder). Obviously, if the resonator has a depth smaller than the diameter of the hole the conductivity is lowered appreciably, as was to be expected<sup>1</sup>. Another feature of the impedance contours is readily explained. The resistance (distance from the imaginary axis) is materially increased by the vicinity of the bottom of the resonator if the depth is of the order of the dia-

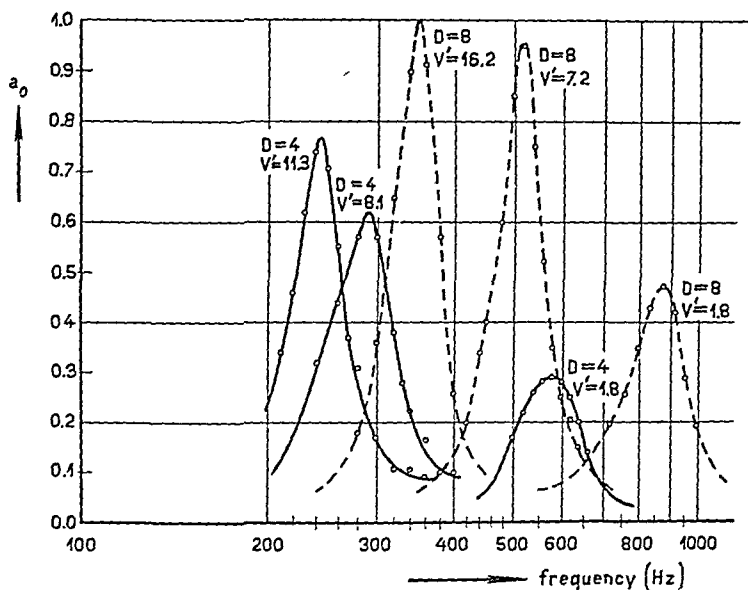


Fig. 85

Absorption characteristics to Fig. 84

meter  $D$ . The curve width in octaves turns out to be in fair agreement with theory (Fig. 82). We may conclude from these results that practical non-filled resonators comply with the theory.

Similar results are obtained (see Fig. 84 and 85 dotted lines) with

$D = 8$ mm,	$V' =$	1.8 mm,	7.2 mm,	16.2 mm resp.
res. freq. measured		870 Hz,	515 Hz,	353 Hz resp.
res. freq. from $D$ and $V$		1063 Hz,	532 Hz,	354 Hz resp.

<sup>1</sup> See also U. Ingård, *J. Acoust. Soc. Am.*, 20 (1948) 665.

The conductivity appears to be lowered some 7% even if the depth is equal to the diameter. For resonators of normal depth the theory holds very well. The number of octaves is again approximately as theoretically predicted from  $a_{\text{res}}$  and  $\Gamma'/\lambda_{\text{res}}$ .

In Fig. 86 results of more practical resonators are given.<sup>1</sup> The resonator was a thin perforated metal plate placed in the interferometer as previously. The air space behind the perforated plate was 30 mm; the gap was filled with glass silk. Unfortunately no impedances were measured. The perforation consisted of circular holes in a "cubical lattice", 5.6 mm apart from each other, 4 mm in diameter; the whole plate had about 175 holes. Variations of

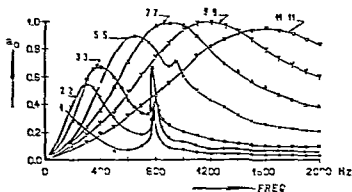


Fig. 86

Absorption characteristics of the same resonator with different perforations

the resonator were made by closing a great number of these holes. The curves in Fig. 86 from left to right correspond to  $1 \times 1$ ,  $2 \times 2$ ,  $3 \times 3$ ,  $5 \times 5$ ,  $7 \times 7$ ,  $9 \times 9$  and  $11 \times 11$  holes opened in the middle of the plate.

The curves of  $1 \times 1$  to  $3 \times 3$  holes show a second resonance at 600 to 900 Hz. This has nothing to do however with the resonator, these irregularities being probably due to a vibration of the metal covering plate.<sup>2</sup> If many holes are opened the force on the metal plate is negligible and the effect therefore, absent. The shifting

<sup>1</sup> Unpublished result of J. van den Esk (1945) whom we thank for the permission of publication.

<sup>2</sup> See also V. L. Jordan, *Acoust. Z.*, 5 (1940) 7.

of this resonance to higher frequency if more holes are opened is explained by the decrease of the mass of the plate by opening the holes.

Qualitatively we see:

- a. increasing the number of holes leads to a higher resonance frequency caused by the increased conductivity  $G$  of the resonator,
- b. if the number of holes increases, the air resistance of the resonator must decrease and therefore  $a_{0\text{res.}}$  should increase (see Fig. 11, 81 and 82), as is actually found,
- c. the curve for  $9 \times 9$  holes almost reaches  $a_{0\text{res.}} = 100\%$ , the curve  $11 \times 11$  holes shows a decreased maximum absorption. Obviously the resistance reaches the critical value  $W_0$  at about  $9 \times 9$  holes.

It is not very easy to estimate the conductivity as a function of the number of holes. Firstly the resonator is filled, so the structure factor might be of influence. Furthermore the holes are so close to each other that the conductivity is probably not proportional to the number of holes. Moreover the depth of the resonator is small, so if many holes are opened the "effective diameter" of the perforations will be greater than the depth, so that then computation is quite impossible.

One easy verification can be made, however.  $a_{0\text{res.}}$  and  $\lambda_{\text{res.}}$  are known for every curve. Since the volume is known the curve width can be read from Fig. 82. The measured curve width agrees fairly well with the computed ones. The discrepancies are systematical and show the trend of a somewhat greater curve width than computed. Almost certainly this is due to a curvature of the impedance contour.

We may conclude from the experimental results of this section that

- a. the simple theory holds for practical constructions,
- b. the curve width actually found is in most cases greater than that theoretically predicted.

## § 5 COMBINATIONS OF RESONATORS

A drawback of any resonator construction is always that it absorbs more or less selectively in the neighbourhood of resonance, although the best constructions of this type are very satisfactory

indeed Especially in those cases where absorption at high frequencies is not necessary because the room in question already contains a considerable amount of porous material (upholstery of seats, auditorium, wood fibre plates, carpets) excellent results can be obtained with a simple perforated panel device

If however a resonator construction is needed that absorbs non selectively in a very broad frequency range recourse should be had to a combination of resonators Series connections (Fig 87a) and parallel connections (Fig 89a) seem equally advantageous in this respect

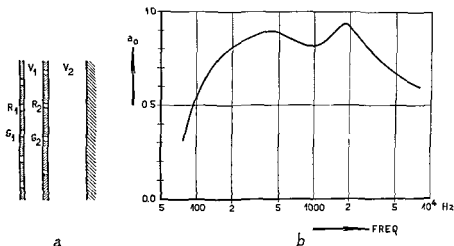


Fig 87  
Double resonator in series

Whereas a single perforated panel has only one degree of freedom (one resonance frequency), the double construction of Fig 87a has two, which manifests itself in two peaks in the absorption curve (Fig 87b)<sup>1</sup>

The theory of such double resonators has been given by Rayleigh<sup>2</sup> For our purpose it is, however, more convenient to make use of the impedance concept. If namely the two perforated panels have a non identical perforation we cannot always divide the whole construction into double resonators, each having

<sup>1</sup> P V Bruel, *Lydsolation og rumakustik*, p 120, Goteborg 1946

<sup>2</sup> Rayleigh, *Theory of sound* II, 2nd ed, § 310, Cambridge 1896

two holes, but the construction must be treated per  $m^2$ . The construction is governed by the conductivities  $G_1$  and  $G_2$  per  $m^2$  (in  $m^{-1}$ ), the volumes  $V_1$  and  $V_2$  per  $m^2$  (equal to the thickness of the respective layers of air apart from the volume of the porous filling material, if any) and the resistances  $R_1$  and  $R_2$  per  $m^2$  (see Fig. 87a).

The electrical analogue of the specific impedance is given in Fig. 88. In view of the six variables it seems hardly possible to use this scheme directly or the computed impedance therefrom for designing adequate constructions. It is, however, easy to give a rough idea of the frequency range in which the construction absorbs, viz., by considering the two values of resonance.

The resonance frequencies are approximated by putting  $R_1$  and  $R_2$  equal to zero and consequently computing the frequencies for

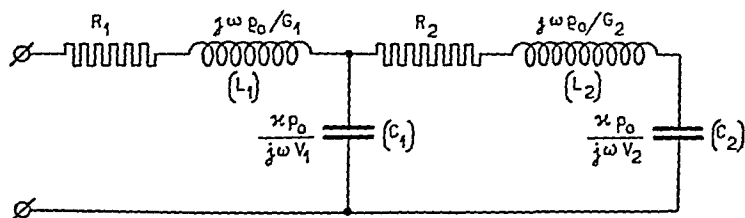


Fig. 88

The impedance of double resonator in series connection (see Fig. 87).

which the (imaginary) impedance becomes zero. Labeling the inductances and capacities for brevity  $L_1$ ,  $L_2$ ,  $C_1$ ,  $C_2$  (see Fig. 88), we have ( $R_1 = 0$ ,  $R_2 = 0$ )

$$z = j\omega L_1 + \frac{1}{j\omega C_1} \left( j\omega L_2 + \frac{1}{j\omega C_2} \right) \bigg/ \left( \frac{1}{j\omega C_1} + j\omega L_2 + \frac{1}{j\omega C_2} \right)$$

which becomes zero for

$$j\omega L_1 \left( \frac{1}{j\omega C_1} + j\omega L_2 + \frac{1}{j\omega C_2} \right) + \frac{1}{j\omega C_1} \left( j\omega L_2 + \frac{1}{j\omega C_2} \right) = 0$$

or

$$\omega^4 - \omega^2 \frac{L_1 C_1 + L_2 C_2 + L_1 C_2}{L_1 L_2 C_1 C_2} + \frac{1}{L_1 L_2 C_1 C_2} = 0. \quad (7.24)$$

Labeling the resonance angular frequencies  $\omega_{\text{res.1}}$ ,  $\omega_{\text{res.2}}$ , we immediately read from (7.24)

$$\left. \begin{aligned} \omega_{\text{res } 1}^2 + \omega_{\text{res } 2}^2 &= \omega_{\text{res } 1 \text{ free}}^2 + \omega_{\text{res } 2 \text{ free}}^2 + \frac{1}{L_2 C_1}, \\ \omega_{\text{res } 1} \omega_{\text{res } 2} &= \omega_{\text{res } 1 \text{ free}} \omega_{\text{res } 2 \text{ free}} \end{aligned} \right\} \quad (7.25)$$

if  $\omega_{\text{res free}}$  is the resonance angular frequency of the single resonator ( $= c_0 \sqrt{G/V} = 1/\sqrt{LC}$ )

From the second equation (7.25) we see that the logarithmic mean value of the resonance frequencies is the same as when the resonators were not coupled at all, from the first equation (7.25) we see that the resonance frequencies are more or less separated due to the coupling. This effect may be neglected for the first

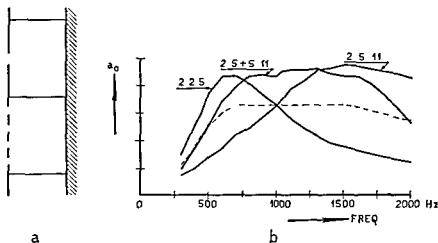


Fig 89

Double resonator in parallel

calculation or estimated to some 20 % of the free frequencies. If for example a construction is wanted absorbing from 50 to 3000 Hz the coupled resonance frequencies will have to be about 150 and 1000 Hz, the free resonance frequencies are to be chosen, therefore, at about 180 and 800 Hz. This can be done with the aid of the rules given in § 5. It is more difficult to find the best adjustment of the resistances  $R_1$  and  $R_2$ . As long as the results of extensive experiments are lacking a good approximation will be the values that make the non coupled resonators not too selective.

A parallel connection unit is shown in Fig 89a. It consists of two resonators quite near to each other with different resonance frequency. If the absorbing wall is supposed to be completely

covered with units of this type the absorption coefficient can be computed from the mean specific admittance of the wall

$$Y = f_1 Y_1 + f_2 Y_2 \quad (7.26)$$

if  $f_1, f_2$  denote the fraction of the surface occupied by resonators of the first and second type resp. and  $Y_1, Y_2$  the specific admittance of a wall containing only resonators of the first and second type respectively. (7.26) is based on the assumption that the resonators are very small compared with the wave length, so that the pressure will be constant over the whole wall (normal incidence being assumed as previously) and the volume displacement is additive.

The absorption coefficient is computed from the well-known formula (7.08) using admittances instead of impedances ( $1/W_0$  instead of  $W_0$ ). Also the circle diagram Fig. 11 is valid ( $1/W_0$  instead of  $W_0$ ).

We have

$$1/Y = R + j\omega\rho_0/G + \kappa\rho_0/j\omega V,$$

$$Y = 1/(R + j\omega L + 1/j\omega C)$$

or

for brevity. It should be borne in mind that all quantities in these equations refer to  $1 \text{ m}^2$ . Inserting  $Y_1$  and  $Y_2$  in (7.26) yields  $Y$ , from which the absorption coefficient can be found. As in the case of the series connection it seems wise, with a view to the six variables, to confine ourselves to the computation of the two resonance frequencies. They will give us a good impression of the absorption region provided the resistances are adjusted well.

Neglecting  $R_1$  and  $R_2$  we conclude that resonance occurs when  $Y_1$  or  $Y_2$  becomes infinite, i. e., for the two resonance frequencies of the single resonators. So in this case there is no influence of the coupling upon the resonance frequencies, greatly simplifying the design. Moreover constructions of this type have the same thickness as normal single-type construction. In Fig. 89b results are given of an experiment of this type. The resonator unit was a circular one, inner diameter 86 mm, thickness 30 mm, filling material glass silk. It was measured in the interferometer (diameter 90 mm) thus giving results as for a wall completely covered with resonators of this type (no dead space in between). The sample was divided into two halves by the insertion of a thin

## CHAPTER VIII

### OBLIQUE AND RANDOM INCIDENCE PRACTICAL ASPECTS

#### § 1 INTRODUCTION

In the previous chapters we confined ourselves to absorption at normal incidence. The reasons are that both theory and experiment become much more difficult when considering oblique incidence. Something must be said, however, about the behaviour of materials at oblique incidence with a view to the great importance of this case in practice.

The measurement of sound absorption at normal incidence is quite simple. As a consequence the properties of materials for this case have been studied extensively. The reverse is true for oblique incidence, the measuring techniques are more complicated, more over a new variable is introduced with the angle of incidence thus materially increasing the number of measurements necessary for describing the properties of a given material. Little is known, therefore from experiment of the behaviour of materials at oblique incidence.

Of the measuring devices the following need mentioning

- a exploration of the interference pattern<sup>1</sup>. Analogous to the interference pattern in normal incidence interferometers a pattern is found for oblique incidence, from which the absorption coefficient can be derived. Plane waves and large samples are required, moreover the experiment should be carried out in free space in order to avoid disturbances of the sound field.
- b Measurement at 45° incidence<sup>2</sup>. If two walls of a room are covered with the material under test and a plane wave is supposed to impinge upon the material in a direction nor-

---

<sup>1</sup> L. Cremer, *Flek. Nachr. Tech.*, 10 (1933) 302, 13 (1936) 36

<sup>2</sup> H. Schuster, *Akust. Z.* 3 (1938) 137



mally to the line of intersection of the walls and symmetrically to both walls an interference pattern is obtained. The absorption coefficient can be computed from the ratio of the extreme values of the pressure-gradient or the pressure along the direction of incidence. In this case too, free space and large samples are required.

- c. Measurement at  $55.7^\circ$  incidence<sup>1</sup>. If a plane wave impinges symmetrically upon a three-plane-corner consisting of three mutually perpendicular walls covered with the material under test, a similar pattern as sub b is obtained. The measurement is as sub b.
- d. Pulse method<sup>2</sup>. If a sound source, situated at a certain distance from the sample (large size) gives a short sound pulse, the microphone at the receiving place will receive two pulses, if the experiment is carried out in free space, viz., a pulse due to the direct sound from source to microphone, and a pulse reflected from the sample. The ratio of the intensities is governed by geometrical quantities and the absorption coefficient of the sample, that can be calculated by adequately taking into account the geometrical configuration or by calibration with a totally reflecting surface.
- e. Standing waves in a rectangular room<sup>3,4</sup>. This method is based upon the well-known fact that the eigenfunctions of a rectangular room with homogeneously covered walls can be described as the superposition of plane waves. This method seems to be the most promising one since no free space nor extremely large samples are necessary. Under certain circumstances it is possible to excite only one single characteristic frequency. From the decay of the intensity after stopping the sound source the absorption coefficient at the corresponding angle of incidence of the wall under test (other walls being totally reflecting) can be calculated.
- f. Reverberation method. In this well-known method the samples

---

<sup>1</sup> K. Schuster, *Akust. Z.*, 3 (1938) 137.

<sup>2</sup> F. Spandöck, *Ann. Physik*, 20 (1934) 328.

<sup>3</sup> H. and L. Cremer, *Akust. Z.*, 2 (1937) 296.

<sup>4</sup> H. Neubert, *Akust. Z.*, 5 (1940) 189.

are used under more or less random incidence. The interpretation of the results is, however, extremely difficult<sup>1</sup>

Since we know only little from experiment about the behaviour of materials under oblique incidence, it seems more adequate to study the problem theoretically. Among all materials those with so called local reaction are the easiest to consider. A layer of material is called locally reacting<sup>2</sup> if the velocity component perpendicular to the surface only depends upon the pressure at the point and not upon the angle of incidence. Typical examples are the samples with glass tubes (VI § 2), the single resonator in an infinite wall (VII § 2), a wall covered with resonators of this type, i.e., with resonators the volumes of which are not interconnected in another way than via the air in front of the wall. In these cases the ratio  $p/v_n$  is independent of the angle of incidence and equal to the impedance used for normal incidence.

In the case of a normal porous layer or of perforated panels with an uninterrupted air gap between panel and wall the impedance  $p/v_n$  will depend upon the angle of incidence, the more so when the sound velocity in the absorbing medium is greater and the damping of the travelling waves in a sideways direction is smaller. This is clearly shown by Morse<sup>2</sup> with different examples.

Now owing to the structure factor  $k$  of porous materials always being much greater than unity (say 4 to 9) the sound velocity in these media is 2 to 3 times smaller than in air. Moreover there is, as a rule, ample damping so there is reason for neglecting the extended reaction also in these cases. That a low sound velocity makes a material locally reacting can also be elucidated by considering the direction of the refracted wave in the material<sup>3</sup>. The incident wave is refracted towards the normal as a light beam impinging upon a glass surface. Even at glancing incidence the refracted wave only deviates by  $20^\circ$  to  $30^\circ$  from the normal so that also in porous media the interconnection of the pores in a sideways direction will not materially affect the impedance  $p/v_n$ .

<sup>1</sup> See e.g., E. Meyer and A. Schoch *Akust. Z.*, 4 (1939) 51

<sup>2</sup> P. M. Morse *Vibration and Sound*, 2nd ed., p. 361, New York 1948

<sup>3</sup> C. W. Kosten, *Thesis*, p. 99, Delft 1942

If perforated panels are used with non-filled air gaps extended reaction is quite sure. This seems to be a disadvantage of resonators of this type as compared with resonators with filled gaps. Extended reaction can be eliminated of course by splitting up the gap in many non-communicating volumes<sup>1</sup>

## § 2 OBLIQUE INCIDENCE ON LOCALLY REACTING SURFACES

Suppose a plane sound wave to impinge on the surface with impedance  $z$ , in a direction making an angle  $\varphi$  with the normal to the surface (see Fig. 90). The reflected wave will be as shown in the figure. Let  $p_i$  and  $p_r$  be the pressures at the surface in any point, then

$$z = \frac{p_i + p_r}{v_{in} + v_{rn}}$$

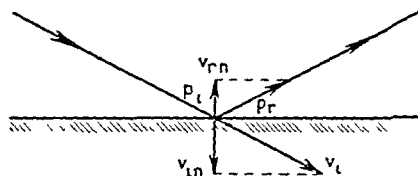


Fig. 90  
Oblique incidence

if  $v_{in}$  and  $v_{rn}$  are the normal components of the respective particle velocities towards the surface. Now

$$v_{in} = \frac{p_i}{W_0} \cos \varphi \text{ and } v_{rn} = -\frac{p_r}{W_0} \cos \varphi,$$

and therefore

$$\frac{z \cos \varphi}{W_0} = \frac{p_i + p_r}{p_i - p_r}.$$

The complex reflection coefficient  $p_r/p_i$ , and, therefore, the absorption coefficient  $1 - |p_r/p_i|^2$  bears the same relation to  $z \cos \varphi$  as to  $z$  in the case of normal incidence. Therefore, the circle-

<sup>1</sup> Note added in proof: The behaviour of perforated panels with non-filled air gaps at oblique incidence has recently been studied by J. Brillouin, Cahiers du Centre sci. et tech. du Bâtiment, Cahier 31, January 1949.

diagram Fig 11 also applies to this case, provided it is supposed to give the absorption coefficient and phase jump in the complex  $z \cos \varphi$  plane

A direct conclusion is the following since the impedance of many materials is larger than  $W_0$  both as to their real and imaginary part, an apparent decrease of the impedance as a consequence of the multiplication by  $\cos \varphi$  will generally increase the absorption coefficient. Only for very small impedances (near resonance) or for very small  $\cos \varphi$  (almost glancing incidence) the diminution of  $z$  to  $z \cos \varphi$  will be disadvantageous. It, therefore, is plausible that the mean value of the absorption coefficient, if all directions are taken into account, is greater than that for normal incidence.

An adequate mean value is found if the energy is considered that is absorbed by a surface element that is exposed to a completely diffuse sound field in terms of the incident energy. The incident energy comprised in a small solid angle  $d\Omega$  in a direction with an angle  $\varphi$  to the normal is proportional to  $\cos \varphi d\Omega$ , since the apparent surface of the surface element under consideration is proportional to  $\cos \varphi$ . Let the fraction  $a$  be absorbed. Then the mean value  $\bar{a}$  is defined as

$$\bar{a} = \frac{\text{absorbed energy}}{\text{incident energy}} = \frac{\int a_{\varphi} \cos \varphi d\Omega}{\int \cos \varphi d\Omega}$$

Now  $a$  is only dependent upon  $\varphi$ , therefore take as elementary solid angle  $d\Omega$  the small solid angle between a circular cone around the normal with top angle  $2\varphi$  and a similar cone with top angle  $2(\varphi + d\varphi)$ , then  $d\Omega = 2 \sin \varphi d\varphi$  and

$$\bar{a} = \int_0^{\pi/2} a_{\varphi} \sin 2\varphi d\varphi \quad (8.01)$$

For locally reacting surfaces  $a_{\varphi}$  is known as a function of  $\varphi$ , so the integral can be evaluated. This seems to have been done independently by Morse et al.<sup>1</sup> and the authors.<sup>2</sup> If the impedance  $z$  is written as  $R + j\Lambda$ , we obtain

<sup>1</sup> P. M. Morse, R. H. Bolt, and R. L. Brown, *J. Acoust. Soc. Amer.*, 12 (1940) 217.

<sup>2</sup> C. W. Kosten and C. Zwikker, *Physica* 8, (Febr. 1941) 251.

$$a = 8 \frac{W_0 R}{R^2 + X^2} - 8 \left( \frac{W_0 R}{R^2 + X^2} \right)^2 \ln \left( \frac{R^2 + X^2}{W_0^2} + \frac{2R}{W_0} + 1 \right) + 8 \frac{R}{X} \left( \frac{W_0 X}{R^2 + X^2} \right)^2 \left( \frac{R^2}{X^2} - 1 \right) \arctan \frac{X}{R + W_0}. \quad (8.02)$$

A more adequate representation is, of course, giving contours of constant  $\bar{a}$  in the complex  $z$ -plane. This is done in Fig. 91, which is the parallel of Fig. 11 for random incidence. The contours can

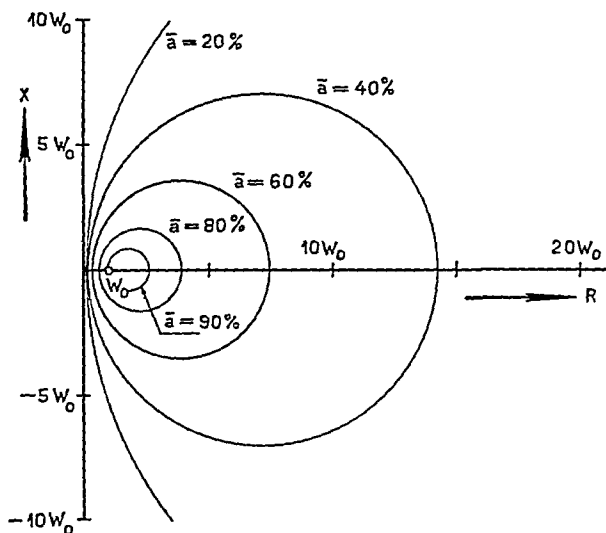


Fig. 91

The mean value of the absorption coefficient of a locally reacting surface as a function of the impedance

hardly be distinguished from circles, but actually are not. Another way of representation is given by Morse<sup>1</sup>. The maximum value of  $\bar{a}$  turns out to be 0.95. In Fig. 92  $\bar{a}$  is compared to  $a_0$  on the supposition that the impedance is real. The dotted part of the curve refers to impedances less than  $W_0$ . One sees that for impedances greater than  $W_0$ ,  $\bar{a}$  is appreciably larger than  $a_0$ .

<sup>1</sup> P. M. Morse, *Vibration and sound*, 2nd ed, p. 458, New York 1948.

## § 3 OBLIQUE INCIDENCE ON A SINGLE RESONATOR

Suppose a plane sound wave impinges obliquely upon a surface containing one single resonator. Since the acoustical 'e m f' is unchanged equal to  $2p$ , and the internal source impedance is the radiation impedance as previously and moreover the resonator impedance is unchanged too, the amount of the absorbed power is independent of the angle of incidence. Dividing this absorbed power by the power impinging upon  $1 \text{ m}^2$  wall surface, i.e., by

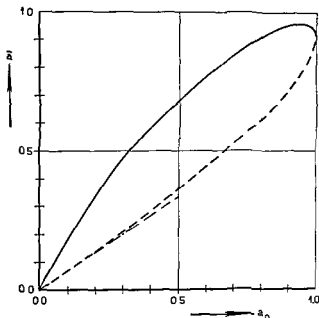


Fig. 92

The comparison between mean and normal value of the absorption coefficient for locally reacting surfaces with real impedance

$(\hat{p}^2/2W_0)\cos\varphi$  yields the surface in  $\text{m}^2$  of the equivalent open window, and since the absorbed power is independent of  $\varphi$ , the open window surface is inversely proportional to  $\cos\varphi$ . The average surface of open window for random incidence of sound within a cone with top angle  $2\varphi$  is readily computed to be

$$\frac{\bar{A}}{A} = \frac{-\ln \cos \varphi}{1 - \cos \varphi}, \quad (8.03)$$

if  $\bar{A}$  denotes the mean value and  $A$  the surface of open window at normal incidence

$\varphi$  cannot be extended to  $90^\circ$ , since then  $\bar{A}$  increases to infinity, which seems meaningless. There seems to be no theoretical objection against this extension. It is only of no practical value since the effect could only be verified with samples of unlimited dimensions.

One conclusion is however certain. The effective number of  $m^2$  open window at random incidence will always be greater than the computed number at normal incidence; experiments in a reverberation room are in agreement herewith.

In order to give some idea about the magnitude of this effect, we give the ratio  $\bar{A}/A$  for a few values of the maximum angle of incidence considered,  $\varphi_{\max}$ :

$\varphi_{\max}$	$30^\circ$	$45^\circ$	$60^\circ$	$75^\circ$
$\bar{A}/A$	1.07	1.18	1.38	1.82

Bearing in mind that a practical resonator is always somewhat less selective than according to the theory as a consequence of the slightly curved impedance contour, it seems justified to expect the number of  $m^2$  open window in practice to be about two times higher than the theoretical value at normal incidence.

# AUTHOR INDEX

- Bedell, H H 89, 127  
 Bekkering, D H 96  
 Beranek, L L 85, 90, 113, 124  
 Bohme, H 82  
 Bolt, R H 113, 168  
 Brillouin, J 167  
 Brown, R L 113, 168  
 Bruel, P V 127, 158  
  
 Chrysler, V L 87  
 Costadoni, B C 82  
 Cremer, H 165  
 —, L 164, 165  
  
 Eckhardt, E A 87  
 Eyk, J van den 40, 50, 77, 88,  
 111, 156  
  
 Fay, R D 93  
 Ferrero, M 49  
  
 Geluk, J J 99  
 Gigh, A. 127  
 Goldbaum, G 87  
  
 Hall, W M 88, 93  
 Harmans, J 88  
  
 Ingård, U 130, 155  
 Ingerslev, F 127  
  
 Jordan, V L 127, 156  
  
 Kasteleyn, M L 50  
 Kaye, G W C 40  
 Keidel, L 82  
 Kennely, A E 93  
 Kirchhoff, G R 30, 34  
 Kok, W 88  
 Korringa, J 42  
  
 Kosten, C W 15, 50, 52, 71, 83,  
 88, 93, 96, 111, 117, 119, 121,  
 166, 168  
 Kromg, R 42  
  
 Leonard, R W 77, 80  
  
 Meyer, L 82, 127, 166  
 Morse, P M 113, 166, 168, 169  
  
 Neubert, H 165  
 Nielsen, A K 127  
  
 Parns, E T 87  
 Pedersen, P O 127, 130  
 Pierce, G W 93  
  
 Rayleigh, Lord 30, 34, 43, 86, 127,  
 129, 135, 158  
 Rashevkin 127  
  
 Sacerdote, G 49  
 Schoch, A. 166  
 Schuster, K 164, 165  
 Sherratt, G G 40  
 Smit, A 42  
 Spandock, F 165  
  
 Taylor, H O 87  
 Tuma, J 87  
  
 Van den Eyk, J 40, 50, 77, 88,  
 111, 156  
  
 Wactzmann, E 87  
 Wente, E C 89, 127  
 Willms, W 127  
 Wintergerst, E 127  
 Wust, H 49  
  
 Zeller, W 127  
 Zwikker, C 15, 52, 71, 77, 111, 117,  
 119, 163



## SUBJECT INDEX

- Absorption coefficient 5
  - — , mean value of — 163
  - , measurement of — 85
- Admittance 161
  - diagram 74
- Air, compression modulus of — 29
  - density in cylinders 26
  - -impedance 73
  - resistance 79
  - -wave 62
- Attenuation constant 1
- avity factor 2
- Mular rubber 16, 111
- lotex C—4 114, 124
- relc diagram 12
- sed front surface 65
- mpression modulus of air 29
- nductivity 129, 130
- k 77
- ve width 136
- nping 131
- oupling frequency 62, 63
- opillo 114
- iciency of resonator 136
- tie frame 52, 116
  - corrections 129
- riments 107
  - 50, 63, 77
- air — 47
- , wood- 63, 77
- e-impedance 73
- esonance 69
- rave 62
- ency 1
  - decoupling- 62, 63
- tubes 103
- Hair felt 47
- Heat conductivity 42
- Honeycomb 103
- Impedance, air- 73
  - , frame- 73
  - , measurement of — 85
  - of resonator 132
- Interferometer 86
  - , reaction- 91
- Kirchhoff's theory 26
- Lattice 114
- Local reaction 166
- Loss angle(s) 13, 51
- Mean value of absorption coeffi-  
cient 163
- Measurement of absorption 85
  - of impedance 85
- Multilayer system 122
- Oblique incidence 164
- Perforated material 111
  - panels 127, 143
- Phase constant 1
- Plasters 50, 63, 77, 122
- Porosity 2, 20, 77, 131
- Propagation constant 1
  - , velocity of — 1
- Radiation 131
  - resistance 135
- Reaction interferometer 91
- Reflection coefficient 5, 86
- Resistance, air- 79
  - constant 20
- Resonance 16
  - , frame- 69

- frequency 128
- Resonator(s) 127, 169
- , efficiency of — 136
- , impedance of — 132
- in parallel 160
- in series 158
- Reverberation method 165
- time 142
- Rubber 83
- , cellular — 111
- , sponge — 77, 117
- Selectivity 145
- Sponge rubber 77, 117
- Stiffness 53, 81
- Structure constant 20
- factor 50, 107, 131, 149
- Surface, closed front — 65
- Theory of Kirchhoff 26
- Velocity of propagation 1
- Wave impedance 2
- — of free air 4
- — of impervious media 13
- Wood fibre 63, 77